Emission and Dispersion of Gaseous S, F and Cl from Mt. Erebus, Antarctica

Edward P. Klimasauskas

A Thesis Submitted in Partial Fulfillment of the Requirements for Master of Science in Geology

August 1995

Abstract

Mt. Erebus, Antarctica, provides a unique laboratory to study degassing behavior of a stable alkaline magma body. Sixty four samples of the gas plume emitted from Erebus were collected on filter packs during the 1992, 1993 and 1994 Austral summers. Filter packs consisted of a 2um teflon particulate filter followed by two ^{7}LiOH-impregnated Whatman 41 filters. Filter packs were connected to a small vacuum pump at a site on the crater rim. Total volume of air sampled was determined by multiplying the sample collection time by the flow rate. Samples were collected over intervals of 15 minutes to 2 hours to evaluate temporal variations in F/S, Cl/S and F/Cl. Data collected in previous years was used as a comparison to examine any significant trends.

Variations in F/S, Cl/S and F/Cl appear to be related to processes in the magma chamber and occur on three different time scales. Short term variations range from one to several hours. Three 30 minute samples collected before, during and after a Strombolian eruption document the following changes: Cl/S increased from .91 before the eruption to 4.4 during and dropped to 1.4 after; F/S ratios increased from .27 to .52 and remained at .53 after; F/Cl ratios decreased from .29 to .12 but climbed to .4 following the eruption. These changes are consistent with eruption of a gas "slug" formed by coalescence of bubbles at a shallow obstruction in the magma conduit. The high fluorine and chlorine relative to sulfur suggests the gas pocket formed in a partially degassed melt.

Daily values of Cl/S and F/S from 1992 and 1993 appear to have a cyclic trend with a period of ~ 6 - 8 days. This may be related to large scale overturn or convection in the magma column.

Yearly average values of the relative proportions of S, F and Cl show a two to three year cyclic trend between a more sulfur-rich and a more fluorine/chlorine-rich composition. Superimposed on these variations is an overall shift with time towards a gas which is more sulfur-rich. Pulses of magma recharge from depth followed by periods of repose could account

for the observed trends. The overall shift toward more sulfur-rich composition could herald the arrival of a large diapir at depth.

Gaussian plume dispersion models were used to examine the distribution and potential impact of S, F and Cl from Mt. Erebus on the Antarctic environment. Two plume sector models were used to evaluate seasonal average dispersal patterns and concentration gradients for Mt. Erebus and McMurdo Sound. A third standard dispersion model provides an extreme upper limit of the potential contribution of Erebus plume gases to South Pole based on a 5 hour time average prediction.

Sector model results reveal that distribution and concentration gradients are strongly dependent on emission rate, wind direction and wind speed. Model predictions are essentially zero for ground level concentration of all elements in a 10 km radius from the summit. Distant sector models predict that only the sites with elevations closest to Erebus will have seasonal average atmospheric concentrations of a few 10's of $ng's/m^3$ for SO_2. Atmospheric concentrations predicted by these two models can be tested by future sampling.

Models of dispersion to South Pole predict that Erebus can account for ~10 - 100% of SO_2 and Cl compared to atmospheric samples collected by Maenhaut et al. (1979). Extrapolation of certain model parameters to distances much greater than intended for this type of model appears to be unreasonable. It is likely that any model predictions would be at least an order or two of magnitude higher than reality. However, as a rough first order approximation this model provides a constraint on maximum potential input of Erebus gases to the South Polar troposphere.

Model predictions as well as trace element data from atmospheric and snow sampling clearly show that measurable amounts of Erebus gases can reach South Pole. Based on current levels of activity and the absence of a mechanism responsible for transferring significant amounts of SO_2 and Cl to the stratosphere it is unlikely that gases from Erebus play a large role in ozone depletion.

Acknowledgements

I would like to acknowledge and thank the following for their support and assistance on this project. I would like to especially thank the U.S. Navy VXE-6 squadron for getting me in and out in one piece. For assistance in the field and with collection of samples thank you to Ken Sims, Demetria Newsome, Alexei Ozerov, Richard Esser, Bill McIntosh, Nelia Dunbar and all the folks at McMurdo who made both field seasons truly memorable. Thanks to Mike Glascock and Vicki Spate at the Missouri University Research Reactor for running the '92 and '94 samples, the folks at Texas A&M Research Reactor for putting up with me for a week and recommending great Thai food, Sandy Swartz and the NMBMMR for her patience and use of the IC, and last but not least many thanks to Phil Kyle for things too numerous to mention. This project was funded in part by NSF grant DPP-9118056.

Table of Contents

Abstract.....i

Acknowledgements.....iii

Table of Contents.....iv

List of Figures.....vi

List of Tables.....viii

1. Introduction.....1

    1.1 Magmatic Volatiles.....2

    1.2 Geologic Setting.....7

    1.3 Eruptive History.....10

    1.4 Previous Studies.....11

    1.5 Objectives.....12

2. Methods.....13

    2.1 Filter Sampling.....13

    2.2 Filter Analysis.....15

3. Results.....16

    3.1. Filter Data.....16

4. Discussion.....23

    4.1. Quality Control.....23

    4.2. Solubility Constraints on Degassing.....25

    4.3. Short Term Variations.....29

    4.4. Daily Variations.....33

    4.5. Long Term Variations.....37

    4.6. Estimation of Pre-eruptive Volatile Content.....39

        Saturated vs. Unsaturated.....39

        A Preliminary Model.....41

5. Plume Dispersion Models....43
5.1. Introduction....43
5.2. Model Results....47
30° Sector Models - Local Sites....47
10° Sector Models - Distal Sites....56
South Pole Dispersion Models....61
Potential Contribution to the Stratosphere....63
6. Conclusions....65
Appendix A: Ion Chromatography Procedures....67
Appendix B: INAA Procedures....69
Appendix C: Filter Data....74
References....90

List of Figures

Figure 1.1. Locator Map for Ross Island, Antarctica. 8

Figure 1.2. Mt. Erebus and Ross Island, Antarctica 9

Figure 2.1. Map of summit crater area....14

Figure 3.1. S, F, and Cl as a proportion of the sum of the three for 1992 (A), 1993 (B) and 1994 (C) samples....19

Figure 3.2. Distribution between particulate and gaseous sulfur (A), fluorine (B) and chlorine (C) 21

Figure 3.3. A filter Na versus Cl 22

Figure 4.1. Variations in F/S (A) and Cl/S (B) over 11 Dec 93 30

Figure 4.2. Variations in F/S, F/Cl and Cl/S over the course of an eruption, 10 Dec 94....31

Figure 4.3. Daily averages calculated for F/S, Cl/S and F/Cl for 1993....33

Figure 4.4. Daily averages for F/S, Cl/S and F/Cl for 12 - 19 Dec. 1992....34

Figure 4.5. Daily averages from 1994 filters. 35

Figure 4.6. Mean sulfur, fluorine and chlorine as a proportion of the sum of the three for 1986 - 1994. 37

Figure 4.7. Comparison of Erebus melt inclusion sulfur and iron with values from other sulfur-saturated volcanic rocks. 39

Figure 5.1. Plume sector model results for centerline SO2. 49

Figure 5.2. Plume sector model results for centerline F....50

Figure 5.3. Plume sector model results for centerline Cl 51

Figure 5.4. Monthly wind rose diagrams for McMurdo Sound, Austral Summer, 1993-4....52

Figure 5.5. Monthly wind rose diagrams for McMurdo Sound, Austral Summer, 1994-5.....53

Figure 5.6. Summary wind rose diagram for Austral summer 1993-4. 54

Figure 5.7. Summary wind rose diagram for Austral summer 1994-5. 55

Figure 5.8. 1993 Seasonal average SO_2 centerline concentrations for ten degree sector models. 57

Figure 5.9. 1993 Seasonal average SO_2 ground level concentrations for ten degree sector models. 58

Figure 5.10. 1994 Seasonal average SO_2 centerline concentrations for ten degree sector models. 59

Figure 5.11. 1994 Seasonal average SO_2 ground level concentrations for ten degree sector models. 60

Figure 5.12. Enrichment factors for selected volcanoes and anomalously enriched elements in South Pole snow. 63

Figure B.1. Comparison of chlorine values from short calibration and very short cross calibration, INAA @ MURR, 1995. 73

List of Tables

Table 1.1. Average annual emission rates for SO_2, HF and HCl for 1986 - 1991 12

Table 3.1.a. 1992 Sample data for S, F, Cl, In and Na (ug/m^3) 16

Table 3.1.b. 1993 Sample data for S, F, Cl, In and Na (ug/m^3) 17

Table 3.1.c. 1994 Sample data for S, F, Cl, In and Na (ug/m^3) 18

Table 3.1.d. Particle size fraction concentrations (ug/m^3) for sample 94-301 20

Table 4.1. Elemental ratios for duplicate samples 23

Table 4.2. Variations in elemental ratios over a one hour period on 7 Dec 1994 24

Table 4.3. Correlation coefficients for particulate versus gaseous proportions of S, F and Cl by filter size and year 25

Table 4.4. F/S, F/Cl and Cl/S from melt inclusions and volcanic gases collected from 1986 - 1994 28

Table 5.1. Concentrations of SO_2, F and Cl for South Pole Gaussian plume models and atmospheric measurements 62

Table B.1. Isotopes and peak energies used for F, Cl, In and Na calibrations 69

Table B.2. Irradiation, decay and count times for elements analyzed by INAA 70

Table B.3. Standards used for INAA 71

Table C.1. Blank corrected filter data for 1992 75

Table C.2.a. Blank corrected filter data for 1993-110mm samples 76

Table C.2.b. Blank corrected filter data for 1993-47mm samples 77

Table C.2.c. Blank corrected filter data for 1993-Staplex samples 77

Table C.3.a. Blank corrected filter data for 1994-100mm samples.....78

Table C.3.b. Blank corrected filter data for 1994 size fraction and hut aerosol samples.....78

Table C.3.c. Blank corrected filter data for 1994-47mm samples. 79

Table C.4. Sample collection data for 1992. 80

Table C.5.a. Sample collection data for 1993 (47mm and 110mm filters).....81

Table C.5.b. Sample collection data for 1993 (Staplex samples). 82

Table C.6.a. Sample collection data for 1994 (47mm and 100mm) 83

Table C.6.b. Sample collection data for 1994 (misc. samples).....84

Table D.1. 1993 Gaussian plume model calculations for concentrations of SO_2 at South Pole.....86

Table D.2. 1994 Gaussian plume model calculations for concentrations of SO_2 at South Pole.....87

Table D.3.a. 1993 ground level sector model results for SO_2. 88

Table D.3.b. 1994 ground level sector model results for SO_2 89

1. Introduction.

Volcanic activity has a strong influence on both local and global processes. The early formation of the continents, hydrosphere and atmosphere are largely a result of early magmatic evolution and degassing of the earth through volcanism. Some believe that volcanoes may have played an important role in the origins of life (Nisbet, 1986). Throughout earth history volcanoes have shaped our planet.

Physical manifestations of volcanic activity affect a spectrum of human activities. Small, quiescent eruptions can destroy property, affect agriculture and hurt local economies (e.g. Kilauea, Hawaii). Larger, explosive eruptions have a much more dramatic effect, often resulting in the devastation of large areas and loss of life. An example is the historical eruption of Santorini in 1600 BC, which destroyed the center of Minoan civilization and may have ultimately led to their decline. In 1902 the eruption of Mt. Pelee resulted in 29,000 deaths (Decker and Decker, 1991). Mud flows generated by the 1985 eruption of Nevado del Ruiz, Columbia, killed 25,000 (Voight, 1990). Another recent reminder is the May 1980 eruption of Mt. St. Helens. A large area on the north side of the mountain was devastated by the blast, large tracts of timber were leveled, and 57 lives were lost.

Many of the devastating effects of large eruptions are restricted geographically, but can still have a global impact on the atmosphere and the weather (Decker and Decker, 1991). Large eruptions can inject significant amounts of ash and SO_2 into the stratosphere, resulting in reduced solar insolation and climatic cooling. The 1783 eruption of Laki in Iceland created a poisonous fog that killed livestock and resulted in the "year without a summer"(Decker and Decker, 1991). The release of "greenhouse gases" as well as large amounts of SO_2 aerosol and Cl during eruptive processes may have far reaching effects on climate and the atmosphere that have not been completely evaluated.

1.1 Magmatic Volatiles.

Volatile species emitted from volcanoes are typically atmophile elements or complexes (mainly H_2O, CO_2, SO_2 and/or H_2S with minor amounts of HCl, HF, H_2, CO, S_2, O_2, COS, N_2, HB, CH_4, HI, metal halogens, and noble gases) that are soluble to varying degrees in molten rock at depth. As magma nears the surface, decreasing pressure lowers the solubility of these compounds. At saturation volatiles begin to exsolve through diffusion into a fluid or vapor phase (Anderson, 1975; Krauskopf, 1979; Gerlach, 1982; Fisher and Schminke, 1984).

The presence of a vapor or fluid phase in a magma influences a broad spectrum of geologic and volcanic processes. An important consideration is how the volatiles are distributed in a melt. Volatiles within a melt structure can polymerize or depolymerize a melt, significantly affecting viscosity . Experimental data suggests that H_2O occurs in the melt structure as network modifiers (OH^- groups) which depolymerize the melt, resulting in reduced viscosity (Fisher and Schminke, 1984). On the other hand, a vapor or fluid phase may separate from the magma altogether. The latter process is considered to be important in the generation of hydrothermal ore deposits (Krauskopf, 1957; Krauskopf, 1964; Smirnov, 1976; Hedenquist et al, 1993) as well as metaliferous sulfide bands in layered mafic intrusions (due to the formation of an immiscible sulfide phase coexisting with silicate melt (Campbell and Barnes, 1984; Barnes, 1993)).

Another consideration is whether or not bubbles form. Bubble nucleation and growth depends on partial pressure and solubility of gases, depth of magma (e.g. external pressure), viscosity, presence of surface active agents (Jackson,1994), and torsional forces (Clift et al, 1978; Sparks, 1978; Jackson,1994). Movement of the magma may lead to bubble nucleation and growth at partial pressures lower than the limits of solubility due to cavitation (Oxtoby and Evans, 1988). Volatile content, depth of vesiculation (bubble formation), nucleation rate and growth rate of vesicles directly influence the explosivity of volcanic eruptions (Fisher and Schminke, 1984).

Volcanic gases once released to the atmosphere can influence climate and other atmospheric processes. Stratospheric injections of Cl and SO_2 through sizable volcanic eruptions may affect ozone depletion (Hoffman and Solomon, 1989; Hoffman et al., 1992; Solomon et al, 1993; McCormick et al., 1995). An understanding of the processes responsible for ozone destruction is needed to evaluate the potential contribution from volcanic sources.

Chemical depletion of ozone during the Antarctic spring occurs chiefly in the 15 - 20 km range of the stratosphere (Solomon et al., 1986). Two processes have been determined to govern the rate and amount of ozone destruction: homogeneous gas phase chemistry in which chloride species break down O_3 and heterogeneous chemical reactions which take place on stratospheric aerosol surfaces.

The first process operates as long as there are reactive chloride species present in the stratosphere (Solomon et al., 1986; Hoffman and Solomon, 1989):

$$Cl + O_3 \text{ (ozone)} = ClO + O_2 \qquad (1)$$

$$ClO + O = Cl + O_2 \qquad (2)$$

Model results show that the impact of homogeneous chemistry is minimal in the altitude range where the majority of Antarctic stratospheric ozone depletion occurs (Solomon et al., 1986).

Heterogeneous reactions on aerosol surfaces appears to be responsible for the majority of ozone depletion. Springtime observations in Antarctica show increases of ClO concentration of about two orders of magnitude accompanied by dramatic reductions in NO_2 and NOx (Hoffman and Solomon, 1989). Free nitrogen compounds suppress reactive chloride through the formation of more inert $ClONO_2$ (Solomon et al., 1986). The coupled reduction of NOx with increased Cl has led researchers to the conclusion that the two are related through heterogeneous chemical reactions which occur rapidly on stratospheric aerosols. Polar stratospheric clouds (PSC's) have been observed during winter and spring conditions in Antarctica at temperatures less than -80° C (Solomon et al., 1986; Collins et al., 1993). PSC's can catalyze ozone destruction through denitrification of the lower stratosphere (Collins et al., 1993) and by providing aerosol surfaces

for heterogeneous chemical reactions (Solomon et al., 1986; Collins et al., 1993). Free nitrogen compounds can be directly removed through condensation of HNO_3 or nitric acid trihydrate in PSC's (Hoffman and Solomon, 1989; Collins et al., 1993). Reactions that would otherwise proceed very slowly have been shown to occur rapidly on aerosol surfaces (Solomon et al., 1986):

$$HCl + ClONO_2 = HNO_3 \text{ (nitric acid)} + Cl_2 \quad (3)$$

$$Cl_2 + h\nu \text{ (light)} = Cl + Cl \quad (4)$$

This reaction efficiently removes free nitrogen compounds while at the same time converting inert chlorine reservoirs (HCl, $ClONO_2$) into more reactive species (Cl_2, HOCl, ClO). The resultant Antarctic springtime ozone depletion occurs on a time scale of ~ 3 weeks (Hoffman and Solomon, 1989).

It has been proposed that volcanic eruptions contribute to ozone destruction through injection of large amounts of HCl, SO_2 and to a lesser extent H_2O into the stratosphere (McCormick et al., 1995). Volcanic gaseous chlorine species can catalyze ozone destruction through homogeneous reactions previously discussed. Once injected into the stratosphere SO_2 undergoes conversion to sulfuric acid droplets which provide surface area for heterogeneous reactions much like PSC's.

Estimation of stratospheric HCl input from volcanic activity has been a matter of debate. Ryan and Mukherjee (1975) suggest that volcanic HCl contributes up to 70% of the stratospheric reservoir. Cadle (1975) on the other hand maintains that only ~ 3.7% of volcanic emissions actually reach the stratosphere. The main reason for large differences is that while eruption plumes contain high concentrations of HCl, the amount that reaches the stratosphere may be less by up to four orders of magnitude (Tabazadeh and Turco, 1993).

Factors affecting stratospheric input are the volcanic emission rate, explosivity (Delmas et al., 1985), water content of the plume (Lazrus et al., 1979), ambient humidity, tropopause altitude and temperature (Tabazadeh and Turco, 1993). Observations following the 1974 eruption of Fuego (Central America) showed significant stratospheric increase in SO_2

accompanied by no increase in HCl (Lazrus et al., 1979). Similar observations during the 1991 eruption of Mt. Pinatubo suggest that Cl removal into condensed, supercooled water is extremely efficient (Tabazadeh and Turco, 1993). At Mt. Sakurajima (Japan) studies indicate that wet deposition effectively removes HCl but not SO2 from the plume (Kawaratani and Fujita, 1990). Because HCl is highly soluble, almost all of it is probably "rained out" from eruption plumes with high water content or in humid climates. Should large amounts of volcanic-derived halides reach the stratosphere it is unlikely that they would have any long term effects on ozone due to estimated residence times of a few months (Cadle, 1975).

The case for SO_2 is much different. Large amounts of SO_2 are often injected into the stratosphere through explosive eruptions. This volcanic SO_2 is rapidly converted to sulfate aerosols and ultimately sulfuric acid droplets (McCormick, 1992). Over 95% of the SO_2 injected into the stratosphere from Mt. Pinatubo was converted to H_2SO_4 within six weeks (Hoffman et al., 1992). Estimates of the stratospheric residence time for these small (0.1 - 0.3 um) acid droplets are ~ 1 year (Lazrus et al., 1979). Atmospheric transport and mixing occurs over a much shorter time scale. Stratospheric SO_2 from the June 1991 eruption of Mt. Pinatubo completed a circuit of the globe in 22 days (Bluth et al., 1992). By the fall of 1992 Pinatubo aerosols were detected in large amounts in the Antarctic stratosphere (Solomon et al., 1993). Isotopic studies indicate that the stratospheric sulfate reservoir is primarily maintained by periodic volcanic input superimposed on a background source of tropical upwelling (Castleman et al., 1973, 1974).

Recent laboratory studies suggest that the same reactions which are catalyzed on PSC surfaces also occur on H_2SO_4 aerosols, but at a slower rate. It is believed that the total aerosol surface area is the most important factor controlling the extent of these heterogeneous reactions (Hoffman and Solomon, 1989). Because these aerosols occur independent of temperature, they can catalyze ozone destruction at latitudes and temperatures where PSC's do not form (Solomon et al., 1993). Observations of a 10 to 20% reduction in ozone at the 20 km level for northern mid-latitudes in the years following the 1982 eruption of El Chichon (Central America) support this conclusion. Concurrent measurements of aerosol surface area over Texas fall in the observed range for PSC's in Antarctica (Hoffman and Solomon, 1989). An August 1991 eruption of Mt.

Hudson (Chile) injected significant SO_2 into the lower stratosphere. By September the eruption cloud had encircled the Antarctic polar vortex below 16km. Introduction of these aerosols resulted in an unprecedented 50% reduction of ozone in the 11 - 13 km range. Reductions in the 25 - 30 km range the same year have been attributed to the appearance of Pinatubo aerosols (Hoffman et al., 1992).

Other evidence for long-range transport of volcanic gases exists. Peaks in sulfate concentration in Antarctic snow have been linked to the 1963 eruption of Agung (Delmas et al., 1985). Delmas et al. (1982) estimate that volcanism contributed about a third of the sulfate in South Pole snow over the last 1000 years. Variable peaks in sulfate, fluorine and chlorine in Greenland ice cores have been correlated with distant volcanic activity (Herron, 1982). Anomalous enrichment of Si and Cl in aerosols at South Pole have led to speculation on Mt. Erebus as a possible source (Shaw, 1983). Enrichment of Pb, Cd, Cu and Zn in East Antarctic snow layers from 1910 to 1915 may be related to an Antarctic eruption at this time (Boutron, 1980).

Mt. Erebus currently provides a continuous supply of Cl and SO_2 to the Antarctic atmosphere. A close examination of emission and dispersion of these gases is important to quantifying any potential effect they may have on ozone depletion. It is likely that a large explosive eruption from Erebus would have a significant impact.

1.2 Geologic Setting.

Mount Erebus is an active alkaline intraplate hot spot volcano located on Ross Island, Antarctica (Figure 1.1)(Kyle et. al., 1992). Other radially (~120° angles) distributed volcanic centers on Ross Island (Mt. Terror, Mt. Byrd and Hut Point Peninsula)(Figure 1.2) may represent surface expressions of upwelling, fracture, and intrusion of a mantle plume (Kyle and Cole, 1974; Kyle et al., 1992). Volcanic rocks on Ross Island comprise the Erebus volcanic province of the McMurdo Volcanic Group (Kyle, 1990). Compositional evolution from basanite through anorthoclase phonolite via fractional crystallization has been documented by Kyle et. al. (1992). The upper reaches of Mt. Erebus consist of younger flows infilling an older caldera collapse. The older caldera rim is prominent at the 3200 meter level. Younger flows are chiefly anorthoclase phonolite, which also comprises possibly greater than 75% of the volcano (Kyle et. al., 1992). Recent $^{40}Ar/^{39}Ar$ age dates constrain the onset of current phonolitic activity to 121±7 Ka, although older phonolitic rocks have been dated at Turks Head (243±5 Ka) and on Inaccessible Island (542±3 Ka). An age of 1310±7 Ka for a basanite dike at Cape Barne provides age constraints on the evolution of the Erebus Lineage rocks (Esser, unpub. data; Kyle et. al., 1992).

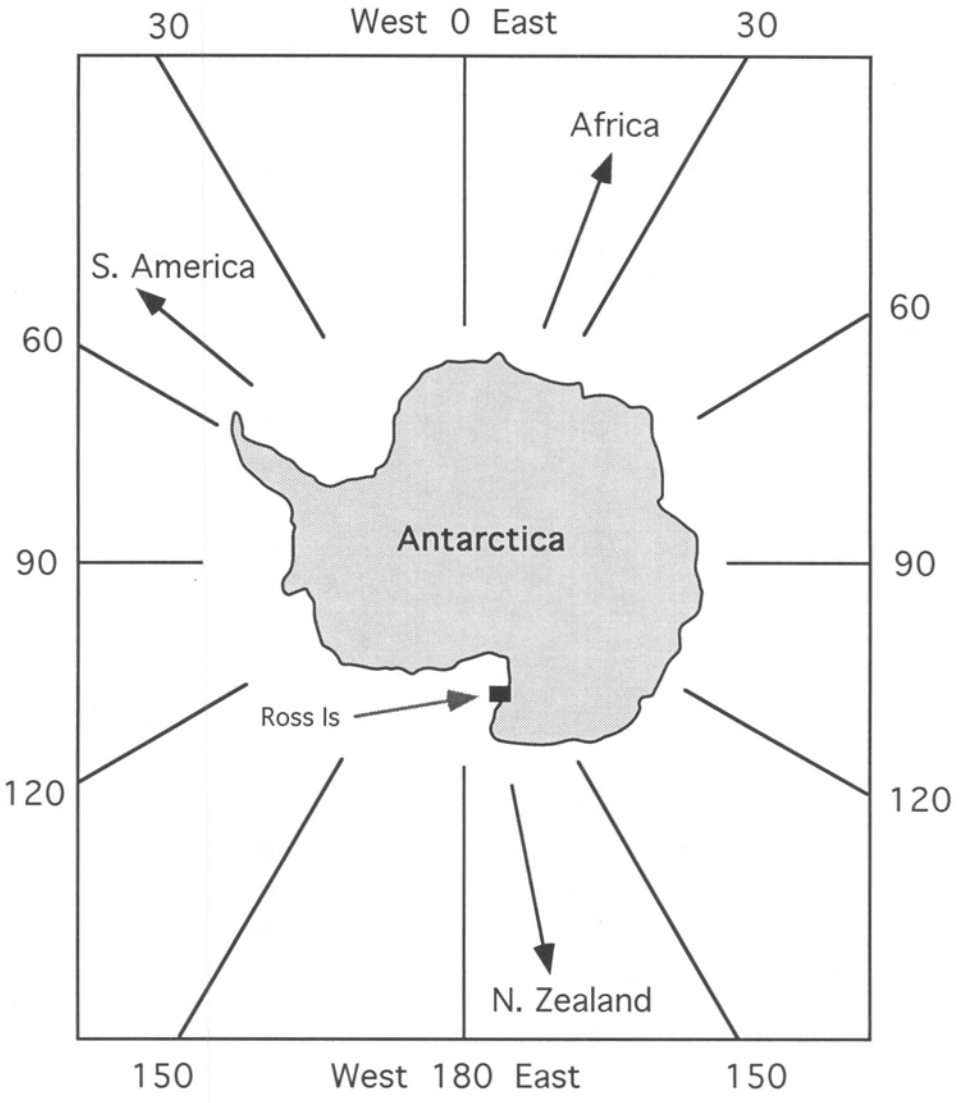


Figure 1.1. Location Map for Ross Island, Antarctica.

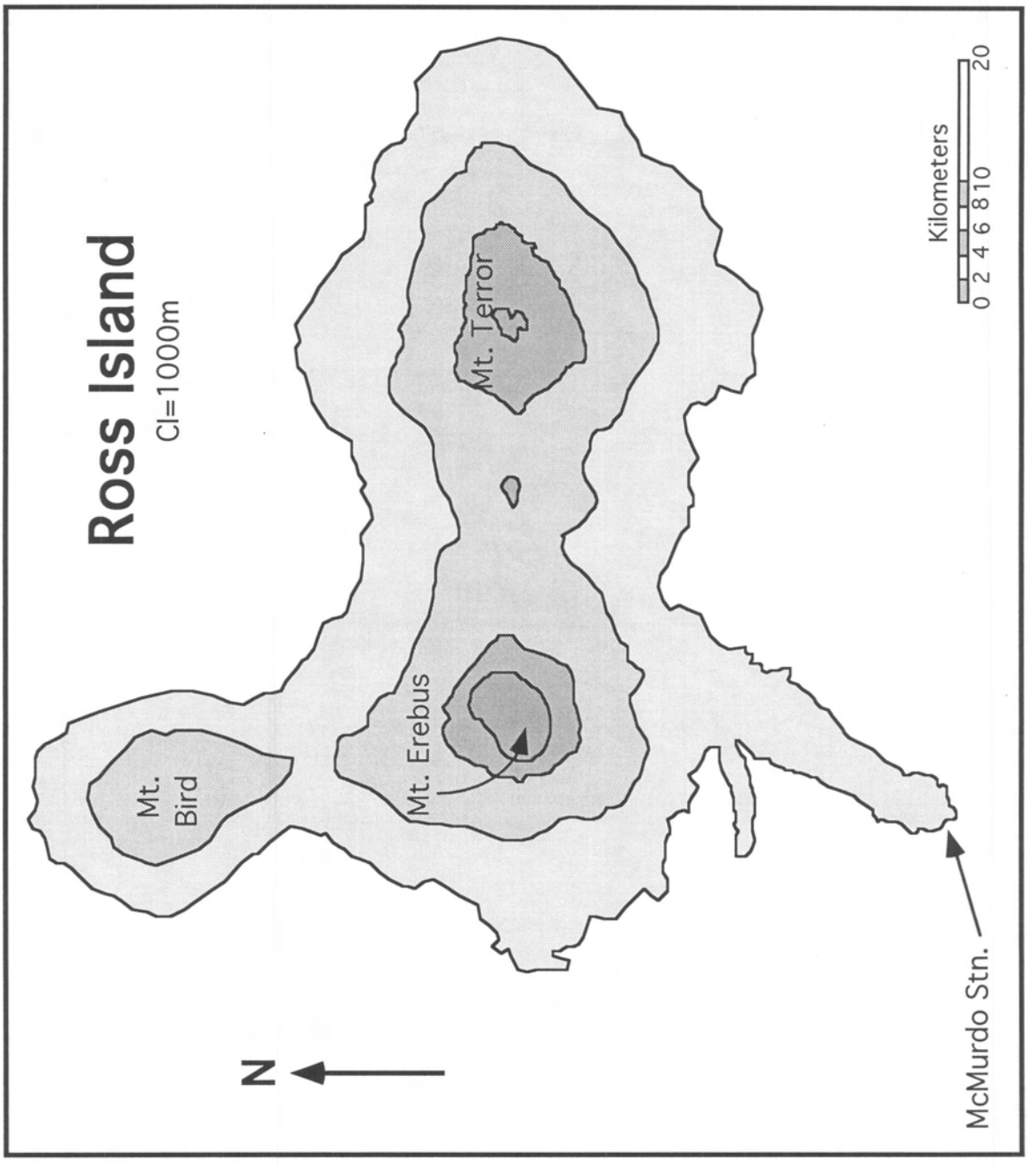


Figure 1.2. Mt. Erebus and Ross Island, Antarctica.

1.3 Eruptive History.

Volcanic activity at Mount Erebus was first witnessed by Ross (1847) in 1841 when the volcano was seen to "emit smoke and flame in unusual quantities, producing a most grand spectacle." The first summit observations by Shackleton in 1908 and the Scott expedition in 1912 revealed the absence of an Inner Crater and fairly continuous Strombolian activity. Depth to the crater floor was measured at 270m, approximately 100m deeper than at present. Over the next fifty years ongoing Strombolian activity was noted by visiting expeditions.

In 1963 the U.S. Navy produced the first aerial photo of Mount Erebus clearly showing the Inner Crater (Caldwell, 1991). Giggenbach et al (1973) first reported the appearance of a small anorthoclase phonolite lava lake in 1972. Careful examination of the 1963 photo suggests the lava lake may have been present at that time (Kyle et al, 1982). A steady increase in the surface area of the lava lake was observed from 1972 through 1976, when it reached a maximum diameter of 60 meters. From 1976 to 1978 the lava lake surface area remained fairly uniform. An increase in seismic activity in 1978 was accompanied by increased activity (an average of 3.5 Strombolian eruptions per day for 1978 over 2 per day for 1977-78). A gradual decrease in the level of the lava lake (~5-10 meters) was observed over the next three years, possibly due to magma withdrawal or erupted ejecta. Increased activity (4-6 eruptions per day) occurred during the 1981-82 season. During the 1982-83 season another drop of 3 meters was observed in the lake level (McClelland et al, 1989).

Strombolian activity jumped significantly during September, 1983. During the week of the 13th through the 19th, 8 to 19 large eruptions occurred per day. A decrease in activity was noted from the 20th through the 25th (2 to 8 eruptions per day) followed by peak activity from the 26th through the 29th (12 to 27 eruptions per day)(McClelland et al, 1989). Large bombs (up to 10m diameter) were thrown up to 1 km from the summit region(Caldwell, 1991). In the later part of 1983 the persistent anorthoclase lava lake appeared to be buried by ejecta.

During the 1985 season a reduction in seismic and eruptive activity (lower than pre-1984 levels) was observed. Subsequent field observations revealed the reappearance of the

lava lake from beneath the rubble. The lake continued to increase in size until 1988, when a 36% reduction in size accompanied by reduced SO_2 emissions was observed (Sybeldon, 1991).

During the 1991 field season, Mount Erebus neared pre-1985 levels of activity (Zreda-Gostynska, 1995), followed by a drop in Strombolian activity to the present. A small phreatic eruption occurred in October of 1993 which formed a small crater in the west side of the main crater floor. No juvenile material was reported from samples collected at the summit (Kyle, pers. comm.). At this time the lava lake appeared as a kidney-shaped pool situated against the NW wall of the inner crater. Observations made during the 1994-95 season revealed a deepening of the phreatic crater and slumping of several large blocks of the north side of the main crater floor which partly buried the lava lake. On closer observation the floor of the phreatic crater appeared flat, possibly reflecting fill of fine-grained ejecta (Dunbar, pers. comm.).

Minor, intermittent Strombolian activity was observed during the 1993-94 and 1994-95 seasons. No fresh bombs were observed outside the main crater. Only a few fresh bombs were noted on the main crater floor; the majority fell within a few tens of meters of the lava lake in the inner crater. Analyses of ejecta since 1973 are identical, suggesting a very stable convecting magmatic source (Caldwell and Kyle, 1994).

1.4 Previous Studies.

A significant amount of work on the physical (Giggenbach et al., 1974; Kyle and Cole, 1974; Kyle et al., 1977; Kyle et al., 1982), petrologic (Kyle and Cole, 1974; Kyle et al., 1977; Caldwell, 1991; Kyle et al., 1992; Dunbar et al., 1994), and geochronological (Armstrong, 1978; Esser, unpub. data) characteristics of Erebus already exists (see sections 1.2, 1.3 for relevant details).

Numerous studies of gaseous emissions have also been completed. With the exception of 1990, sulfur dioxide emissions have been measured annually since 1983 (Rose et al., 1985; Symonds et al., 1985; Meeker, 1988; Kyle et al., 1989; Sybeldon, 1991; Zreda-Gostynska et al., 1993; Kyle et al, 1994; Zreda-Gostynska, 1995; Kyle et al, in press.). Studies of halogen and trace metal emissions have also been completed (Meeker, 1988; Kyle et al., 1990; Meeker et al.,

1991; Zreda-Gostynska et al., 1993; Chuan, 1994; Zreda-Gostynska, 1995). Emission rates of sulfur, fluorine and chlorine for 1983-94 are tabulated in Table 1.1.

Table 1.1. Average elemental ratios and emission rates for SO2, HF and HCl. Data for SO2 from Kyle et al. (1995), elemental ratios from 1983 - 1991 from Zreda-Gostynska (1995).

Year	F/S	Cl/S	SO2 (Gg/yr)	HF (Gg/yr)	HCl (Gg/yr)
1983	.69*	1.41*	84	30.5	60.9
1984	.69*	1.41*	9	3.3	6.5
1985	.69*	1.41*	6	2.2	4.3
1986	.99	1.75	7	3.6	6.3
1987	.69*	1.41*	16	5.8	11.6
1988	.44	1.09	10	2.3	5.6
1989	.92	1.8	19	9.2	17.6
1991	.44	1.00	26	6.0	13.4

HF and HCl emission rates determined using SO_2 emission rates and F/S and Cl/S ratios for each year. * Years for which no fluorine or chlorine data was available - average value of F/S and Cl/S for 1986, 1988, 1989, and 1991 (Zreda-Gostynska et al., 1993).

1.5 Objectives.

Objectives of this study are addressed in two parts. The first part of the study involved collection of COSPEC and filter data as part of a program of annual monitoring of emissions and gas composition. Short term as well long term systematic variations in elemental ratios were investigated in an attempt to constrain degassing behavior. The second part of this research involved the collection of meteorologic data combined with EPA-approved air pollution models in an attempt to quantify the environmental impact of volcanic gases on the Antarctic environment.

2. Methods.

2.1 Filter Sampling.

Samples of volcanic gases were collected at Mt. Erebus using a variety of sizes of filter packs in a manner similar to that described by Finnegan (1984). Filter packs consist of a teflon particulate filter (A-filter) followed by two Whatman 41 cellulose filters (B&C) impregnated with 3M ^{7}LiOH. A solution of 3M ^{7}LiOH was prepared by dissolving near pure ^{7}Li metal in 18mΩ deionized water. Lithium-7 hydroxide was chosen because of it's properties as a strong base and low thermal cross section, which allows us to analyze filters by neutron activation for trace constituents that occur in the gas.

Filter packs were connected to a vacuum pump on the NE crater rim (Figure 2.1) at a site where the plume was drifting over. Measurements of the flow rate using a rotameter and sample time are used to compute the total volume of air sampled in cubic meters (m^3). Plume rise rate at the crater rim is typically 5 m/s (Sybeldon, 1991). Based on this velocity it takes less than a minute for gases emitted at the lava lake surface to reach the sampling site. This short travel time precludes significant loss of gaseous elements through wall rock interaction en route to the crater rim.

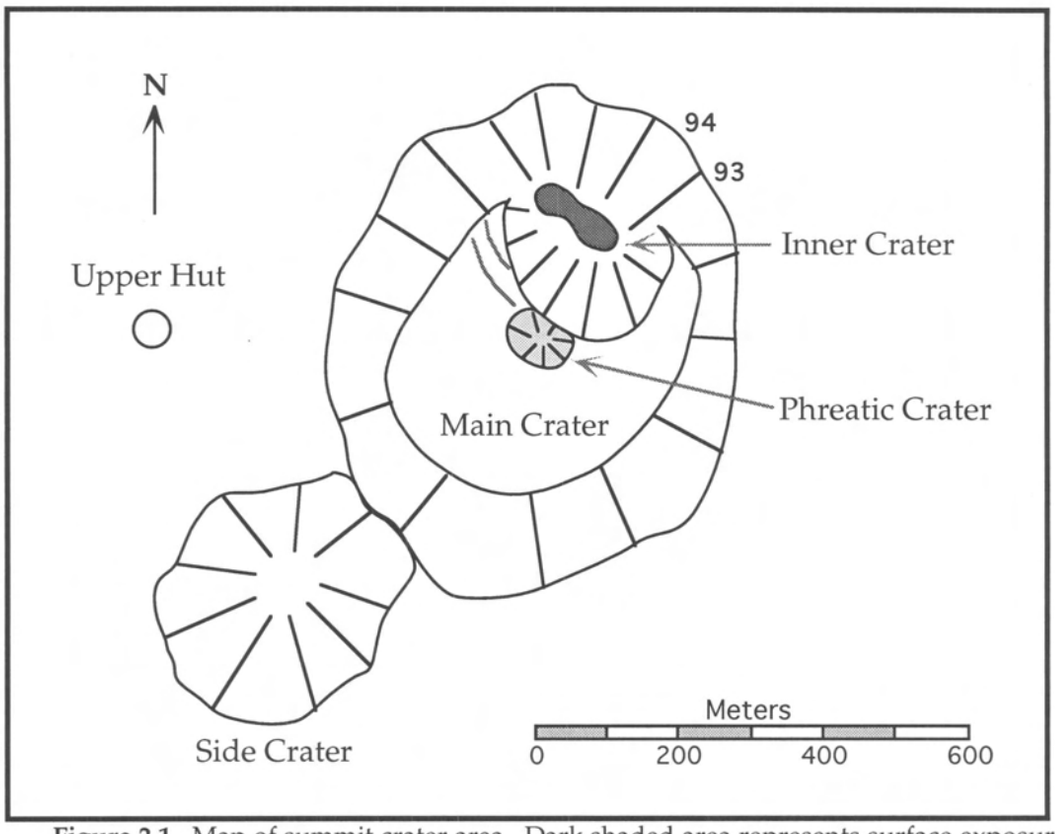


Figure 2.1. Map of summit crater area. Dark shaded area represents surface exposure of the lava lake. Numbers represent sampling locations for respective field seasons.

Two hour samples on large (100 or 110mm) filter packs were collected to provide an average representative sample of gases. Short term samples (15 min to 1 hour) were also collected to evaluate possible short term fluctuations in the gas composition.

Most of the particulate fraction of the samples are collected on the A-filter. Acid gases (SO_2, HCl, HF etc.) are absorbed on the base-treated filters that follow. Concentrations of F and Cl are typically highest on the B-filters, with minor amounts collected on C-filters, suggesting the base adequately absorbs all the acid gases for the sample times used.

2.2 Filter Analysis.

Analysis for S, F, Cl and other trace constituents were carried out using a combination of ion chromatography and neutron activation. Filters were divided into halves (47mm) or quarters (100 and 110mm sizes). One portion was leached in clean centrifuge vials for analysis of sulfur (all filters) and fluorine (particulate filters) by ion chromatography.

A second portion of the filters was packed for analysis by neutron activation. Particulate filters were analyzed for Cl, In and Na. Treated filters were analyzed for F and Cl. Samples from 1993 were analyzed in September of 1994 at the Texas A&M Research Reactor. Samples from 1992 and 1994 were analyzed in the Spring of 1995 at the Missouri University Research Reactor. Details of the analytical procedures are provided in appendices A and B.

3. Results.

3.1. Filter Data.

Filter data consists of a number of samples collected over a period of a few weeks during 1992 (16 samples), 1993 (26 samples) and 1994 (22 samples). Analytical results presented in Tables 3.1.a, b, and c represent the sum of all filters in a sample in ug/m3. Individual filter concentrations for sample 94-301 in ug/m^3 are given in Table 3.1.d.

Table 3.1.a. Analyses of filters collected in 1992 (in ug/m^3 except In - ng/m^3).

Samples	S	F	Cl	In	Na	vol.(m^3)
92-1	56.00	19.26	35.26	5.6	4.28	2.25
92-3	241.89	129.26	463.47	37.6	15.83	2.97
92-5	78.51	37.32	52.83	7.9	2.75	5.9
92-6	90.00	20.40	99.61	3.9	3.44	4.8
92-7	46.38	38.81	69.84	7.7	1.57	3.7
92-8	61.22	24.33	107.31	7.3	5.81	3.6
92-9*	39.14	22.74	114.34	4.8	.87	1.4
92-10*	35.54	35.35	141.18	8.5	6.48	1.3
92-11*	53.85	46.35	119.01	10.1	5.19	1.3
92-13	111.37	32.31	49.67	10.3	1.14	1.9
92-14	167.18	51.15	109.31	11.4	6.52	3.9
92-15	84.29	30.53	169.19	5.5	1.11	1.4
92-16	129.37	104.74	174.80	9.9	6.17	4.1
92-19	165.16	89.49	245.13	16.3	11.61	3.1
92-21	86.90	32.11	127.32	5.8	5.05	2.9
92-22	89.15	30.93	120.45	7.7	3.16	6.6

* indicates 47mm samples, all others are 110mm. Volume is calculated from flow rate and sample time.

Table 3.1.b. Analyses of filters collected in 1993 (in ug/m^3 except In - ng/m^3).

Samples	S	F	Cl	In	Na	vol.(m^3)
93-1	189.11	59.84	278.39	22.3	14.31	1.44
93-2	928.24	293.50	1021.80	80.8	52.29	2.88
93-3	185.74	41.19	152.57	50.3	28.19	4.32
93-4	425.49	69.75	339.05	41.7	24.54	4.8
93-5	324.46	53.5	75.73	40.5	34.25	2.4
93-6	222.26	76.52	102.35	3.7	2.61	3.6
93-8	163.89	29.55	31.74	7.1	3.72	3.6
93-9	66.52	15.97	47.23	5.7	3.53	3
93-10	72.86	36.07	27.35	9.7	5.27	3
93-11	73.86	34.93	24.7	5.6	2.84	3.45
93-13	76.65	16.57	15.79	15.2	14.17	2.64
93-15	185.55	38.61	46.29	2.3	4.22	6.12
93-16	263.24	52.18	116.59	13.3	8.40	2.83
93-17	79.5	39.93	72.29	8.0	5.13	2.46
93-52*	560.29	205.60	539.01	36.4	19.44	1.58
93-54*	412.90	130.47	375.56	17.1	10.99	1.58
93-55*	192.11	173.48	292.93	18.8	8.57	.63
93-56*	412.00	133.16	160.69	15.0	7.11	1.8
93-58*	282.18	131.92	186.99	20.1	12.67	.6
93-59*	853.56	372.20	433.27	19.7	9.50	1.2
93-60*	330.47	107.91	222.76	15.7	8.12	.69
93-61*	211.18	140.55	236.22	17.3	7.70	2.16
93-62*	66.14	35.45	209.63	5.4	3.04	1.38
93-63*	146.32	60.78	359.28	12.3	6.4	1.63

* indicates 47mm samples, all others are 110mm. Volume is calculated from flow rate and sample time.

Table 3.1.c. Analyses of filters collected in 1994 (in ug/m^3 except In - ng/m^3).

Samples	S	F	Cl	In	Na	vol.(m^3)
94-1	113.62	85.41	145.24	9.7	26.37	2.743
94-3°	175.04	131.06	232.46	25.2	31.48	2.725
94-4°	71.75	49.46	71.52	11.6	24.50	3.625
94-6	27.77	17.15	51.10	2.77	7.62	5.04
94-9	13.36	9.10	59.64	.9	8.25	2.34
94-11	19.33	15.41	56.63	3.6	2.64	3.25
94-51*	135.09	62.33	122.61	14.0	13.05	.57
94-52*	174.06	61.52	250.42	9.9	1.51	.465
94-53*	179.81	87.29	213.00	12.4	22.54	.465
94-54*	233.99	70.80	175.31	17.5	6.14	.42
94-57*	25.70	16.00	26.87	1.2	1.16	.396
94-58*	68.40	17.99	62.58	10.9	3.59	.396
94-59*	24.77	12.76	110.84	4.6	7.07	.396
94-60*	95.92	50.84	130.49	6.6	0	.462
94-61*	442.18	176.77	360.49	38.1	26.06	.264
94-62*°	36.10	16.19	63.75	2.2	0	.81
94-63*°	47.86	17.07	139.94	2.2	7.44	.573
94-65*	133.62	49.70	113.33	10.3	7.21	3.64
94-67*	62.17	29.91	71.43	6.0	3.29	3.51
94-69*	89.80	38.58	101.78	7.0	5.36	3.713
94-70*	24.33	11.43	48.47	2.2	1.24	4.05

* indicates 47mm samples, all others are 100mm. Volume is calculated from flow rate and sample time. ° indicates duplicate samples.

Sulfur, fluorine and chlorine for each sample are presented as a proportion of the sum of the three for each sample in Figure 3.1.

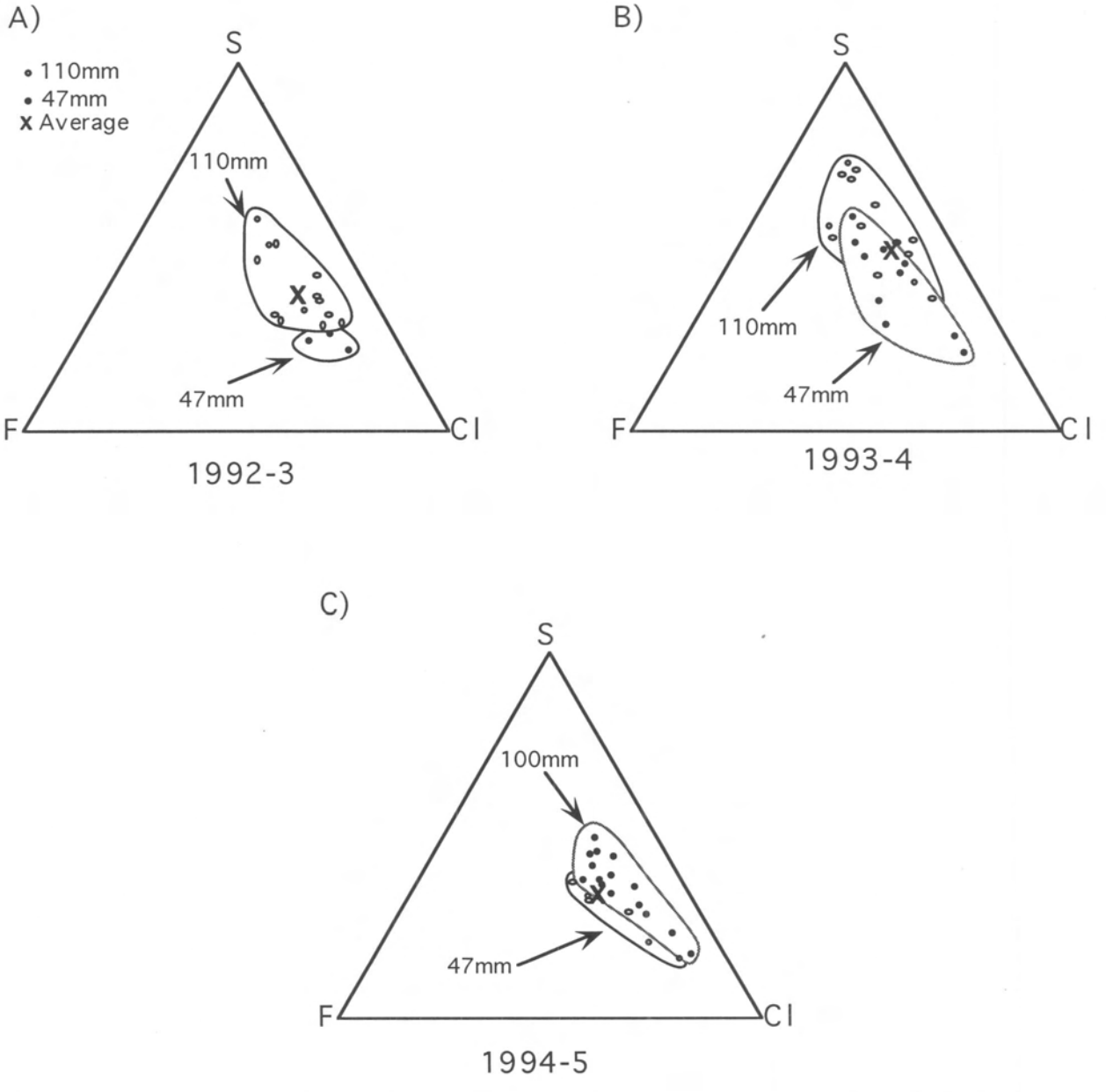


Figure 3.1. Sulfur, fluorine and chlorine for each sample plotted as a proportion of the sum of the three for 1992 (A), 1993 (B) and 1994 (C). Circled areas represent grouping by filter size.

A comparison of particulate and treated filter concentrations provides little insight into the partition of elements between the particulate and gaseous fractions. Indium and sodium only occur on the A filters. Very little particulate sulfur or fluorine is observed. Occasionally 10's of ug's of chlorine are collected in the particulate fraction (Figure 3.2). These are likely NaCl or KCl particles derived from the volcano. Chuan (1994) has identified both NaCl and KCl particles collected from the Erebus plume. Thermodynamic models of gases from Mt. St. Helens show NaCl as a predominate sodium species at temperatures estimated for the lava lake at Erebus (Symonds and Reed, 1993). Zreda-Gostynska (1995) also found a very good correlation between total Na and Cl collected in filter samples from 1986-1991. A plot of Na versus Cl on particulate filters (Figure 3.3) shows that NaCl accounts for most of the particulate chlorine, but this does not preclude the presence of other particulate chloride species.

A 47mm filter pack sample (94-301) collected in 1994 contained 8um, 2um and .2um particle filters. Fluorine was absent on all filters. Indium and sodium only occurs on the 2 um filter. Chlorine is mostly on the 2 um filter, but a small amount does occur on the 8um filter. These larger particulates may be other metal-chloride complexes or larger aggregates formed around condensation nuclei. Particulate sulfur in the .2 - 2um size range suggests two possibilities; either sulfur is scavenged during sample collection or there is a component of < 2um particles which can pass through the A filter of other samples. In the first case it is likely that these are newly formed H_2SO_4 condensation nuclei.

Table 3.1.d. Analysis of elemental concentrations on sample E94-301 which consisted of 3 particulate filters of 8 um, 2 um, and .2 um pore sizes. All data in ug/m^3 except In (ng/m^3). Total sample volume was .495 m^3.

Pore Size	Type	S	F	Cl	In	Na
8 um	Np	3.53	0	.99	0	0
2 um	Zef	9.21	0	4.10	5.74	6.91
.2 um	Np	9.75	0	0	0	0

Zef = Zefluor teflon filter, Np = Nucleopore polycarbonate filter

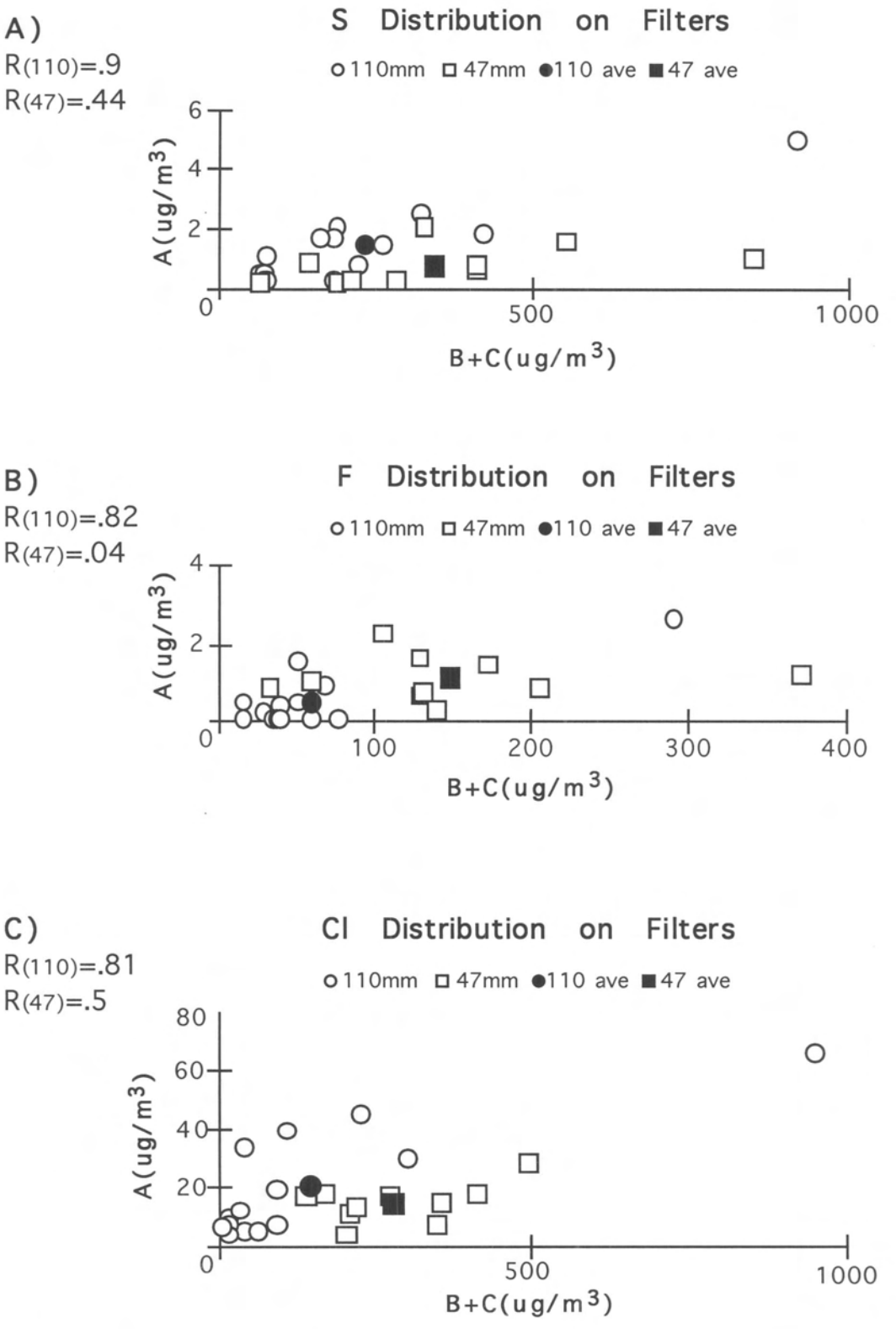


Figure 3.2. Distribution of sulfur (A), fluorine (B) and chlorine (C) between teflon (A) and treated filters (B + C) for 1993 . Correlation coefficients (R) are listed for each filter size. Plots for 1992 and 1994 show similar scatter and are not presented.

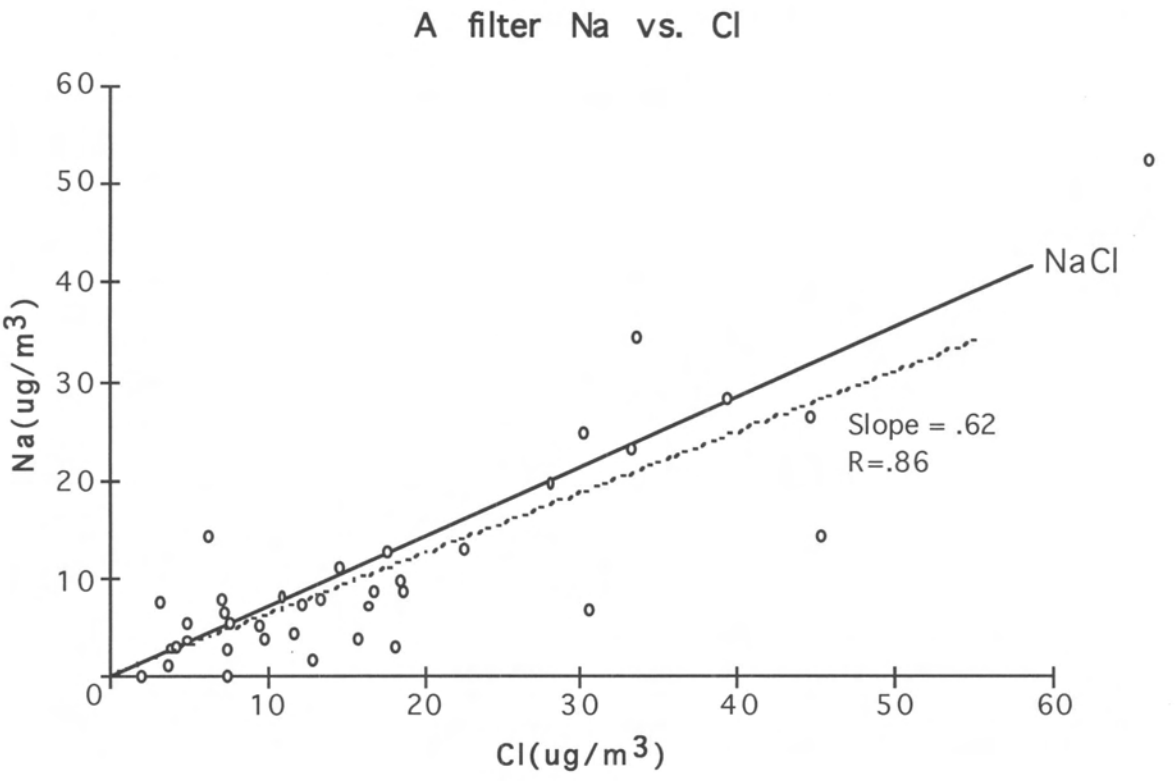


Figure 3.3. Concentrations of A filter Na vs. Cl. Dashed line represents regression of data points. Solid line (slope = .64) represents 100% NaCl. The good correlation (R = .86) of A filter Na and Cl and the similarity of the slope of the "100%" NaCl line with the regression of data points suggests that most of the particulate chloride occurs as NaCl.

4. Discussion.

4.1. Quality Control.

Absolute elemental concentrations collected on filter samples can vary widely depending on wind direction, plume dilution, wall rock and atmospheric interaction(Yoshida, 1990), however, elemental ratios can provide insight into degassing behavior (Giggenbach, 1975; Malinconico, 1979; Hirabayashi et al., 1982; Miller et al., 1990; Yoshida, 1990; Yoshida et al., 1994). The following discussion of quality control is directed primarily at elemental ratios. The basis for the use of elemental ratios in constraining degassing behavior of Mt. Erebus will be explained in the next section.

During the 1994 season, "duplicates" of both 100mm and 47mm samples were collected to assess the precision of the sampling technique (Table 4.1). These samples were collected approximately one meter apart over the same sample time. Because each filter was run on separate vacuum pumps, flow rate and hence total sample volume varied slightly. Although the samples are not exact duplicates, they do provide a test of precision for the sampling procedure.

Table 4.1. Elemental ratios for duplicate samples. The average and mean deviation (d) are used to constrain the precision of sampling method. Note the 47mm duplicates show consistently lower precision. Samples -003 and -004 are 100mm filters, samples -062 and -063 are 47mm samples.

Sample	vol. (m^3)	F/S	Cl/S	F/Cl	In/Cl*	Na/Cl
94-003	2.725	.75	1.33	.56	.11	.14
94-004	3.625	.69	1.00	.69	.17	.34
Average		**.72**	**1.165**	**.625**	**.135**	**.24**
d		**.03**	**.165**	**.065**	**.035**	**.10**
variation		4 %	14 %	10 %	26 %	42 %
94-062	.810	.45	1.77	.25	.35	.00
94-063	.573	.36	2.92	.12	.16	.05
Average		**.40**	**2.34**	**.185**	**.255**	**.025**
d		**.04**	**.58**	**.065**	**..095**	**.025**
variation		10 %	25 %	35 %	37 %	100 %

* In/Cl ratios are mulitplied by 1000 for comparison.

The difference in elemental ratios is significantly smaller in duplicates of 100mm compared to 47mm ones. Both smaller sample volume and surface area analyzed for 47mm filters (868mm^2) compared to 100mm filters (1964mm^2 analyzed) result in much smaller concentrations. At lower concentrations the same variability will result in a higher percentage of error. For the purpose of interpreting temporal variations in plume composition, only departures in elemental ratios larger than these variations will be considered significant.

A series of 4 - 47mm filter pack samples were collected over 15 minute intervals on 7 Dec. 1994 to assess the sensitivity of this method in detecting short term variations in plume composition (Table 4.2). With the exception of F/S, elemental ratios show a much lower variation than that observed in 47mm duplicate samples. These data confirm the possibility of obtaining short term samples of gas in strong plume conditions. It is also clear that the plume composition remained constant throughout the one hour sample period.

Table 4.2. Short term variations in elemental ratios collected over a total of one hour on 7 Dec 1994.

Sample	vol. (m^3)	F/S	Cl/S	F/Cl	In/Cl*	Na/Cl
94-051	.570	.46	.91	.51	.11	.11
94-052	.465	.35	1.44	.25	.04	.01
94-053	.465	.49	1.18	.41	.06	.11
94-054	.420	.30	.75	.40	.10	.04
Average		**.40**	**1.07**	**.39**	**.08**	**.06**
σ		**.09**	**.30**	**.11**	**.03**	**.05**
variation		22 %	28 %	28 %	24 %	85 %

* In/Cl ratios multiplied by 1000 for comparison.

Based on this set of data, it seems that it is reasonable to expect ±25 to 30% error in all ratios except Na/Cl, where the expected error can be much larger. In the case of the 100mm duplicates the mean deviation is very close to analytical uncertainty. For 47mm duplicates the much lower concentrations could result in a higher percentage variability in the elemental ratios. In either case analytical uncertainties can account for most of the observed variability.

Statistical analysis of particulate versus gaseous sulfur, fluorine and chlorine yields interesting results. Although there is a good correlation for these elements in 110mm samples from 1993 (Table 4.3), data from other years do not confirm any systematic behavior. The correlation coefficients for 1992 - 47mm samples are good because there are only three samples.

Table 4.3. Correlation coefficients for particulate versus gaseous proportions of S, F and Cl.

Year	1992		1993		1994	
Size	110	47	110	47	100	47
#	13	3	16	10	7	15
S	.23	.82	.9	.44	.14	.44
F	0	.76	.82	.04	.07	.33
Cl	.44	.35	.81	.5	.7	.49

In plots of proportional S, F, and Cl (Figure 3.1) mean values for 1992 differ according to filter size. This is primarily due to the paucity of 47mm filters collected that year. Data sets containing a large number of both 47mm and 110mm samples (1993) overlap sufficiently so that the 47mm and 110mm mean values are indistinguishable. This suggests that both 47mm and 110mm filter samples are comparable. The average of a large population of both 47mm and 110mm filter samples should provide a representative gas composition for the field season.

4.2. A Basis for the Interpretation of Changes in Gas Composition: Solubility Considerations.

Many attempts have been made to find a single indicator of volcanic activity. Changes in elemental ratios (e.g. F/S, Cl/S, F/Cl etc.) in volcanic gases at active volcanoes have been correlated with eruption frequency (Giggenbach, 1975; Malinconico, 1979; Hirabayashi et al., 1982). Others have noted systematic changes in elemental ratios before, during and after eruptive activity (Miller et al., 1990). Most of these interpretations are based on the relative solubilities of sulfur, fluorine and chlorine. The basis for my interpretation of changes in Erebus gas composition related to magmatic activity relies on the relative solubilities of S, F and Cl as well as their observed degassing behavior at other volcanoes.

The solubilities of sulfur, fluorine, and chlorine are controlled by a variety of parameters which are only poorly understood. Carbon dioxide solubility shows a strong dependence on pressure and to a lesser degree bulk composition (Fisher and Schminke, 1984). The exsolution of CO_2 may have effects on the solubility and exsolution of other volatiles. Magmatic systems represent complex interactions of volatile species, bubbles, and the melt.

Sulfur solubility in a melt is dependent on temperature, fO_2, fS_2, FeO content, and bulk composition (Haughton et al., 1974; Poulson and Ohmoto, 1990; Wallace and Carmichael, 1992). Based on estimates of fO_2 ($10^{-12.2}$)and temperature (1000°C) for Erebus magma (Kyle, 1977), sulfur is probably dissolved in the Erebus melt as HS^- or FeS complexes (Burnham, 1979). As pressure decreases and fO_2 increases, reduced sulfur is converted to SO_2 which has a low solubility. Degassing of CO in a shallow magma chamber is one possible mechanism of increasing oxygen fugacity in the melt through the following reaction (Mathez, 1984):

$$CO_3^{2-}{}_{(melt)} = CO_{(vapor)} + 1/2\ O_{2(melt)} \qquad (5)$$

Exsolution of this low solubility species allows for efficient removal of sulfur from magma at shallow levels. The controls of FeO content on a melt have led to speculation on fractional crystallization as a mechanism of supersaturating sulfur in a melt.

Factors affecting chlorine solubility are more complex and not as well understood. Experimental data coupled with observations of natural systems show a strong dependence on pressure and water content (Kilinc and Burnham, 1972; Shinohara et al., 1989; Metrich and Rutherford, 1992) as well as melt composition (Anderson, 1974; Metrich, 1990). In experiments with water-saturated melt compositions increases in pressure result in decreased solubility (Metrich and Rutherford, 1992). Other experiments show that chlorine is strongly partitioned into a H_2O-rich fluid phase (Kilinc and Burnham, 1972; Anderson, 1974). Chlorine loss through degassing of H_2O has been suggested as a mechanism to explain the almost constant Cl/H_2O ratios in the Laacher See tephra sequences (Worner and Schminke, 1984). A good correlation between Cl and K_2O and P_2O_5 have led to speculation that fractional

crystallization may enrich Cl content of a melt (Anderson, 1974; Metrich, 1990). The SiO_2 content shows a good inverse correlation with chlorine solubility (Anderson, 1974). In high-silica melts, Cl solubility increases with increasing FeO content. Primary compositional controls on solubility are Al/Si and the Na+K/Al molar ratios for melt compositions where Na+K/Al $\geq$ 1. These studies suggest that chlorine occurs as alkali-chloride complexes in high-SiO_2 melts and that Cl is concentrated in aqueous fluids in equilibrium with these melts (Metrich and Rutherford, 1992).

With the exception of a few studies on the solubility of fluorine in topaz rhyolite melts (Webster, 1990), little is known about factors affecting solubility in natural systems. In water-poor felsic melts temperature and composition are primary controls (Carroll and Webster, 1994). In water-saturated felsic melts, fluorine solubility increases with increasing peralkalinity. Metrich (1990) found a good correlation between F and both K_2O and P_2O_5 content of lavas from Mt. Etna. Because fluorine is incorporated into fluor-apatite, it has been suggested that apatite fractionation could remove fluorine preferentially over chlorine. The effects of pressure and water content have yet to be evaluated

Controls on the solubility of sulfur differ slightly from those of fluorine or chlorine. Fluorine and chlorine share some of the same controlling factors. Sulfur is the least soluble of these three after a threshold of fO_2 and pressure reached. Experimental studies show that fluorine is much more lithophile than chlorine and that exsolution of chlorine is strongly tied to that of water (Yoshida, 1990). Based on these considerations a generalization of the relative solubilities of S, F and Cl can be made:

$$\mathbf{F_{sol} > Cl_{sol} > S_{sol}}$$

This relationship is confirmed by numerous studies of natural systems. Ancient and historic lavas erupted from Mt. Etna appear to have lost little fluorine during eruption (Metrich, 1990). Homogeneous F but variable Cl content in erupted products at Izu-Oshima, Japan, have been explained by differential degassing after effusion (Yoshida et al., 1994). Measurements of volcanic gases from cooling lava flows at Piton de la Fournaise found sulfur-rich, chlorine-rich, and fluorine-rich gases with increasing distance from the vent (Toutain et

al., 1990). Other experimental data confirms that F is less volatile than Cl (Yoshida, 1990; Yoshida et al., 1994). High S/Cl ratios in high temperature fumaroles at White Island are thought to represent primary magmatic gases (Giggenbach, 1980). Increases in S/Cl corresponded to increases in eruptive activity at Central American volcanoes (Giggenbach, 1980). Malinconico (1979) observed increases in S/Cl and total SO2 output prior to increased eruptive activity at Mt. Etna. Studies of water soluble components of ash from Mt. Sakurajima showed increased molar HCl/SO2 one to one and a half months prior to increases in explosive frequency (Hirabayashi et al., 1982). Increases in F/Cl and decreases in In/Cl at Kilauea corresponded with older, more degassed magma (Miller et al., 1990).

A recent study of volatiles in melt inclusions (Dunbar et al., 1994) provides an estimate of S, F and Cl content of highly degassed Erebus magma. A comparison of elemental ratios from these melt inclusions with gas ratios confirms the relative efficiency of degassing for S, F and Cl (Table 4.4).

Table 4.4. Comparison of ranges in elemental ratios from melt inclusions of feldspar and pyroxene (Dunbar et al., 1994) and from volcanic gas measurements from 1986 - 1994. Gas data (1986 - 1991) from Zreda-Gostynska (1995). Gas data from 1992 - 94 this study.

	F/S	Cl/S	F/Cl
MI(1)	4.2 - 5.5	2.6 - 3.4	~ 1.6
Volc. Gas (2)	.32 - .69	.71 - 1.8	.36 -.57

The much lower ratios of F/S and Cl/S in evolved gas compared to melt inclusions is evidence for the relative efficiency of sulfur loss compared to fluorine and chlorine. A similar difference in the F/Cl ratios suggests that chlorine is lost more efficiently than fluorine.

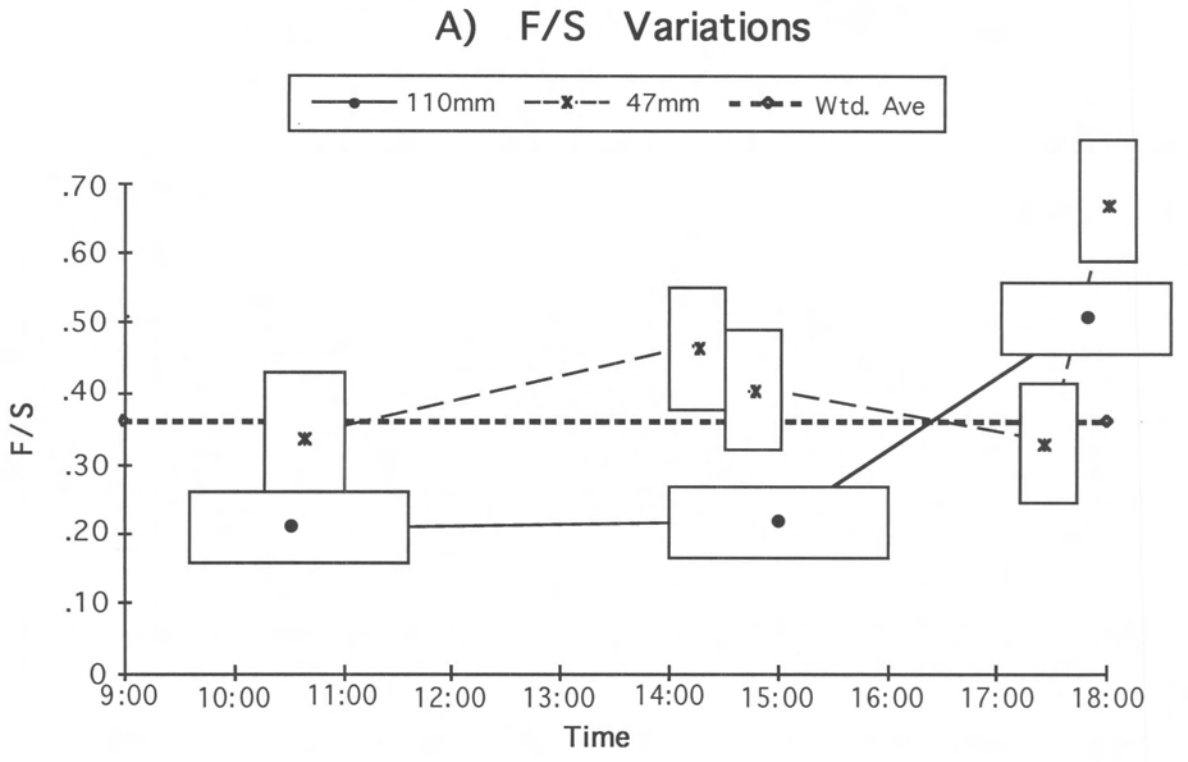
4.3. Short Term Variations.

A number of samples were used to study changes in gas composition over intervals of a few hours to a few days. The best short term data were collected on 11 Dec 1993. Over the course of the day, F/S ratios increased from ~ .2 - .7 and Cl/S ratios increased from ~ .3 - 1.15 (Figure 4.1). Although the data points represent 2-hour time periods for the large and 30-min. time periods for the small filters, an overall increases is seen in both filter sizes collected in the evening. These changes are outside those expected from analytical error. It is also interesting to note that these samples may document the beginning of a continued enrichment of F and Cl relative to S for the following day (the average data for filters collected on 12 Dec 1993 show higher Cl/S). The increase in both ratios suggests that the surface lava has undergone significant degassing.

A series of 3 - 47mm samples were collected over 30 minute intervals on 10 Dec 1994. A small Strombolian eruption occurred approximately halfway through the second sample. These data (Figure 4.2) are one of the only records of changes in gas composition over the course of an eruption at Erebus.

The sample interval prior to the eruption has relatively low F/S and Cl/S (.27 and .91 respectively). The sample interval covering the eruption records much higher F/S and Cl/S (.52 and 4.4 respectively). A decrease in F/Cl from .29 to .12 occurs between the pre-eruption sample and the sample covering the eruption. The sample following the eruption records a drop in Cl/S (1.4), consistently high F/S (.53) and an increase in F/Cl (.4).

Laboratory models of Strombolian eruptions demonstrate that an obstruction in the magma conduit is essential to eruption dynamics (Jaupart and Vergniolle, 1988; 1989; Tait et al., 1989). Bubbles rise and accumulate in a foam layer at the obstruction. Once a critical foam thickness is reached bubbles coalesce to form a gas pocket.



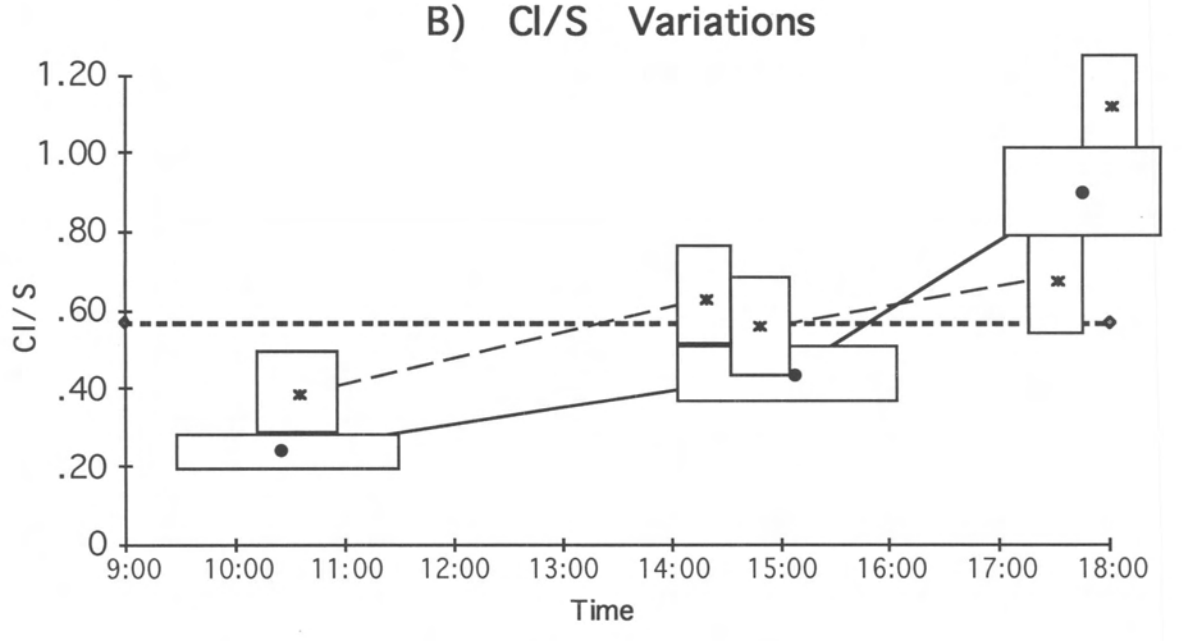


Figure 4.1. Variations in F/S (A) and Cl/S (B) over 11 Dec 93. Data points are plotted at the middle of the sample interval. Boxes define sample interval (horizontal distance) and an uncertainty of ± 25% (vertical distance). Increases in F/S and Cl/S occur later in the day for all filter sizes.

The size of the gas pocket and eruption dynamics are dependent on the viscosity and surface tension of the magma. In higher viscosity fluids smaller pockets form which erupt as intermittent gas "slugs" (Jaupart and Vergniolle, 1989). Large bubbles (~10's of meters in diameter) have been observed to breach the surface of the Erebus lava lake.

Changes in the elemental ratios during one of these events constrains the depth of the obstruction in the magma conduit based on three important considerations:

1) Overall chlorine emissions increase as evidenced by a 400% increase in Cl/S and 50% decrease in F/Cl, but return to "normal" rapidly.

2) Overall fluorine emissions increase relative to S during the eruption and continue to increase afterwards as evidenced by continued high F/S during and after eruption.

3) Late fluorine degassing is evidenced in the continued high F/S and higher F/Cl in the post-eruption sample.

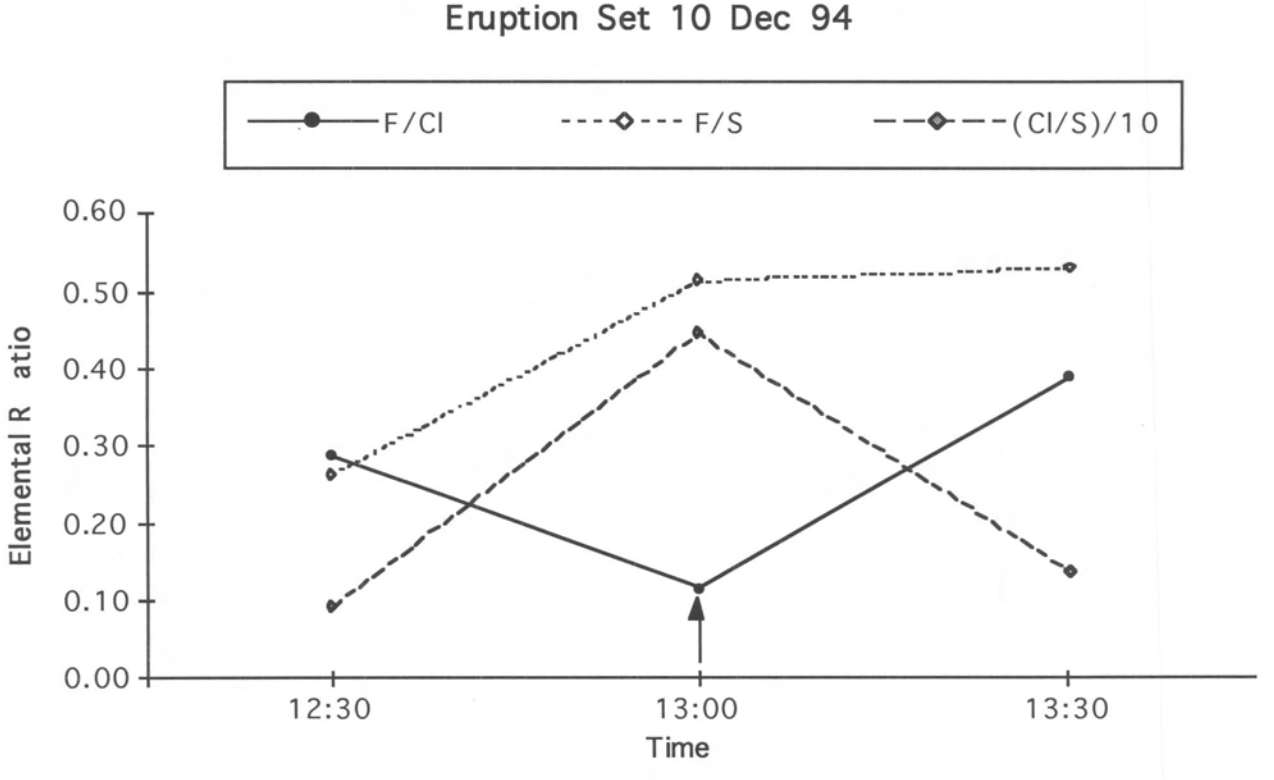


Figure 4.2. Variations in elemental ratios over the course of an eruptive cycle. Points are plotted at the middle of the sample interval. Strombolian eruption occurred at 12:58. Note that Cl/S is divided by 10 to fit scale.

The very high chlorine content of the eruption sample suggests the source gases for the eruption originated in a partially degassed magma. This is also consistent with the high levels of fluorine in the eruption interval. The continuous high fluorine following the eruption could result from surficial degassing of the lava lake due to stirring or overturn in the wake of the eruption. All the evidence is consistent with the eruption of a gas "slug" formed through bubble coalescence at a shallow obstruction in the magma conduit.

Jaupart and Vergniolle (1989) have shown that the time scale of "slug" formation is inversely proportional to gas flux and proportional to pocket volume. It would be useful in the future to determine if the frequency of bubble eruptions correlate with COSPEC measurements.

4.4. Daily Variations.

A daily value for elemental ratios was computed by averaging all samples collected that day. The best continuous data set with the largest number of samples was collected on 7 - 12 Dec. 1993 (Figure 4.3). Other somewhat continuous data sets were collected in 1992 and 1994.

Over the course of 7 - 12 Dec 1993 the average gas composition varied significantly (figure 4.3). The Cl/S ratio dropped over a two day period, remains relatively stable for two days, then began to climb again. The F/Cl ratio behaves in the opposite manner. Stable F/S and SO2 emission rates (Kyle et al., 1995) throughout the sampling period suggest that these changes are a result of changes in Cl flux with possible minor fluctuations in F flux. Initial decreases in Cl/S and increases in F/Cl may result from continued degassing of a batch of magma followed by recharge of a fresh material on the 11th or 12th or slow overturn in the magma conduit.

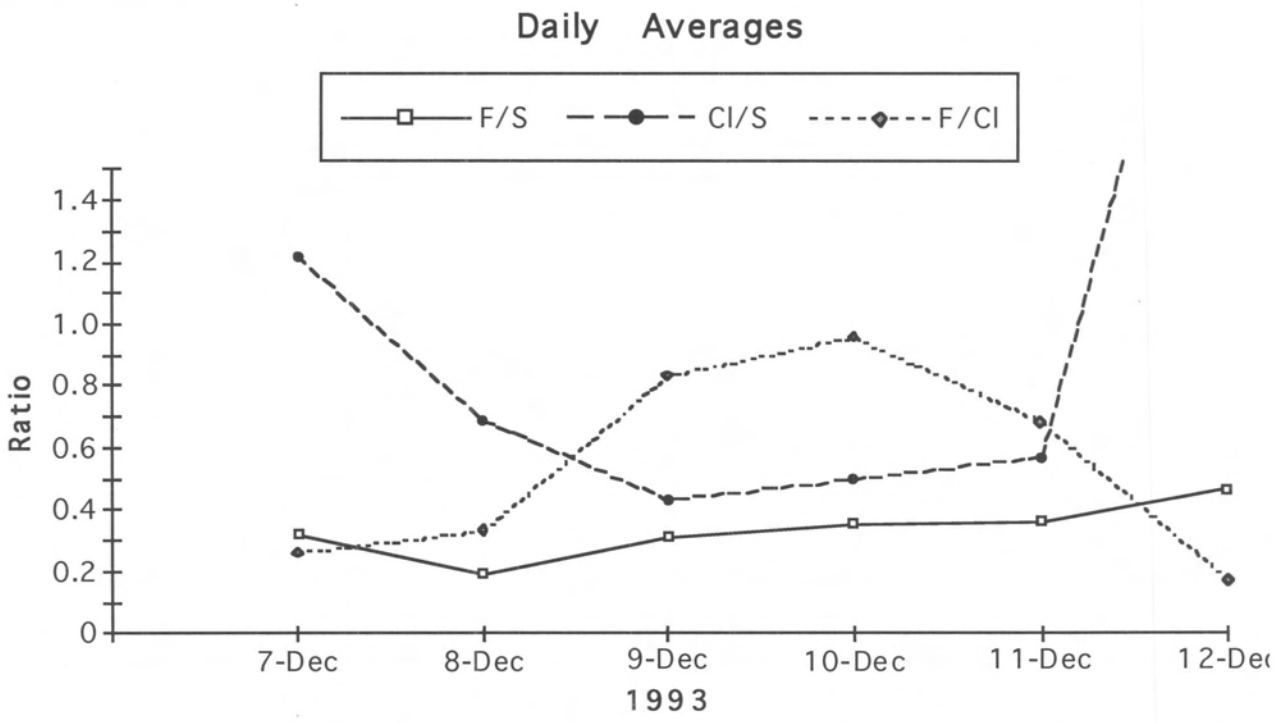


Figure 4.3. Daily averages calculated for F/S, Cl/S and F/Cl for 1993. Major changes occur for Cl/S and F/Cl while F/S remains relatively constant.

Gases collected over 12 - 19 Dec. 1992 display a different behavior (Figure 4.4). Continuous increases in Cl/S occur from the 12th through the 16th followed by a sharp decrease on the 18th. Variations in F/S and F/Cl fluctuate on a daily basis. On the 19th Cl/S begins to climb again. Increasing chlorine relative to sulfur could indicate continued degassing of a batch of magma, which begins as sulfur-rich and progresses to more chlorine-rich. In this case degassing does not proceed far enough for significant increases in the relative proportion of fluorine before fresh magma (low Cl/S on the 18th) reaches the surface.

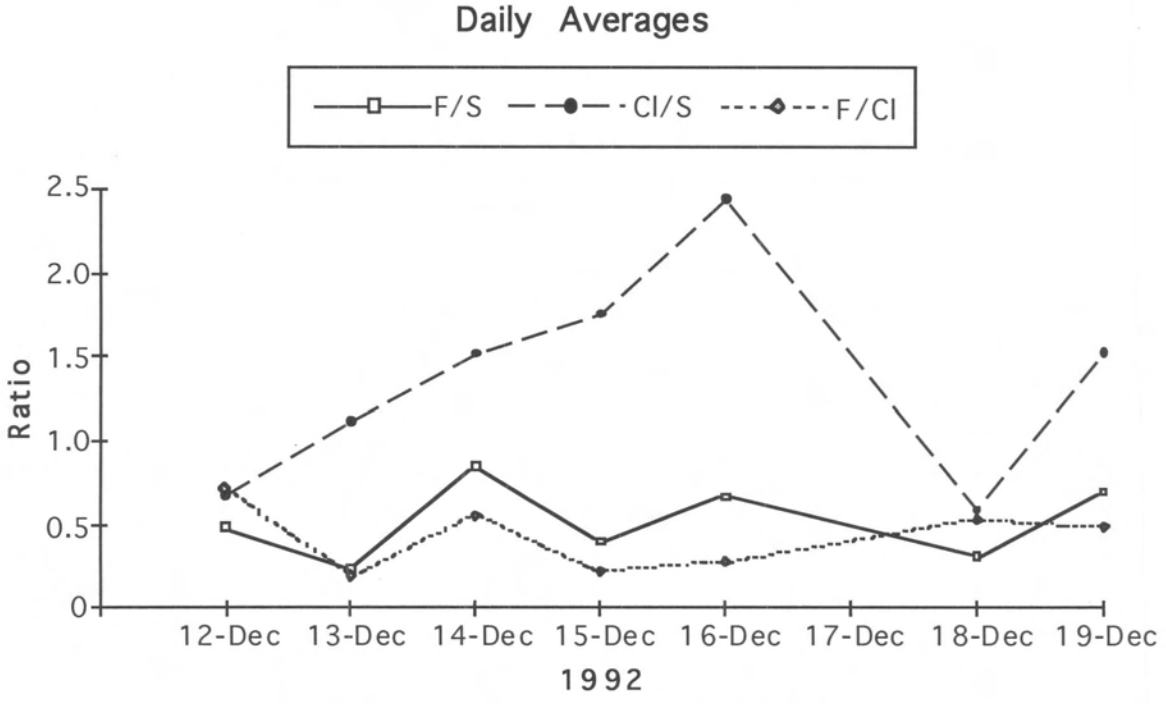


Figure 4.4. Daily averages for F/S, Cl/S and F/Cl for 12 - 19 Dec. 1992.

Variable F/S and F/Cl ratios could be due to small eruptions combined with sample bias. Only one sample was collected each day for the 12th through the 15th, three on the 16th and two on the 18th and 19th. Based on changes that occur on a much shorter time scale (Figures 4.1, 4.2) it is likely that the daily values based on a single sample may not be representative of the daily average gas composition. The relatively smooth trends documented for 1993 are based on a large number of samples, with at least 2 to 3 collected each day. I conclude that one

sample is insufficient to reflect the average daily composition unless it is collected over an 8 to 12 hour time period.

A total of seventeen samples were collected between the 6th and the 13th of Dec. 1994. Although no samples cover the 9th, 11th or 12th, some overall variations can be seen (Figure 4.5). Much like 1993, F/S ratios remain relatively constant while there appears to be a steady increase in Cl/S from the 8th through the 13th. This is consistent with continued degassing of a single batch of magma. There is no observable cyclic behavior of the 1994 data.

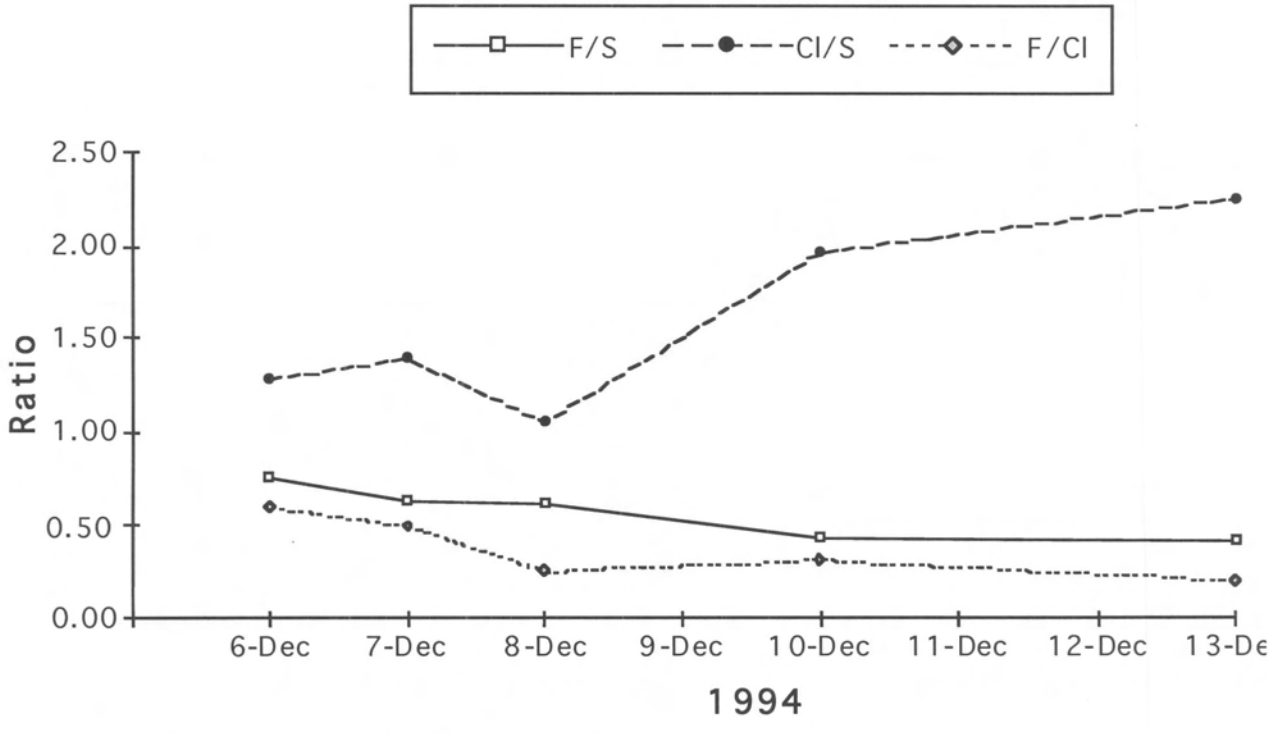


Figure 4.5. Daily averages from 1994 filters. Note relatively constant F/S ratio.

Daily average values for F/S, F/Cl and Cl/S for 1993 and 1992 suggest the possibility of a six to eight day "degassing cycle". Each cycle begins with a somewhat fresh batch of magma which evolves a sulfur-rich gas. As time progresses the gas evolved becomes more chlorine-rich (1992 data). If degassing proceeds far enough, the gas evolves a more fluorine-rich component (1993 data). The degassing cycle is terminated with injection of fresher material or large-scale overturn in the magma column.

Superimposed on this cyclic behavior are short term fluctuations due to explosive eruption of large bubbles at the surface of the lava lake. These bubbles form by coalescence of gas at a shallow obstruction in the magma conduit. It is possible that the timing of eruptive cycles stirs the magma column causing overturn. This would account for the six to eight day cyclic degassing behavior observed in the 1992 and 1993 data.

In all of the data sets the F/S ratio remains constant. Major changes in gas composition are reflected by large variations in Cl/S. Short term fluctuations result primarily from occasional Strombolian eruptions. Variations over a longer time scale (~ 6 - 8 days) could represent overturn of the magma column.

4.5. Long Term Variations.

Annual to bi-annual variations in average gas composition from Mt. Erebus were first proposed by Zreda-Gostynska et al. (1993). Based on relative proportions of sulfur, fluorine and chlorine two populations (1986/1989 and 1988/1990-1) of statistically different gas composition were suggested. In order to determine statistical similarity of all data, t-tests were performed on elemental ratios for all data. Three populations were determined (figure 4.6):

1) 1986/1989

2) 1989/1992/1994

3) 1988/1990-1/1993

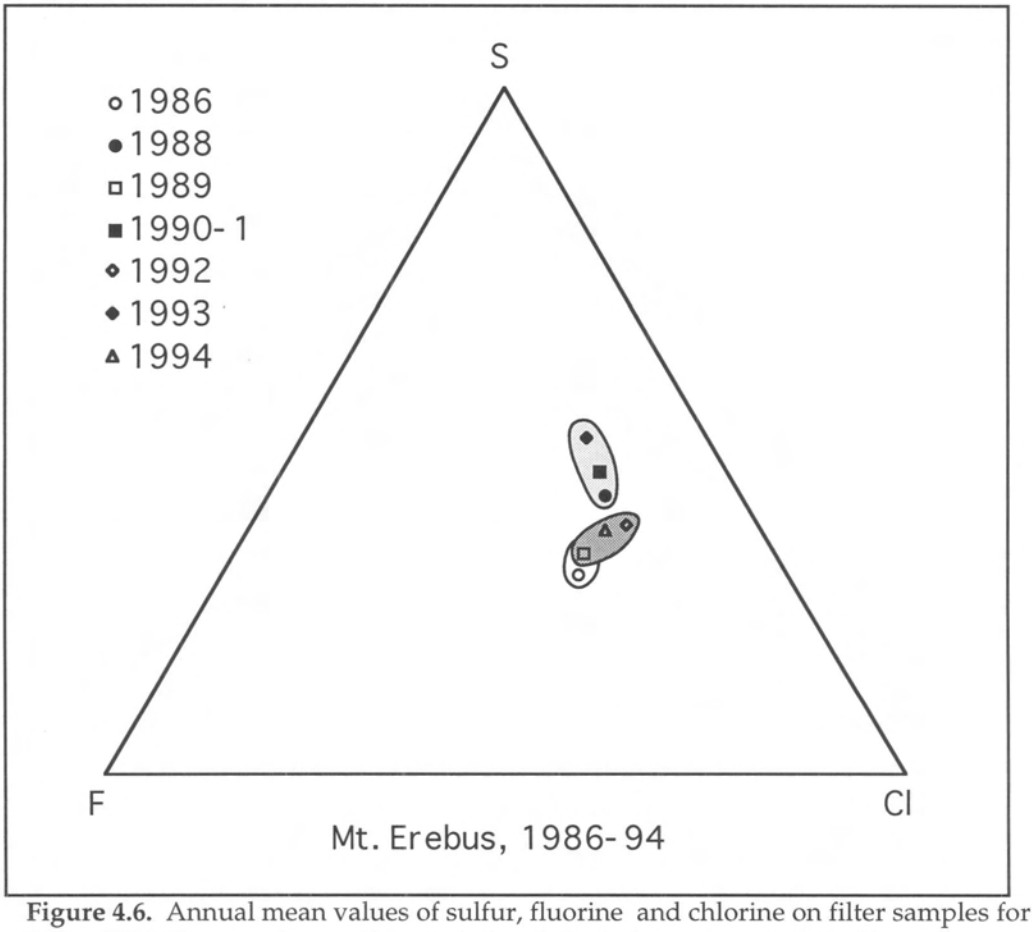


Figure 4.6. Annual mean values of sulfur, fluorine and chlorine on filter samples for 1986 - 1994. Mean values within circled and shaded areas are statistically indistinguishable from one another. Each circled region represents a population that is statistically different from others. Unshaded - population 1, dark shading - population 2, light shading - population 3.

Although the mean for 1986 is indistinguishable from 1989, it is statistically different from all other years. From 1986 to the present there is a trend which alternates between a more fluorine/chlorine-rich and a more sulfur-rich average composition. The time required to return to a given population after each "cycle" varies between two and three years. It is possible that the more sulfur-rich years (population 3) document the appearance of fresh magma at depth while more chlorine-rich years (populations 1 & 2) record time periods between recharge.

Superimposed on this see-saw behavior is an overall shift towards a more sulfur-rich gas composition. There are two ways to interpret these trends. The first is that there has been a significant recharge of magma at great depth over the last ten years which reaches the surface in two to three year pulses. The alternative is that these changes occur over a much shorter time scale. Because the field season on Erebus is so short, sample collection typically occurs over a two to three week period and at best a month. In this case it may be that the "yearly average" fortuitously coincides with large scale convection of the magma chamber that operates on the order of a month or more. In any event, the gas composition of Mt. Erebus has remained remarkably consistent over the past ten years, suggesting a large stable magma body at depth.

4.6. Estimation of Pre-eruptive Volatile Content.

Pre-eruptive volatile content in magma can usually be estimated from studies of volatile content of melt inclusions (Anderson et al., 1989). Microprobe studies of feldspar and pyroxene from Mt. Erebus indicate that melt inclusions were trapped from an already degassed melt (Dunbar et al., 1994). In order to obtain preliminary constraints on initial volatile content of Erebus magma several relationships between volatile and major elements will be extrapolated to encompass available data and combined with simple mass balance calculations.

Saturated vs. Unsaturated

A primary consideration in constraining initial volatile content is whether or not the magma is saturated with respect to a volatile species. Several relationships such as Cl/K_2O and S/FeO (Figure 4.7) ratios in natural systems combined with experimental data are useful in this respect.

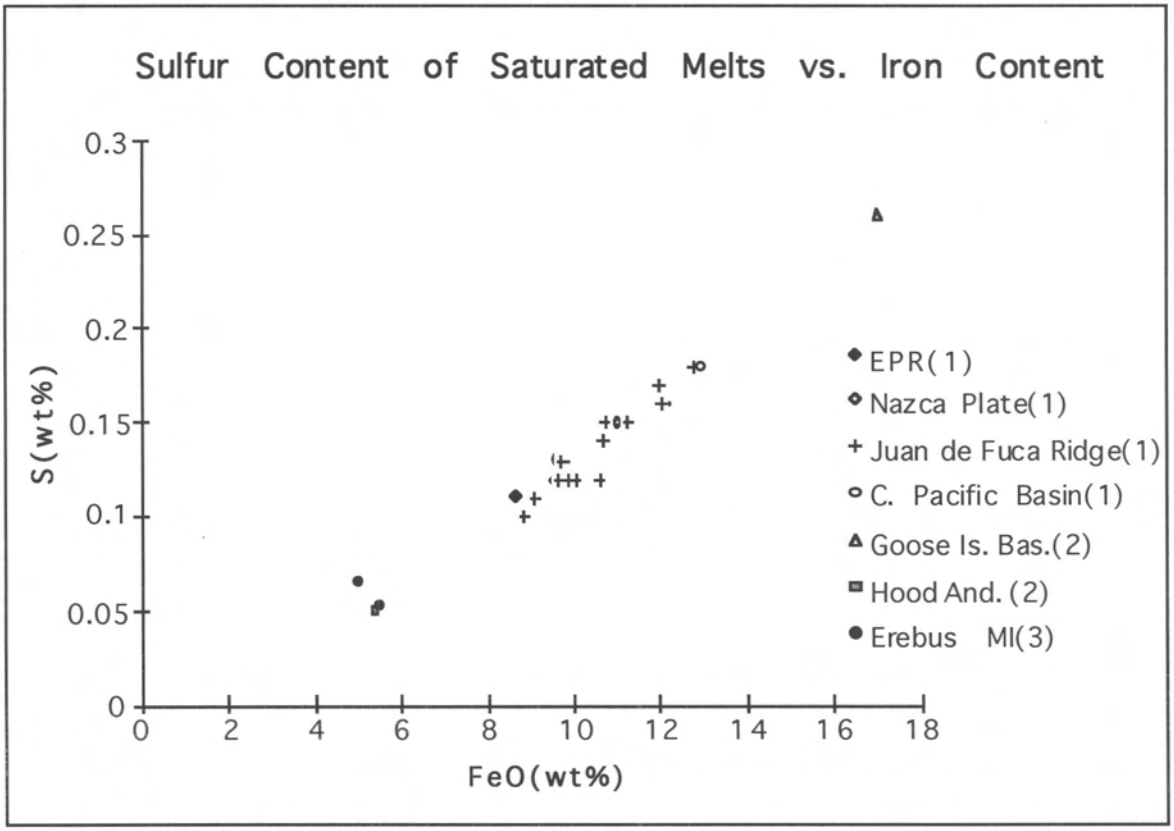


Figure 4.7. Comparison of Erebus melt inclusion sulfur and iron with values from other sulfur-saturated volcanic rocks. (1) from Mathez (1976), (2) from Wendlandt (1982) and (3) from Dunbar et al. (1994).

Magmas saturated with reduced sulfur show a good correlation with iron content (for FeO 5-20%). Erebus melt inclusion sulfur and iron data are comparable to values measured in other saturated rocks (figure 3.8). This implies that Erebus melt inclusions are saturated with respect to sulfur. The presence of pyrhotite in erupted products (Kyle et al., 1992) confirms that Erebus magma is saturated with sulfur as H_2S.

Experimental data combined with observations in natural systems constrains whether or not chlorine is saturated in Erebus magmas. Anderson (1974) found a good correlation between Cl and K_2O content in basalts from Kilauea and Hat Creek, California. He found a consistent Cl/K_20 ratio of .023 to .026 for a range of potassium and chlorine contents. Experimental results on chlorine solubility in phonolite (Metrich and Rutherford, 1992) yields a Cl/K_2O of .066 at 1 kbar. Using a Cl/K_2O of .066 and the K_2O content of Erebus phonolite (4.3 - 4.7 wt. % - Kyle et al., 1992) the estimated content of chlorine in Erebus magma is .28 - .31 wt. % at 1 kbar. This is in contrast to a range of .17 to .18 wt. % Cl and a Cl/K_2O of .03 to .033 for mineral inclusions (Dunbar et al., 1994).

Another constraint on chlorine solubility can be imposed by experimental and theoretical solubilities of H_2O. In the phonolitic Laacher See tephra Cl/H_20 ratios are constant throughout the magma column with a maximum Cl content of .3 wt % (Worner and Schminke, 1984). This is very close to the solubility limit estimated for Erebus magma above. By assuming a constant Cl/H_2O for Erebus and that the melt inclusions (Cl/H_2O = .8 - 1.8) are saturated with water, we can use the experimental estimate of H_2O solubility (Dunbar et al., 1994) of 3.5% at 1 kbar to obtain a range for chlorine solubility (2.8 to 6.3 wt. % at 1 kbar). The upper limit is close to the experimentally determined value for phonolites (~6.27 wt. % Cl) from Metrich and Rutherford (1992). These experimental results combined with the inverse relationship of pressure and chlorine solubility in water-saturated melts implies that Erebus melt inclusions are under saturated with respect to chlorine, probably as a result of H_2O degassing.

There is little to no evidence to constrain whether or not fluorine is saturated in the melt. Based on the relatively "lithophile" nature of fluorine, it is likely that it is not saturated in Erebus lava.

A Preliminary Model

By making certain assumptions it is possible to place first order constraints on the initial volatile content of Erebus magma estimate the time scale required for magma resupply and degassing. I assume a perfect cylinder of magma defined by the following parameters. A diameter of 50 m is assumed based on observations of the maximum lava lake size over the past 15 years. A column height of 75 m is used based on two considerations: 1) observations that few vesicles are observed in MORB's that form at depths > 200 m and calculating the equivalent pressure depth of phonolite ($\rho = 2.6$) and 2) seismic velocity models of the maximum depth of vesiculation in the Erebus magma column (Dibble et al., 1994). This cylinder is equivalent to a mass of 3.828×10^8 kg of phonolite. The volatile content in wt. % in melt inclusions is assumed to represent a thoroughly degassed melt. The degassed magma column would then contain a residual 230 Mg of S, 690 Mg of Cl, and 1147 Mg of F. The average flux of SO_2 for 1986 - 1994 is used to calculate an average flux of S, F and Cl (2 Mg/hr., 1 Mg/hr., and 3 Mg/ hr. respectively). If steady state degassing of a closed system is also assumed, then the following mass balance relationships apply:

$$S_i = S_r + (S_{flux} \times t)$$

$$Cl_i = Cl_r + (Cl_{flux} \times t)$$

$$F_i = F_r + (F_{flux} \times t)$$

Where "i" subscript represents initial volatile content (g), "r" subscript represents remaining volatile content from mineral inclusion data (g), "flux" subscript represents emission rates of volatiles (Mg/hour) and t represents time (hours). This leaves three equations and four unknowns. In order to start the model an initial Cl content of .3 wt. % is assumed based on maximum content measured in Laacher See tephra (Worner and Schminke, 1984). This value is also in agreement with the predicted values using the Cl/K_20 method above. This results in a time scale for degassing of ~ 153 hr.s or 6 - 7 days for a column of magma this size. Based on

daily variations in elemental ratios for 1992 - 1994 this appears to be a reasonable estimate. Back calculation of mass flux results in initial concentrations of .14 wt. % S and .34 wt. % F.

This model can be applied one step further. An estimated 4080 km^3 of basanite is the parental magma of the current Erebus edifice. This translates into ~ 1.06×10^{19}g of basanite. By using FeO content of a typical Erebus basanite (11 - 12 wt. % - Kyle et al., 1992) and the previously mentioned correlation of S and FeO a sulfur content of .14 wt. % is estimated. This is equivalent to 1.5×10^{10} Mg S. A loss of .08 wt% S through degassing (the difference between initial and residual S concentrations from the above model) results in a loss of 8.6×10^9 Mg of sulfur. Assuming steady state degassing of SO_2 using average values from 1986 - 1994 this loss would occur on a time scale of ~ 850 Ka. This is not much shorter than the age of basanite rocks thought to represent the onset of the Erebus Lineage.

5. Plume Dispersion Models.

5.1. Introduction.

Mt. Erebus is the only active volcano in Antarctica and the sole source of certain trace metals in the local atmosphere (Meeker et al., 1991). Antarctica is located far from large industrialized areas or other volcanic sources of trace elements found in the atmosphere. The result is a very clean background which provides a unique laboratory to evaluate the volcanic contribution of specific compounds to the atmosphere.

Based on previous measurements of gas emissions, Mt. Erebus is considered an important source of sulfur, halogens, and trace metal compounds in the Antarctic atmosphere, at least locally (Meeker et al., 1991). Elemental gold particles unique to the Erebus plume have been collected at an altitude of 8 km, which coincides with the altitude of the tropopause for most of the 1993-4 and 1994-5 summers. This raises certain questions about possible dispersion to and mixing with the stratosphere of gases from Mt. Erebus. Emission rates combined with meteorological data and empirical dispersion equations can constrain the contribution of Erebus gases to the Antarctic atmosphere. Particular emphasis is placed on the South Polar region to quantify the maximum possible contribution of certain compounds which may affect ozone.

Zreda-Gostynska (1995) estimated potential contributions of S, F and Cl to South Pole snow by assuming complete mixing of steady state emissions from Erebus throughout an estimated volume of atmosphere for one year. Although these estimates agree with the amount of excess chlorine in South Pole snow determined by Delmas et al. (1982), certain considerations are overlooked. During the winter months when the polar vortex isolates the Antarctic atmosphere the assumption of complete mixing may approximate true conditions. Summer wind and weather patterns display significant seasonal and annual variability. This can prevent emissions from reaching the continental interior, lead to heterogeneous distribution, or loss to mixing with air from higher latitudes. In order to evaluate either case, a model that incorporates wind trajectories for the time period in question would be necessary. This is beyond the scope of this project.

A much more simplified approach is to use available air pollution models to evaluate potential contributions for a specific time period. The Gaussian Plume model is the most common air pollution model approved by the EPA. It is typically used to evaluate the downwind concentration of contaminants generated by a point source over a period of time from 10 minutes to an hour. Long-term average concentrations have also been made (Runca et al., 1976). The standard form of the equation taken from Zanetti (1990) is:

$$C = \frac{Q}{2\pi\sigma_y\sigma_z\bar{u}} \exp\left[-\frac{1}{2}\left(\frac{y}{\sigma_y}\right)^2\right] \exp\left[-\frac{1}{2}\left(\frac{H-z}{\sigma_z}\right)^2\right]$$

Where C is the downwind concentration, Q is the emission rate (ug/s), u is the average horizontal wind speed(m/s), y is the horizontal distance from the receptor to the plume centerline(m), z is the vertical distance from the receptor to the plume centerline(m), H is the effective stack height(m), and σ_y and σ_z are the standard deviations of the horizontal and vertical plume concentration spatial distribution.

Mount Erebus is essentially a very large point source for SO_2, Cl, F and trace metals. A simple Gaussian model may be used as an initial estimation of Mt. Erebus contributions to pollutant transport to the South Pole. Application of the Gaussian plume model to this problem is based on the following assumptions. The average emission rate (Q) for each year is assumed constant and is used for all model calculations. The effective stack height (H) is assumed to equal the summit elevation of Erebus (3784m). Observational data suggests the plume often rises several hundreds of meters above the summit, but compared to the elevation of Erebus this is considered insignificant. These are probably the most reasonable assumptions.

In order to assess the potential contribution of Erebus gases to South Pole, several basic assumptions must be stretched beyond their intended limits. Typical model concentrations are averaged over several minutes to hours. A time correction factor of $C^* = C(10/t)^{.5}$ was used to

compute a five hour average concentration for Erebus SO_2. One problem with this approach is that travel time to the pole (5 m/s) is probably at least three days, so the 5 hour average is only meaningful by assuming the winds carrying the plume maintain constant velocity and direction for at least three days. Given the downwind distances modeled and Antarctic weather patterns this is very unreasonable. However, this model is still useful in providing a constraint on maximum potential contributions.

Radiosonde data provided detailed temperature, wind direction and velocity profiles from sea level up to 60,000 ft. Wind direction and speed were determined for the altitude of the Erebus plume. Estimates of σ_y and σ_z are determined empirically based on Pasquill stability class and downwind distance to the receptor. Each model time period is given a Pasquill stability classification based on the vertical temperature profile. Based on stability class and downwind distance, σ_y and σ_z were calculated using Brigg's rural dispersion parameter equations taken from Zannetti (1990). Dispersion parameters are typically considered valid for distances of a few hundred meters up to 10,000 meters. Extrapolation of these parameters over distances from Erebus to South Pole (~1400 km) is outside the accepted range by approximately an order of magnitude.

Clearly the modeling of gas dispersion from Erebus to South Pole is much more complicated than this model is capable of dealing with. However, under the ideal conditions assumed above it can provide an estimate of the extreme upper limit of potential input.

A second approach is to use a Gaussian plume sector model for a continuous point source to evaluate the seasonal dispersion of S, F and Cl from Erebus. Sector models provide a means of examining the seasonal dispersion of the Erebus plume and allows for comparison between different years. It also provides estimates of concentrations at ground level around the volcano and on the mainland that could be tested through future analysis of seasonal snow samples at certain model locations. The form of the equation, taken from Hanna et al. (1982), has been modified from the previous model to account for long term time averaging and horizontal dispersion within a sector:

$$C = \left[\frac{2}{\pi}\right]^{.5} \left[\frac{fQn}{2\pi\sigma_z x u}\right] \exp\left[-\frac{1}{2}\frac{h^2}{\sigma_z^2}\right]$$

This sector model is based on seasonal wind data which has been compiled into wind roses for 1993-4 and 1994-5. Wind data for the five month summer (October through February) was divided up into increments of 30° or 10° to evaluate local and regional dispersion patterns and concentrations over the summer. In this case, u represents the average wind velocity for all measurements in that sector, n is the number of sectors (12 or 36), f is the fraction of time the wind blows in the direction of that sector determined from the wind roses, h (m) is the distance from the receptor to the plume centerline, and Q, x, and σ_Z are the same as in the initial plume model. Therefore, C represents the average downwind sector concentration for the months of October through February.

In order to evaluate the annual variations in concentration and dispersion patterns of the Erebus plume in the surrounding area, a model for each site representing the midpoint of each 30° sector was computed for centerline and ground level elevations at points corresponding roughly to the 1000 and 2000 meter contour intervals around Mt. Erebus. This simplified the calculations by normalizing the distance from the receptor to the plume centerline for all model locations (for centerline models h=0). The model calculations for the 1000 meter interval correspond roughly to a 10km downwind distance (x), which is the upper limit for empirical calculations of σ_Z.

Additional models are computed for 10° sectors for sites up to 120km away on Black Island and the mainland. In this case the parameter σ_Z was extrapolated to distances greater than 10,000 meters, which makes these model predictions less reliable than the 30° sector models. Distant receptor sites were chosen based on elevation, proximity to the coast, and elevation control to provide h values as accurately as possible and to minimize any terrain effects that would be generated due to reflection or sedimentation. An air quality monitoring

station is located on Black Island which could provide a test of modeled SO2 contributions. Unfortunately, McMurdo station is much closer and the signal of SO2 resultant from burning of fossil fuel most likely overwhelms any input from Erebus. In the future short term average concentrations could be modeled in conjunction with simultaneous atmospheric samples to test this model.

5.2. Model Results.

30° Sector Models - Local Sites

Plume sector modeling analysis for localized dispersion of Erebus gases showed widely different results for 1993 and 1994. The five month plume centerline seasonal average concentrations computed for each thirty degree sector were plotted and contours were manually drawn to describe dispersion patterns and concentration gradients (Figures 5.1, 5.2, 5.3). It is clear from the graphic representations of model results that the dispersion patterns and concentration gradients are strongly dependent on emission rate and wind direction. This raises the question over how stable respective annual wind patterns are in this area. A comparison of wind rose diagrams for each month as well as both seasons reveals that wind patterns can vary significantly from month to month (Figures 5.4, 5.5) as well as year to year (Figures 5.6, 5.7). In order to obtain a model prediction of long term average concentration a much larger database of emission rates and wind patterns is required.

Ground level model values were found to be much less than a few ng's/m^3 for S, F and Cl (Tables D.3.1, D.3.2). The slope of the volcano is at a high enough angle so that no significant plume touchdown is expected based on model dispersion parameters. In other words, the typical atmospheric stability of McMurdo Sound (Pasquill stability class D or E - corresponding to slightly stable and stable categories) is such that the dispersion of the plume has a narrow, funnel-shaped vertical cross section. Poor vertical "fanning" may allow significant concentrations of S, F and Cl to penetrate into the interior of the continent. These model predictions are in contrast to snow data collected by Palais et al. (1994) which shows that significant local deposition occurs. One of the limitations of this model is that observed

fumigation conditions (where the plume flows down along the ground level) should not occur. Fumigation enhances the possibility of both wet and dry sedimentation at the snow surface. More complicated Gaussian-based models would have to be used to accurately simulate these conditions.

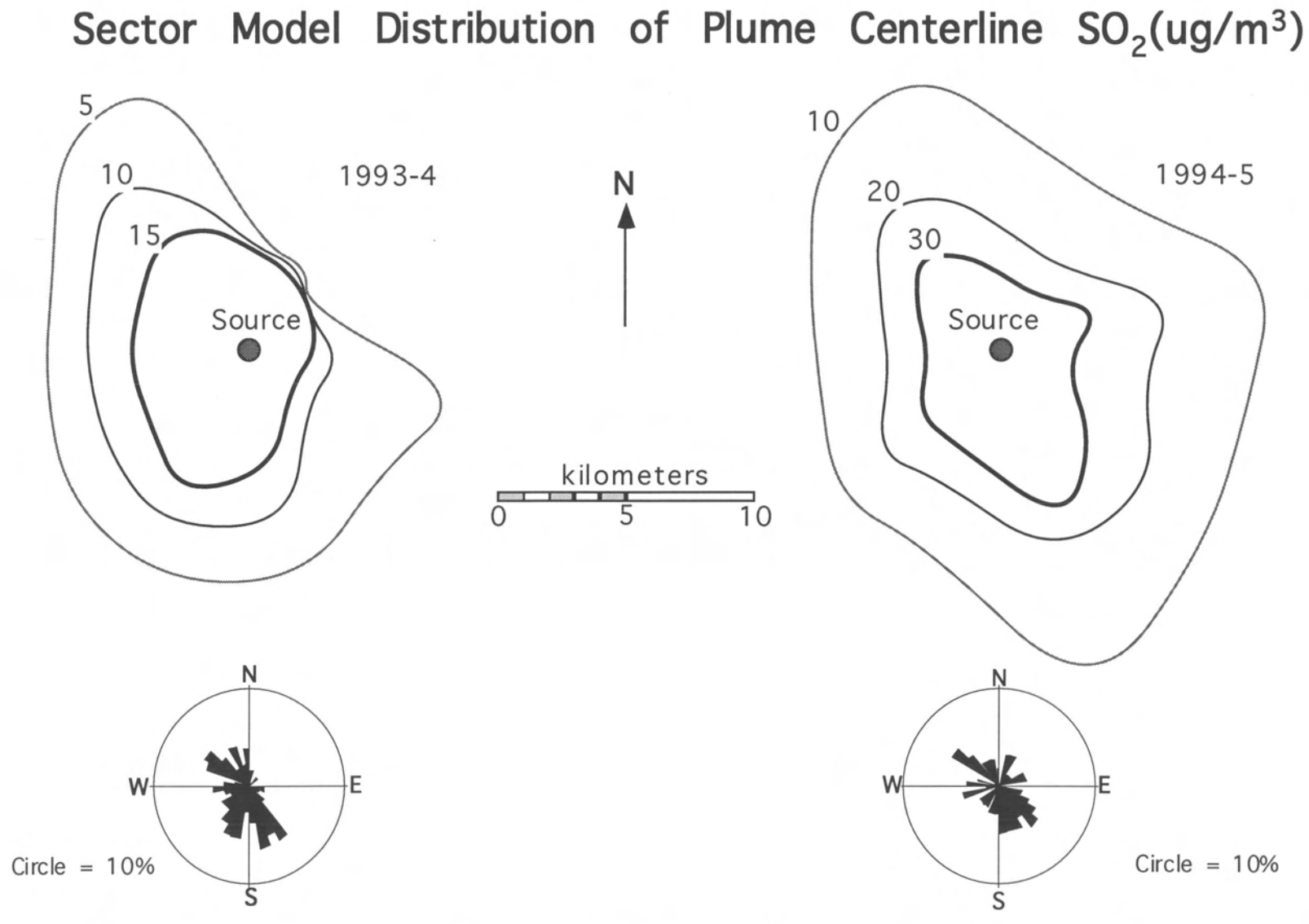


Figure 5.1. Seasonal average plume centerline SO_2 for 1993 and 1994. Wind rose data provided for comparison. Higher values during 1994 primarily due to higher emission rates.

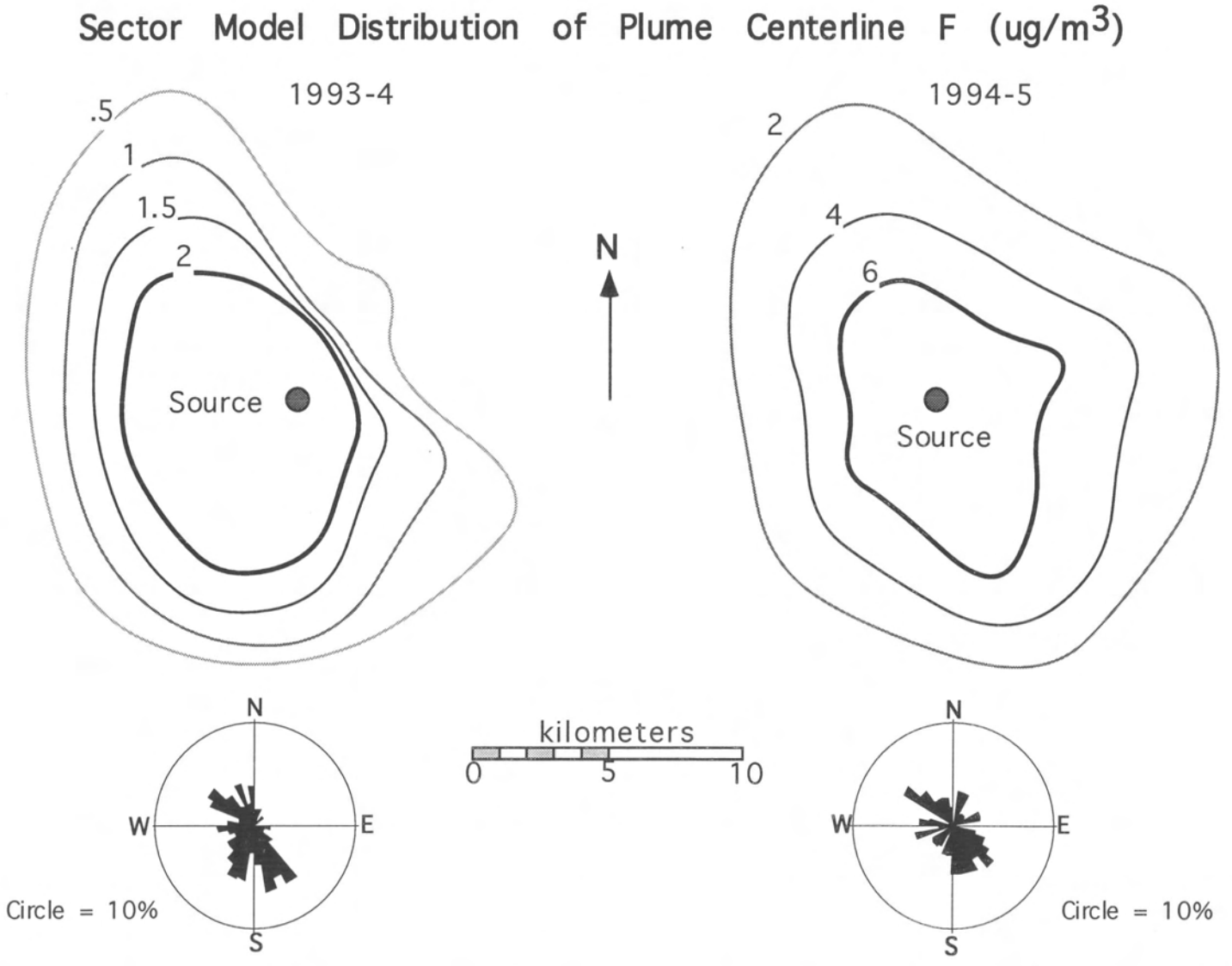


Figure 5.2. Seasonal average plume centerline F for 1993 and 1994. Wind rose data provided for comparison. Higher values during 1994 primarily due to higher emission rates.

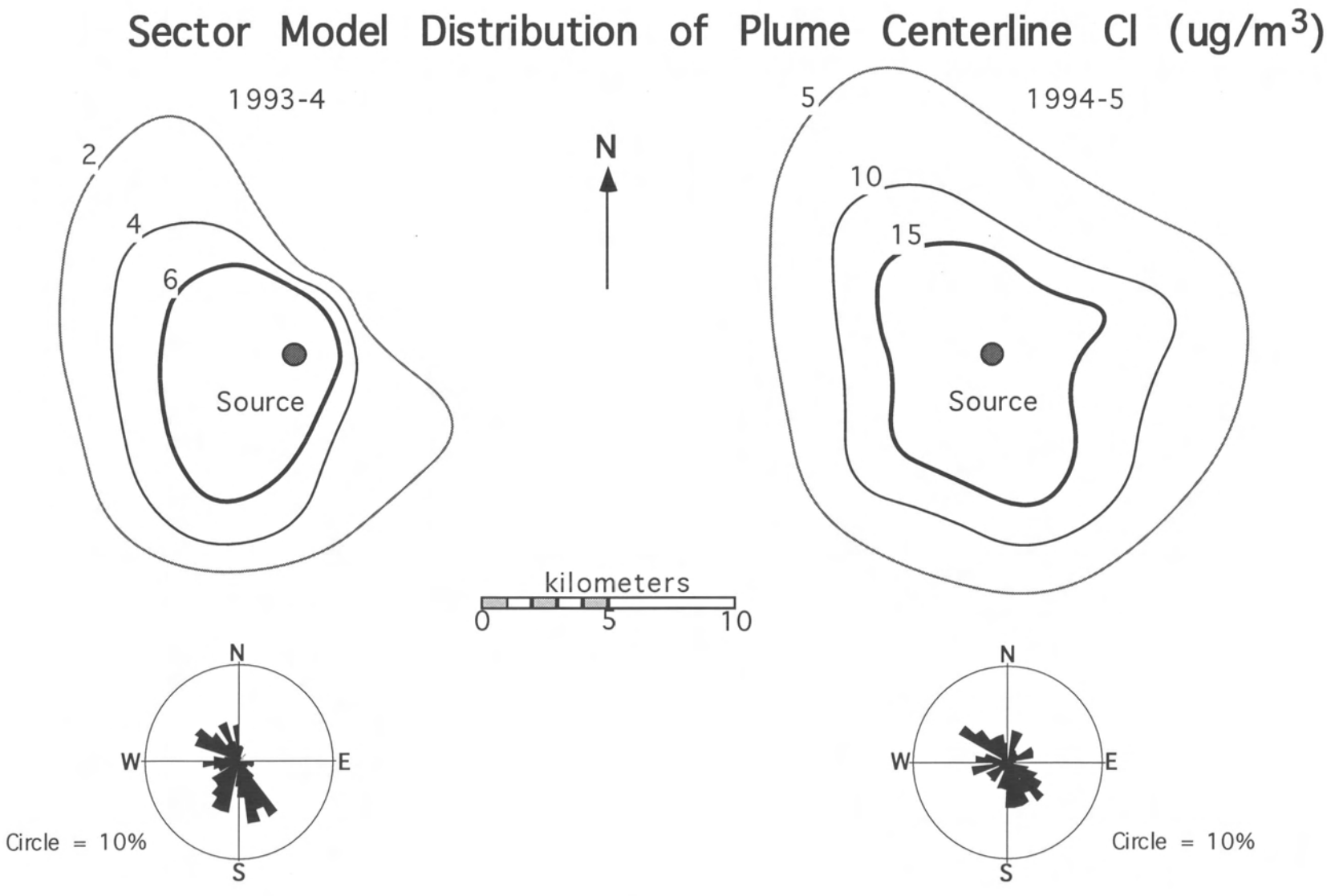


Figure 5.3. Seasonal average plume centerline Cl for 1993 and 1994. Wind rose data provided for comparison. Higher values during 1994 primarily due to higher emission rates.

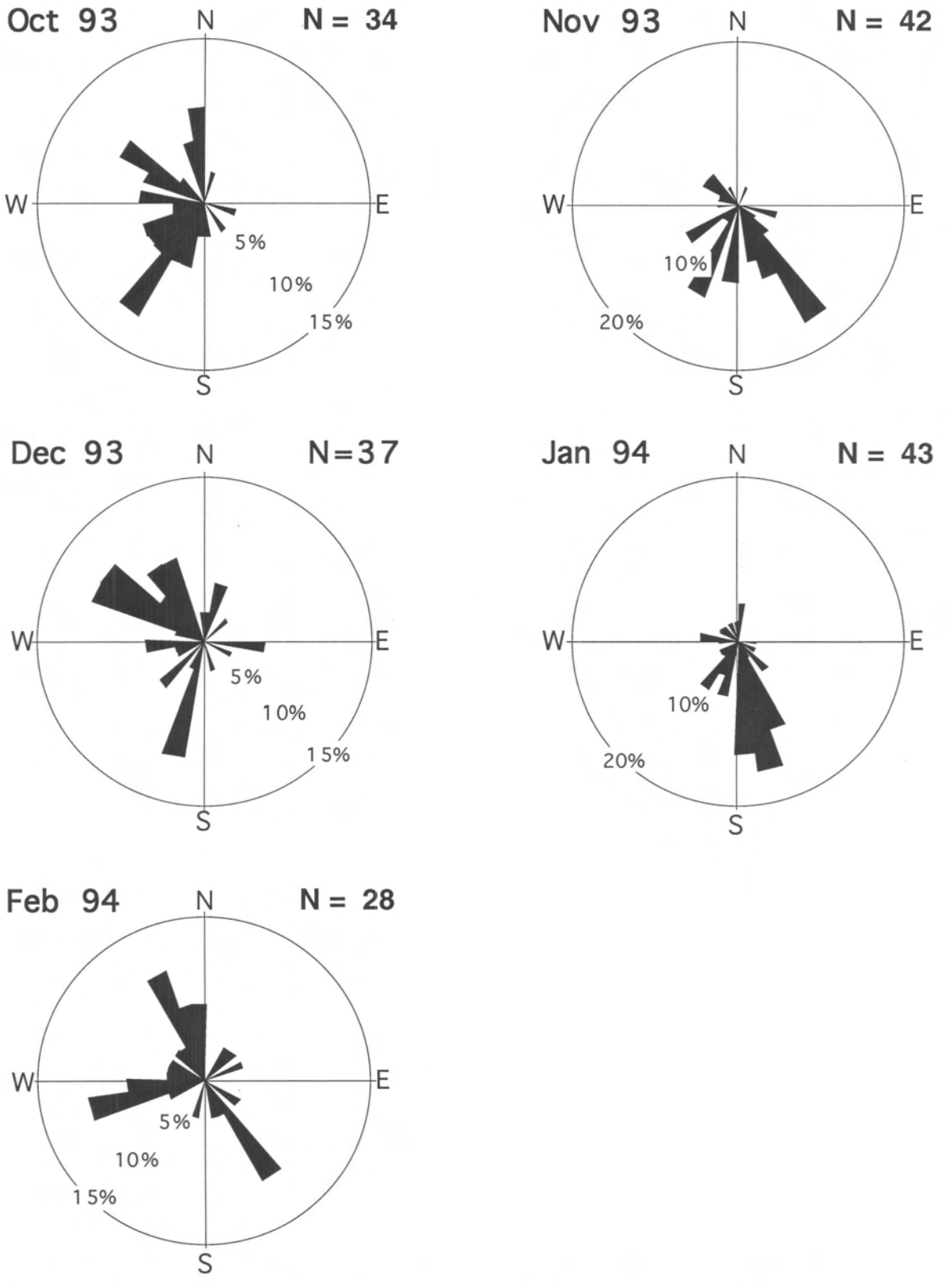


Figure 5.4. Monthly wind rose diagrams corresponding to the elevation of the Erebus plume for McMurdo Sound, Austral Summer, 1993-4.

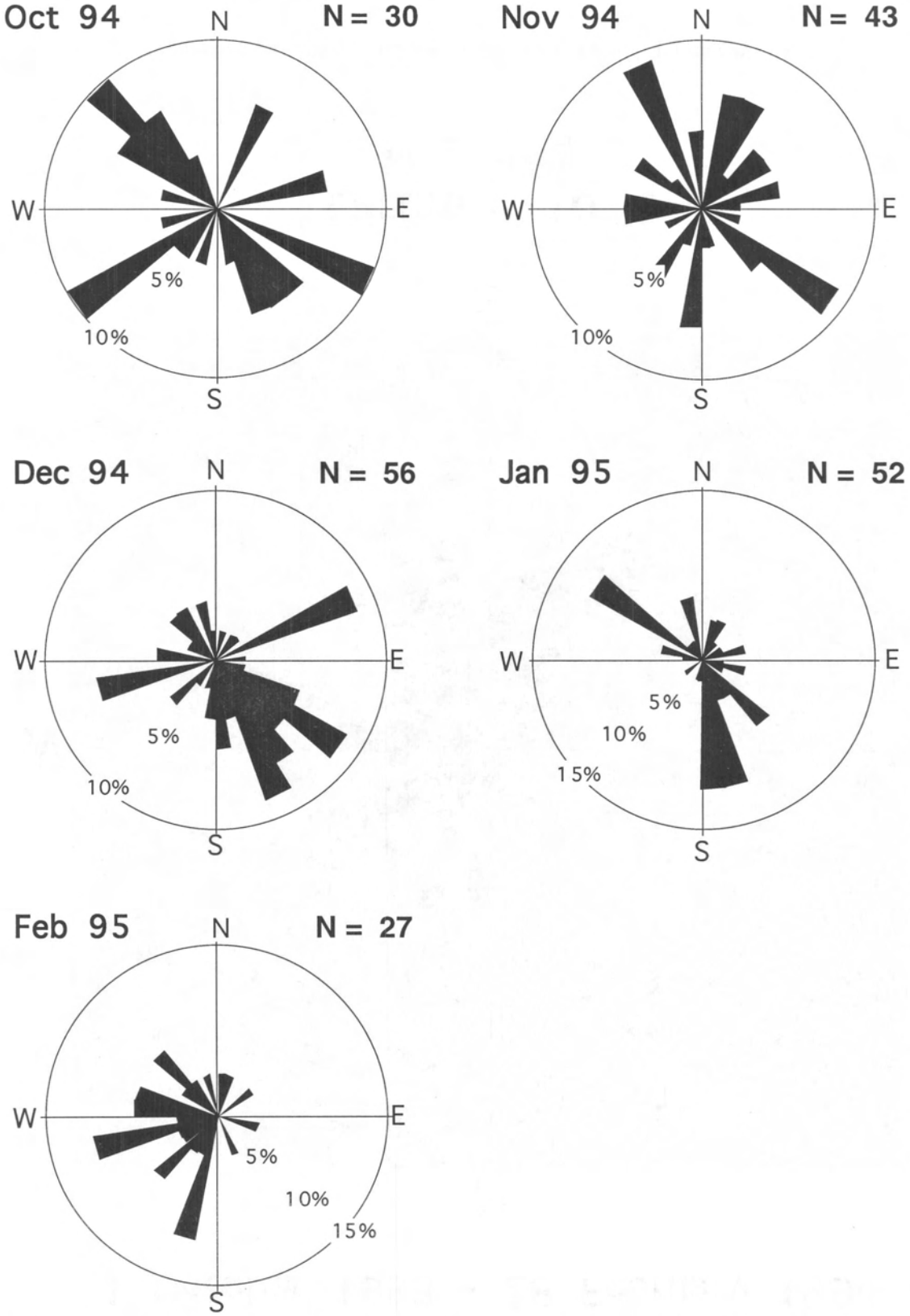


Figure 5.5. Monthly wind rose diagrams corresponding to the elevation of the Erebus plume for McMurdo Sound, Austral Summer, 1994-5.

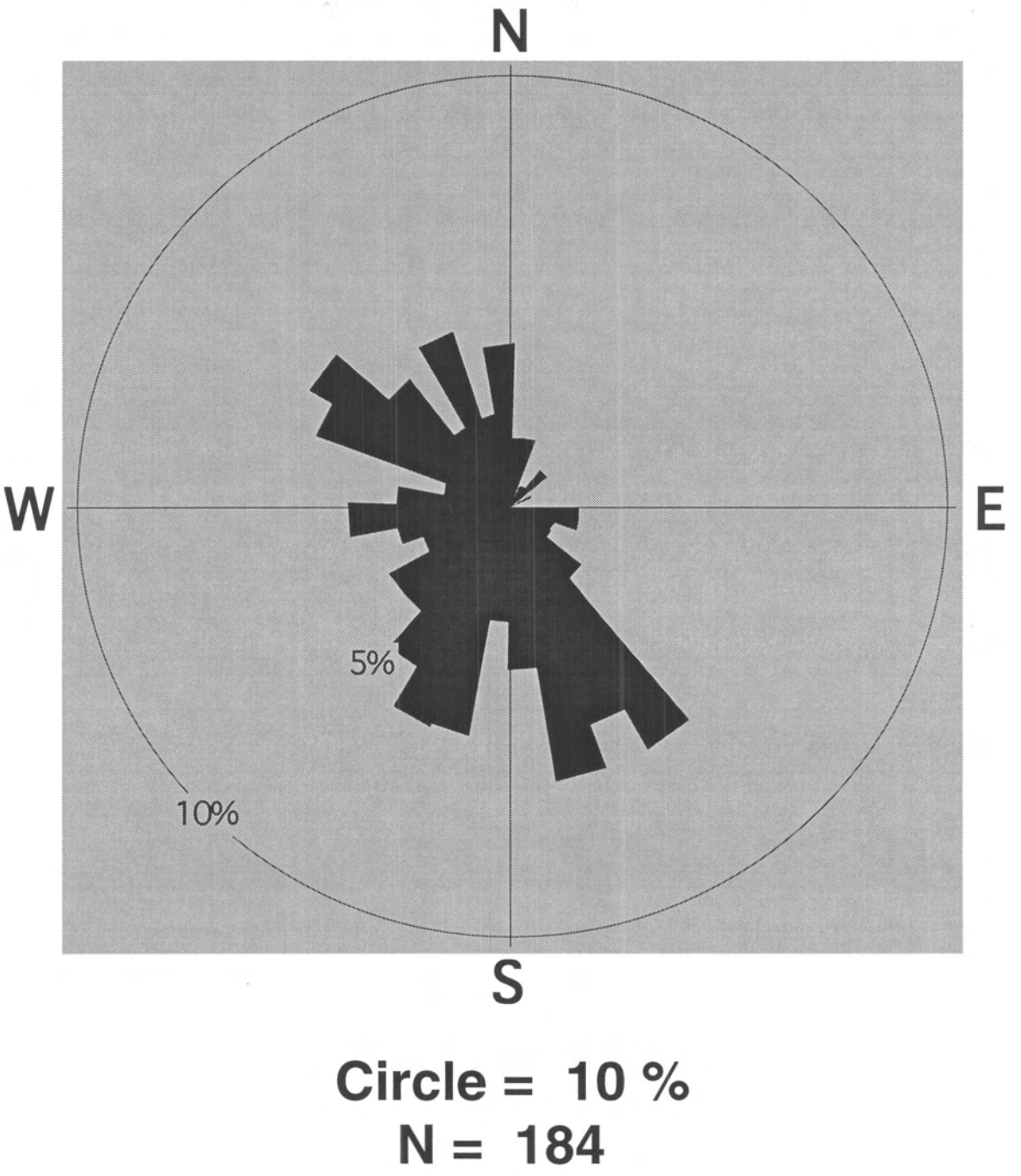


Figure 5.6. Summary wind rose diagram for Austral summer 1993-4.

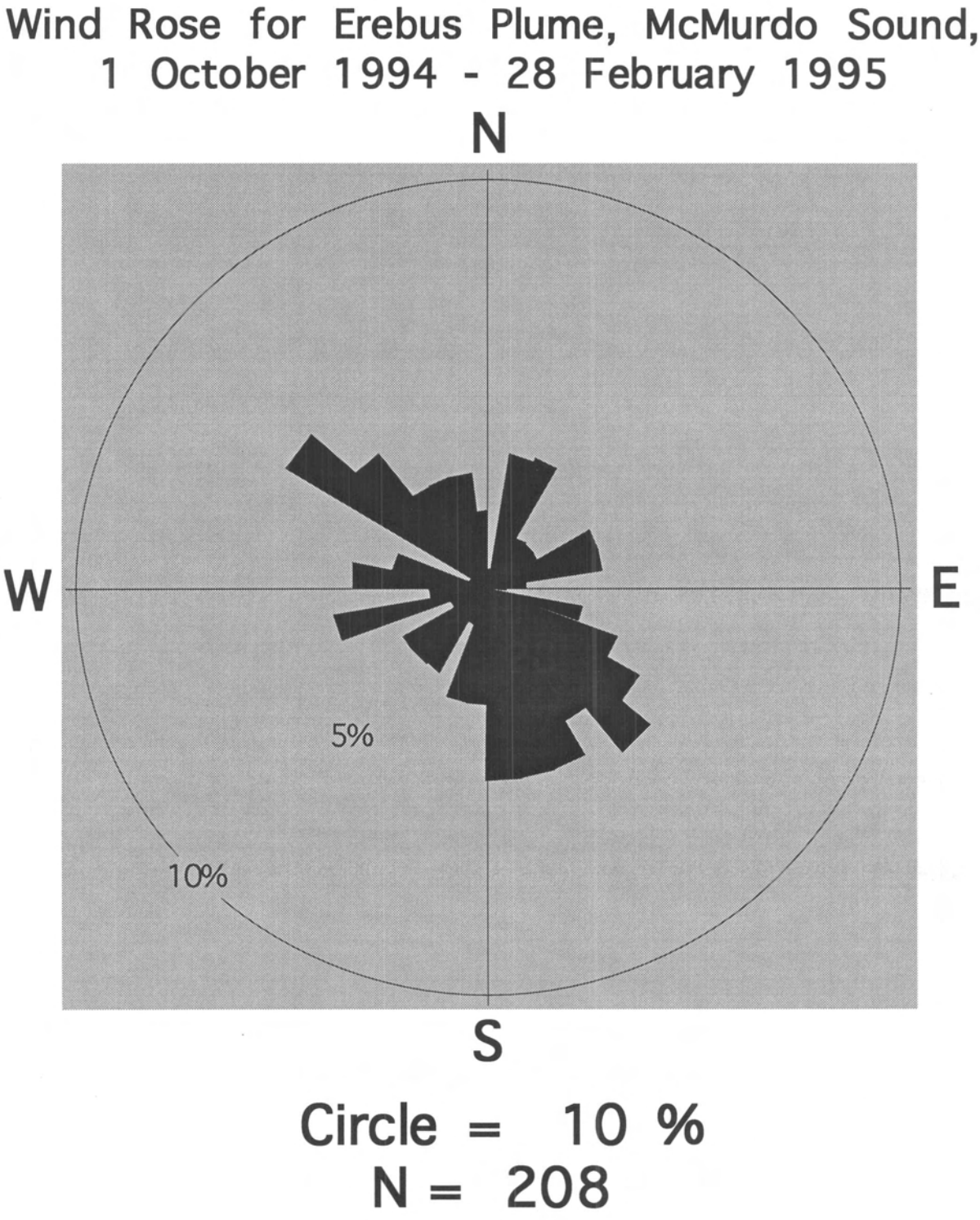


Figure 5.7. Summary wind rose diagram for Austral summer 1994-5.

10° Sector Models - Distal Sites

Ten degree sector models were used for distant receptor sites to obtain finer resolution at known locations. Data from the ten degree distal sector models show maximum atmospheric concentrations of a few hundred ng's/m^3 for SO_2, F and Cl at plume centerline altitudes. Ground level models predict that only the sites closest in elevation to plume centerline should contain potentially detectable values of Erebus gases (a few 10's of ng's/m^3). Ten degree sector model results for SO_2 are provided as plume centerline and ground level atmospheric concentrations (ng's/m^3) in Figures 5.8 - 5.11.

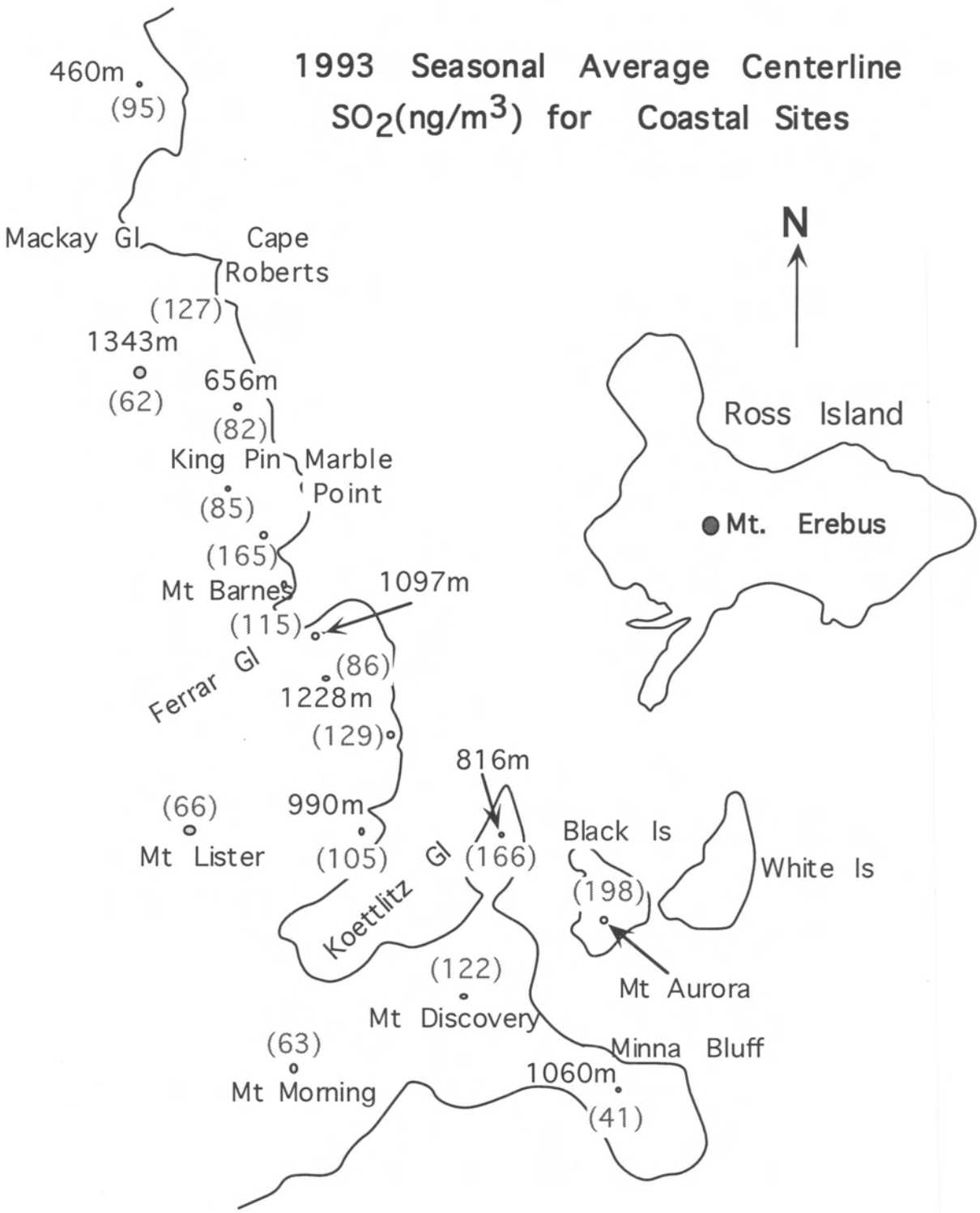


Figure 5.8. Ten degree sector model seasonal average atmospheric SO_2 concentrations for plume centerline altitudes, 1993. Values in (ng/m^3).

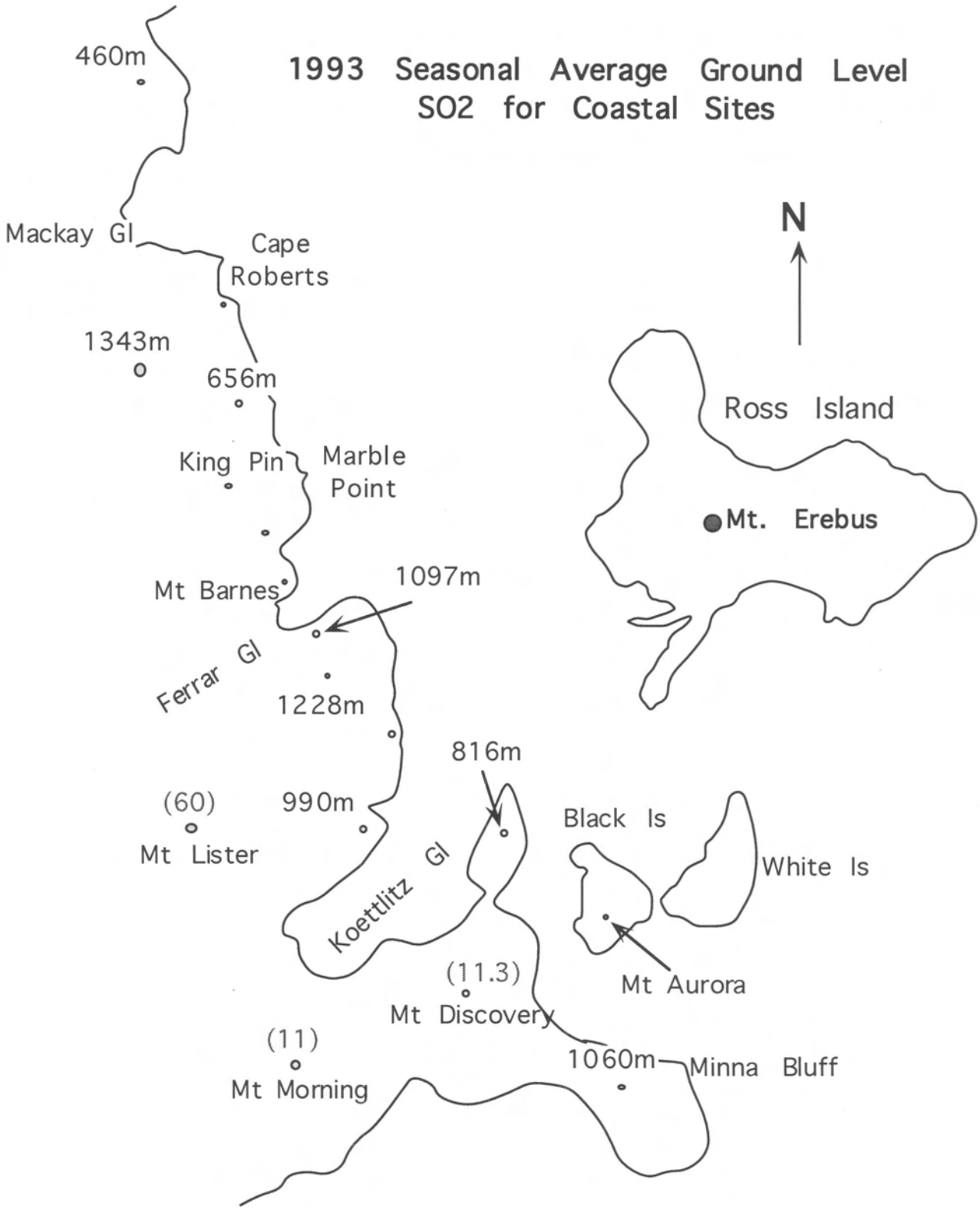


Figure 5.9. Ten degree sector model seasonal average atmospheric SO_2 concentrations for ground level sites, 1993. Values in (ng/m^3).

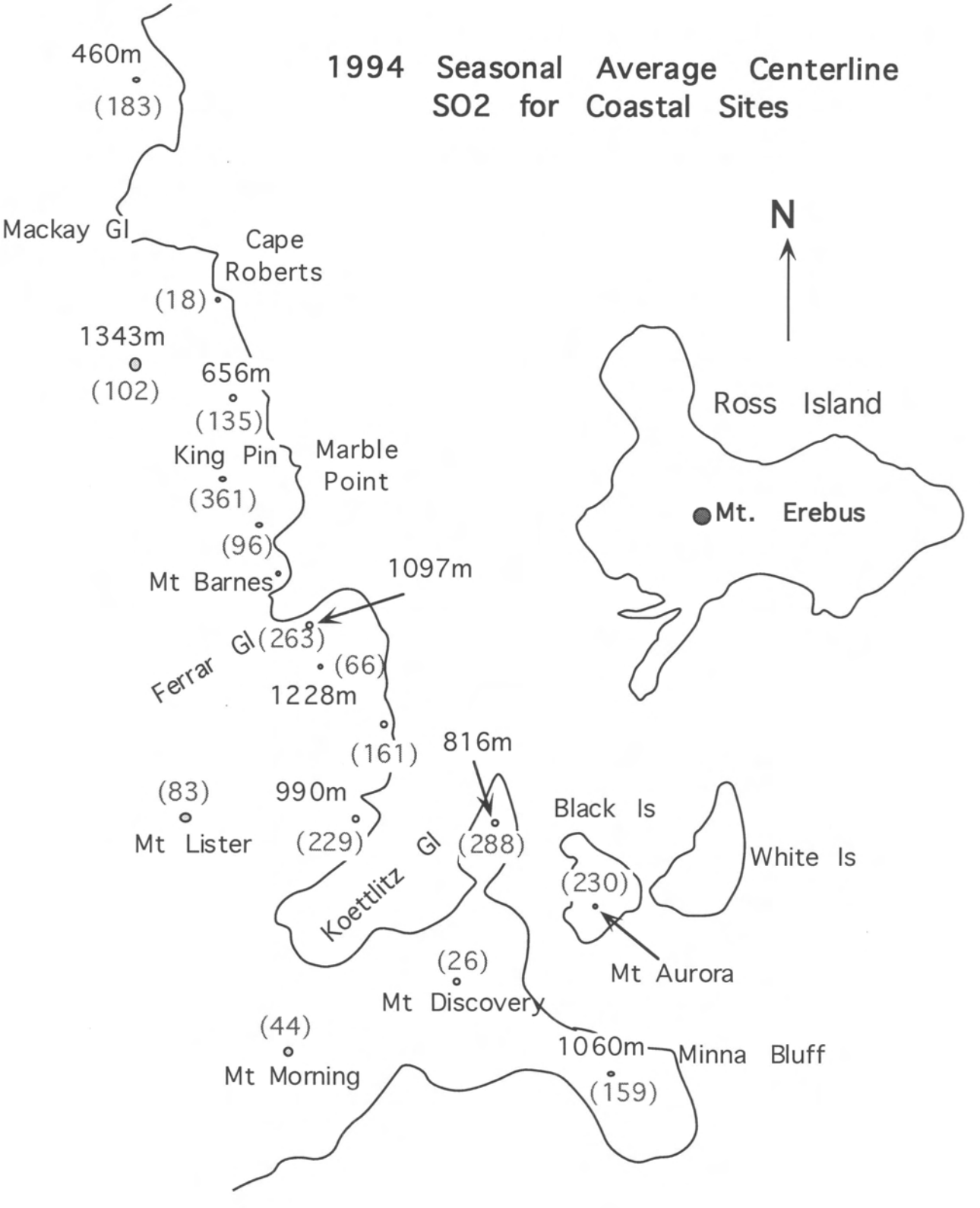


Figure 5.10. Ten degree sector model seasonal average atmospheric SO_2 concentrations for plume centerline altitudes, 1994. Values in (ng/m^3).

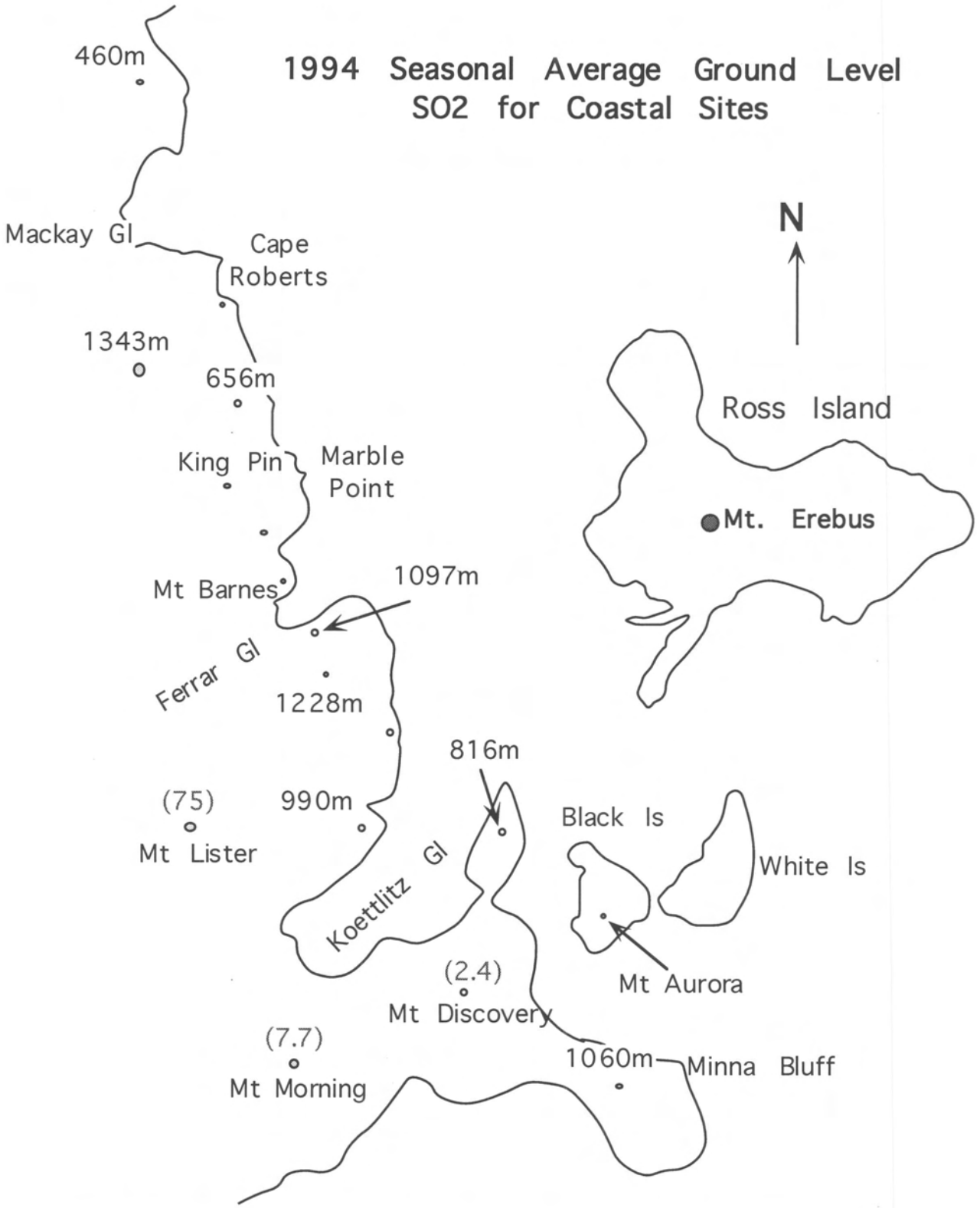


Figure 5.11. Ten degree sector model seasonal average atmospheric SO_2 concentrations for ground level sites, 1994. Values in (ng/m^3).

South Pole Dispersion Models

Results from South Pole dispersion models will be considered qualitatively with respect to other data to evaluate the potential of significant amounts of S, F and Cl reaching the pole. Preliminary calculations show that values obtained for wind directions greater than ten degrees off true south are meaningless. For this reason model calculations were limited to those days when the wind was blowing ±10° off due south. A five hour average concentration for each data point was calculated. The average of these five hour concentrations was determined. Because of the distance and travel time required for the plume to reach South Pole any significance attached to this number must be done so with care. The model prediction does provide an extreme upper limit to any contribution of Erebus gases (Tables D.1, D.2) and allows comparison with atmospheric samples collected over a similar time scale by Maenhaut et al. (1979).

The predicted concentration levels are very low in most cases. Clearly this model is very dependent on wind direction. Variance of more than a few degrees off due south has a profound effect on concentration levels at distances greater than 1000km. The other most important factor is emission rate. If winds are favorable and emission rate high, significant concentrations of gases can be transported rapidly to the interior of the continent. Subsequent dilution and sedimentation will readily lower concentrations. Another important factor is wind velocity. For a wind blowing due south with a velocity of 5 m/s, it would take ~ 3 days to transport gases from Erebus to the Pole. Most of the wind data show that velocities around the summit of Erebus are typically > 5 m/s.

A comparison of model results and atmospheric concentrations measured at South Pole in 1978 is provided as a means of quantifying the potential input of Erebus gases (Table 5.1). Based on the range of model predictions Erebus can account for a few percent to all of the SO_2 and Cl measured in atmospheric samples. Subsequent mixing and dilution with clean polar air

will rapidly lower predicted concentration levels. This means that under the best conditions Erebus contributions are probably at least two orders of magnitude less than model predictions.

Table 5.1. Sulfur, fluorine and chlorine (in picograms/m^3) from model predictions (1) and atmospheric measurements (2)(Maenhaut et al., 1979).

Source	SO_2	F	Cl
1993(1)	3880	1440	650
1994(1)	111110	112240	43080
S. Pole (2)	36000 - 62000	-	2200 - 3500

Whether or not these gases remain in sufficient quantities to affect atmospheric processes like ozone depletion is a function of their residence time and whether or not they reach the stratosphere. There is evidence to support the contention that Erebus gases have played a role in South Pole atmospheric and snow chemistry. Snow data from South Pole show anomalous enrichment of certain metals in layers from 1912 - 1916 (Boutron, 1980). It is interesting to note that enrichment factors for which there are data from Erebus and snow show a similar pattern (Figure 5.8). This suggests that at least a partial trace element signature from Mt. Erebus can be detected. A better comparison of other trace elements in snow and plume gases could test this hypothesis further. In any case, the evidence verifies that Erebus plays a role in the tropospheric chemistry at South Pole.

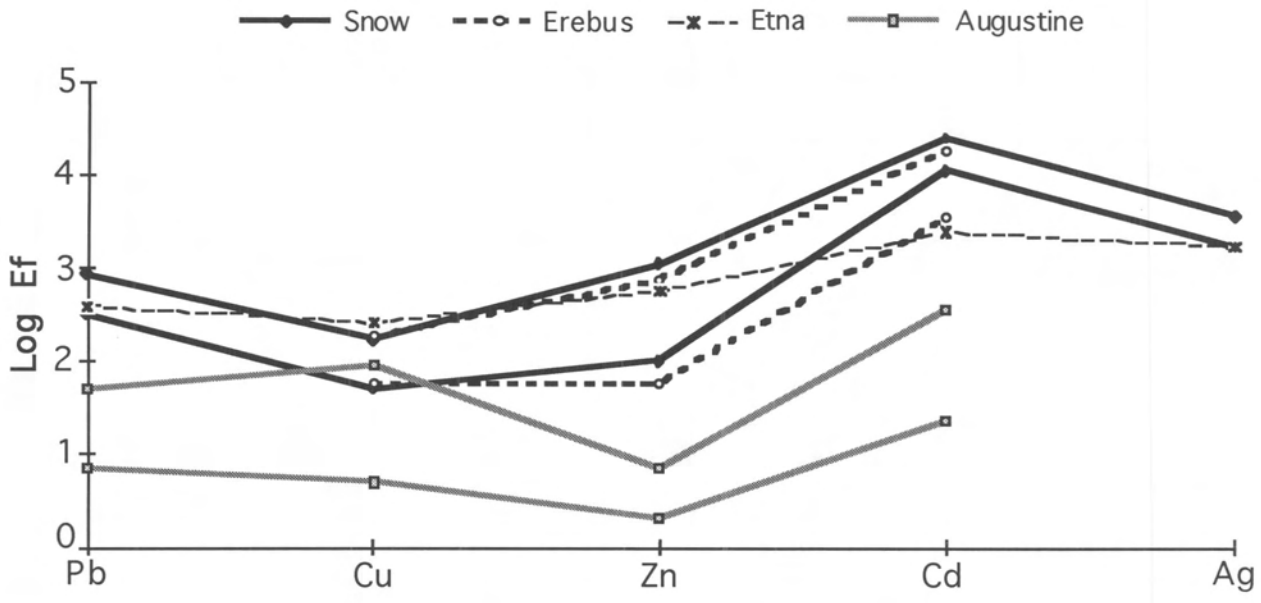


Figure 5.12. Enrichment factors (Ef) selected volcanoes and anomalously enriched elements in South Pole snow (Boutron, 1980). Ef is defined by: $Ef = (El/Al)_{gas\ or\ snow} / (El/Al)_{crust}$. Data for Mt. Erebus (Zreda-Gostynska, 1995), Mt. Etna (Buat-Menard et al., 1988) and Mt. Augustine (Lepel et al., 1978). Note different enrichment patterns for different volcanoes.

Potential Contribution to the Stratosphere

In order to evaluate the potential impact of Erebus gases on ozone depletion it is important to consider that Erebus emissions occur at least 4 km lower than the measured tropopause for 1993 and 1994. If Erebus gases were to account for part of the ozone depletion, a mechanism responsible for transport to the stratosphere is required. Although no such mechanism has been proposed, submicron elemental gold particles unique to Erebus (Meeker et al., 1991) were collected during an airborne sampling transect at 8 km altitude (Chuan, 1994). This roughly corresponds to the same altitude of the summer tropopause for 1993 and 1994. If particulates from Erebus can reach the tropopause it is likely that gaseous SO_2, F, and Cl are also present. Diffusion across the tropopause provides a slow mechanism for removal of gases to the stratosphere. Typically about 2% of gases present at the tropopause can diffuse into the stratosphere (Follows, 1992). The maximum five-hour time average calculation of SO_2 concentration at the tropopause from these models is 9090 ng/m^3. Two percent of this would be 182 ng/m^3.

Based on observed conversion rates of SO_2 to H_2SO_4 (~ 6 weeks for Mt. Pinatubo (Hoffman et al., 1992)) and short transport times to the Pole it is likely that Erebus sulfur reaching South Pole would consist mainly of SO_2. Subsequent conversion to H_2SO_4 could provide surfaces for catalyzed ozone destruction, but would be accompanied by continued dilution. Although sulfuric acid droplets have a stratospheric residence time of ~ 1 year (Lazrus et al., 1979) it is unlikely under even the best conditions that significant amounts of SO_2 from Erebus would reach stratospheric altitudes where they could noticeably impact ozone depletion.

Chlorine has the potential to destroy ozone through homogeneous chemistry, but it's residence time is similar to the plume travel time to the Pole for winds traveling ~ 5 m/s. Given low model predictions and the slow rate of diffusion to the stratosphere it is unlikely that Cl from Erebus has much effect on ozone depletion, but may still appear in measurable quantities in South Pole snow.

A Gaussian plume model based on emission rates from Mt. Erebus and wind data from McMurdo Sound provides the basis for a first order approximation of the maximum potential impact of Erebus gases on atmospheric chemistry at South Pole. Model predictions corroborate other evidence that Erebus gases reach South Pole in measurable amounts. Chlorine may reach the tropopause, but due to it's short residence time will not be present long enough for substantial diffusion to the stratosphere to occur. Erebus sulfur has the best chance to impact ozone due to a longer residence time. However, low model predictions combined with continuous dilution with "clean" polar air and the difficulty of transporting SO_2 to the stratosphere suggest that any contribution to ozone depletion is minor. The most important case for this is the observation that Erebus has been active for at least a hundred years, while the growth of the ozone hole is a new phenomena. Any contribution from Mt. Erebus would be minor and must have been present as long as the volcano has been active.

6. Conclusions

The sulfur, fluorine and chlorine composition of volcanic gases from Mt. Erebus collected between Dec. 1992 and Jan. 1994 was determined to investigate temporal variations related to degassing behavior. Significant variations were observed over three different time frames.

Short term changes over a few hours record infrequent, short-lived eruption events and also define daily trends that may be part of a larger cycle. Data from 1992 and 1993 appear to fluctuate cyclically over a period of 6 - 8 days. These changes are attributed to large scale convection or overturn in the magma column or to periodic injection of fresh material. Data from 1994 do not appear to have any obvious cycle. This suggests that while certain degassing processes may be cyclic, the overall behavior of the system is somewhat more complex.

A comparison of annual values with data form other years reveals a cyclic trend between a more sulfur-rich and a more fluorine/chlorine-rich composition. The periodicity varies between two to three years, but may actually be much shorter due to the nature of the short time period during which samples were collected (~ 2 months) each year. Superimposed on this cycle is an overall shift toward a more sulfur-rich composition. I believe these changes are related to pulses of magmatic recharge (sulfur-rich) followed by periods of repose (fluorine/chlorine-rich) from depth. The trend toward higher sulfur content could represent the approach of a large diapir which periodically resupplies the summit reservoir.

Gaussian dispersion sector models were used to evaluate seasonal dispersion patterns and concentration gradients for the area surrounding Ross Island for 1993 and 1994. Results vary significantly for each year due to differing emission rates and wind patterns. Results of ground level models for a 10 km radius of the summit predict that concentrations for S, F and Cl should all be negligible. This is in direct contrast to visual observations of fumigation conditions on days during the 1994 field season and snow data collected by Palais et al. (1994), who detected a tentative "signature" from Mt. Erebus.

Distal sector model results for nearby coastal sites predict that only elevations similar to Erebus will have measurable amounts of SO_2, F and Cl on the order of a few hundred ng's/m^3.

Plume centerline results suggest that the plume is vertically narrow, which creates the potential for gases to pass over the Trans Antarctic Mountains and into the Polar Plateau.

An extension of the standard dispersion parameters was applied to constrain the maximum potential input of sulfur, fluorine and chlorine to South Pole. Results are computed using a five hour time correction factor. An average of all values was compared to a range of atmospheric sample values collected over a similar time scale by Maenhaut et al. (1979). Given high emission rates and favorable wind patterns it is possible for Erebus gases to account for between 10% and 100% of the tropospheric SO_2 and Cl at South Pole. Erebus gases may play a role in tropospheric chemistry at South Pole, but continued summertime dilution with "clean" air and slow diffusion rates of a small proportion of these gases to the stratosphere preclude the possibility of them significantly affecting ozone depletion. Any impact from Erebus would be "background" and must have been present as long as the volcano has been active.

Appendix A

Ion Chromatography Procedures

Sulfur concentrations on all filters and fluorine concentrations on particulate (A) filters were determined by liquid ion chromatography. All sulfur was measured as sulfate and corresponding mass corrections made to determine total sulfur.

Sample Preparation.

Samples were halved (47mm) or quartered (110 and 100mm), one portion placed in a clean plastic centrifuge tube and another in a poly vial for neutron activation. A solution of approximately 18g of 18mΩ de ionized water and 2g of 3% H_2O_2 was added to the centrifuge vials as leachate and to oxidize reduced sulfur to sulfate. Trays of vials were heated in a water bath at 30 minute increments for a total of 4 to 6 hours, then placed on a reciprocal shaker for 24 hours. Near or total disintegration of Whatman 41 filters usually resulted. Sample solutions were filtered into new poly centrifuge tubes for storage and analysis.

Sample Analysis.

Analyses were conducted at the IC lab at the New Mexico Bureau of Mines and Mineral Resources. Instrumentation consisted of a Dionex 4000i ion chromatograph using carbonate/bicarbonate eluant and H_2SO_4 suppressor on an HP1C AS4A ion column. Retention times varied during the course of the study. Samples analyzed in the spring of 1994 had retention times for F of ~ 1.3 min. and SO4 of ~ 4.6 min. Samples analyzed in 1995 had longer retention times (~1.9 min. for F, ~9.8 min. for SO_4) due to the procurement of a new ion column. In May of 1995 sulfate retention times were shorter (~6.6 min.).

Standards were made by dissolving reagent grade K_2SO_4 and KF salts in a matrix solution to obtain concentrations of F and SO_4 of 1000 ug/g. Subsequent dilution of this solution was used to create other standards. In order to compensate for possible matrix effects a number of treated filters were leached in a solution of deionized water and proportional 3% H_2O_2 similar to that used as leachate for unknowns. This matrix solution was filtered and used as a

base for standards. Matrix solution standards were used to calibrate conductivities of treated filter samples. Particulate filters were calibrated using a separate set of standards prepared in the same manner, but with a matrix solution comparable to leachate of unknowns.

Deionized water, H_2O_2 and matrix solution blanks were all run to assure quality and to suggest possible areas of contamination. In most cases the majority of the unknown blank values for sulfate could be related to the peroxide solution blank (typically .2 to .5 ug/g).

Quality assurance standards were created by dilution of a known amount of commercial standard solutions (NIST 3181 for SO_4 and NIST 3182 for Cl) which were incorporated into each run. Accuracy of standards was typically ±5-10%. Standards were run at the beginning, during and at the end of each analysis. Several duplicate unknowns were also run to determine precision. Variation in standard peak height greater than ±5% over the run time was considered significant and unknowns were re analyzed at a later date.

Data Reduction.

Peak height conductivity of unknowns was calibrated against peak height regression of known standards. Concentrations in ug/g were converted to ug by multiplying by the amount of leachate used (g). A filter multiplier was applied (2x or 4x depending on whether or not the unknown was 1/2 or 1/4 of the total sample) to obtain concentrations in ug/filter. Blank corrected values were divided by the volume of air sampled to obtain a value in ug/m^3.

Appendix B

INAA Procedures

Data Acquisition.

Neutron activation was used to obtain measurements of fluorine and chlorine on treated filters and chorine, indium and sodium on particulate filters. Due to the presence of fluorine in the teflon particulate filters, direct measurement of F could not be made. These filters were anlayzed by ion chromatography for F. Samples irradiated at Texas A&M were counted on the same detector over a five day period. Samples irradiated at MURR were counted on a single detector for the very short irradiation and on two separate detectors for the short irradiation. Separate standards were used to calibrate each detector. Twenty five B&C filters from the very short irradiation underwent a subsequent short irradiation and count on a single detector as calibration standards for the very short Cl irradiation. A list of isotopes measured, their half lives and peak energies measured is provided in table B.1.

Table B.1. Isotopes and peak energies used to determine concentrations of F, Cl, In and Na (Glascock, 1991).

Element	Isotope	$T_{1/2}$	Major Energy Lines (KeV)	
F	^{20}F	11s	1633.1	
Cl	^{38}Cl	37.24m	1642.69	2167.68
In	^{116}In	54m	417	
Na	^{24}Na	15.02h	1368.53	

Analyses of 1993 filters were performed at the Texas A&M Research Reactor by the author in September, 1994. Filters collected in 1992 and 1994 were analyzed at the Missouri University Research Reactor by Michael Glascock (Cl, In, Na data) and Vicki Spate (F data) during the spring of 1995. Peak measurements for elements with different half lives were obtained through two separate irradiations, a very short irradiation(vs) and a short

irradiation(s). Irradiation, decay and count times used for each analysis and reactor are listed in table B.2.

Table B.2. Irradiation, decay and count times for elements analyzed by INAA at Texas A&M and MURR.

Element	Samples Analyzed	Irrad. Code	T_{irrad}	T_{decay}	T_{count}	Research Facility	Date Analyze
F,Cl	93 B/C	vs	5s	10s	30s	Texas A&M	9/94
	92,94 B/C	vs	7s	11s	18s	MURR	3/95
Cl, In, Na	93 all	s	5m	15m	15m	Texas A&M	9/94
	92,94 A, 25 B&C*	s	30s	15m	12m	MURR	3/95 (5/95)*

Irradiation codes refer to text: (vs) = very short irradiation, (s) = short irradiation. * = 25 B&C filters from 92/94 were reanalyzed using a short irradiation to provide a calibration of unknown Cl peaks from the very short irradiation.

Data Reduction.

Concentrations of unknowns were calculated based on linear regression of peak area versus known values of standards for each energy line. Many of the same standards were used in both short and very short irradiations at each reactor to insure compatibility of data sets. Standards used are listed in table B.3 along with their known concentrations.

Table B.3. Standards and known values used for calibrations.

Standard #	Texas (vs)	Texas (s)	MURR (s)	Known F(ug)	Known Cl(ug)
603	F,Cl	Cl	Cl*	200	1000
608	F,Cl	Cl		200	200
609	F			200	220
613	F			350	350
616	F,Cl	Cl	Cl(1)	113	334
617	F,Cl	Cl	Cl(1)	121	237
s-32	F,Cl	Cl		607	475
s-33	F,Cl	Cl	Cl(2)	472	490
s-34	F,Cl	Cl	Cl*	625	460
s-35	F,Cl			416	413
s-37	F,Cl			590	470
s-38	F,Cl		Cl*	535	472
	Type			In(ng)	Na(ug)
604	SRM 1633a	Na	Na(1)		45.71
605	SRM 1633a	Na	Na(2)		36.94
606	SRM 1648	Na, In	Na, In(1)	20.34	87.81
607	SRM 1648	Na, In	Na, In(2)	21.48	95.72
618	Sol.	In	In(2)	43	
283	Sol.	In	In(1)	65.44	

MURR standards are designated as follows: * indicates standards used for irradiation of 25 B&C filters, 5/95; (1) indicates used for calibration of detector 1; (2) indicates used for calibration of detector 2.

Concentrations for F, In and Na were obtained from calibration of a single energy line. Concentrations of Cl were determined by averaging values obtained from calibration of both the 1642 and 2167 KeV lines. Most of the 1993 chlorine data is from the short irradiations at Texas

A&M. A few of the 1993 chlorine values are from the very short irradiation. A comparison of values obtained from the very short calibration agrees within 5% of those obtained from the short irradiation calibration. Chlorine concentration for 1992 and 1994 particulate and 25 treated filters was determined from the average of 1642 KeV and 2167 KeV calibrations from the MURR short irradiation. The chlorine values obtained from the short irradiation were then treated as "standards" and regressed against peak areas for the very short irradiations for the same samples. A separate calibration was used for each line and the average of the two used as the final concentration (short 1642 KeV values were used to calibrate very short 1642 KeV peaks, short 2167 KeV values were used to calibrate very short 2167 KeV peaks). These two very short Cl calibrations were used to calculate concentrations which were averaged to obtain a final value. Concentrations obtained from calibration of samples calculated from both short and very short lines agree within ±20% (Figure B.1). Concentrations determined in this manner are used for samples which did not undergo short irradiation.

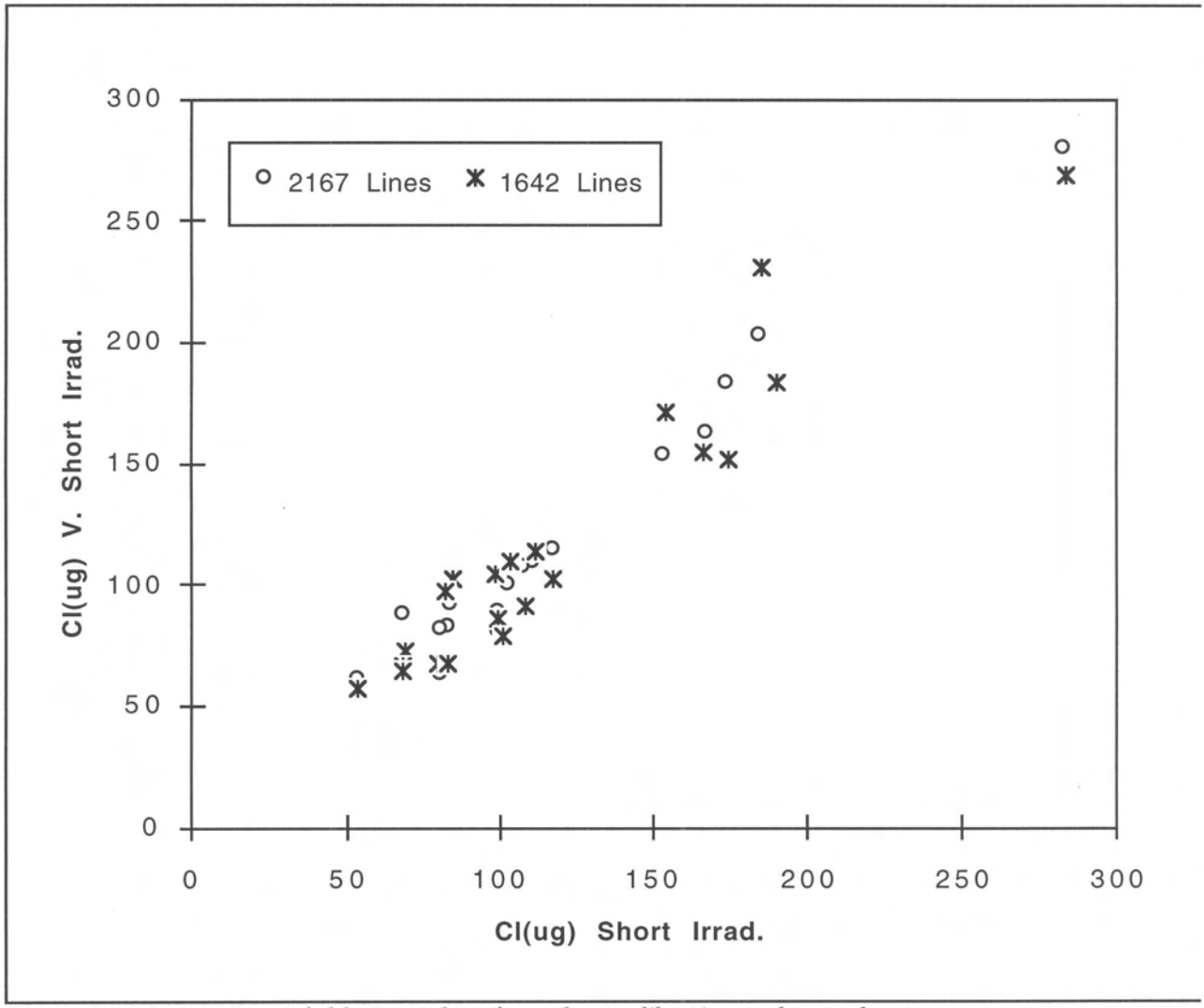


Figure B.1. Comparison of chlorine values from short calibration and very short cross calibration. Both the 1642 and 2167 KeV lines for the very short irradiation were calibrated using values from the short calibration regressed against peak height from the very short irradiation.

Appendix C.

Filter Data.

Filter data for 1992, 1993 and 1994 is presented in the following tables. All values are in ug/m3. - indicates not detected. n.a. indicates not analyzed for this element.

Table C.1. Blank corrected data for 1992 (ug/filter).

E92-	S	F	Cl	In	Na	vol.(m3)
1a	4.8	.8	.9	.013	9.6	2.25
b	99.8	36.6	38.0	-	-	
c	21.4	6.0	40.4	-	-	
3a	22.4	56.8	86.1	.112	47.0	2.97
b	654.6	318.2	1080.9	-	-	
c	41.4	8.9	209.5	-	-	
5a	8.4	8.0	9.9	.047	16.2	5.9
b	420.6	210.1	223.4	-	-	
c	34.2	2.1	78.4	-	-	
6a	4.8	2.8	95.2	.019	16.5	4.8
b	371.8	85.8	281.2	-	-	
c	55.4	9.3	101.7	-	-	
7a	4.8	3.6	2.6	.028	5.8	3.7
b	1410	126.4	162.5	-	-	
c	25.8	13.6	93.3	-	-	
8a	10.0	27.6	0	.026	20.9	3.6
b	208.6	59.2	267.5	-	-	
c	1.8	.8	118.8	-	-	
9a*	1.4	7.0	0	.007	1.2	1.4
b*	22.5	20.7	119.8	-	-	
c*	30.9	4.2	40.3	-	-	
10a*	0	0	0	.011	8.4	1.3
b*	57.7	44.3	174.4	-	-	
c*	27.5	1.6	9.1	-	-	
11a*	0	1.0	10.9	.013	6.7	1.3
b*	34.9	557.1	131.7	-	-	
c*	35.1	2.2	12.1	-	-	
13a	9.6	28.0	16.9	.020	2.2	1.9
b	177.4	22.4	77.5	-	-	
c	24.6	11.0	0	-	-	
14a	10.0	74.4	0	.045	25.4	3.9
b	633.0	120.4	379.6	-	-	
c	9.0	4.7	46.7	-	-	
15a	9.6	19.6	34.2	.008	1.6	1.4
b	93.8	22.2	128.0	-	-	
c	14.6	.9	74.6	-	-	
16a	7.6	4.8	33.0	.041	25.3	4.1
b	512.6	420.4	563.3	-	-	
c	10.2	4.3	120.4	-	-	
19a	7.6	6.4	39.2	.051	36.0	3.1
b	472.2	241.6	620.0	-	-	
c	32.2	29.5	100.6	-	-	
21a	7.6	16.0	0	.017	14.6	2.9
b	235.4	77.1	369.2	-	-	
c	9.0	0	0	-	-	
22a	15.6	45.6	44.2	.051	20.9	6.6
b	545.4	153.0	689.1	-	-	
c	27.4	5.5	61.6	-	-	

* indicates 47mm, all others 110mm.

Table C.2.a. Blank corrected data for 1993 - 110mm filters (ug/filter)

E93-	S	F	Cl	In	Na	vol.(m3)
1a	2.9	.1	65.3	.032	20.6	1.44
b	209.0	80.5	293.2	-	-	
c	60.8	5.6	42.3	-	-	
2a	14.2	7.5	190.3	.233	150.6	2.88
b	2432.7	832.8	2715.7	-	-	
c	229.0	5.0	36.8	-	-	
3a	6.9	1.65	170.7	.218	121.8	4.32
b	775.2	163.0	479.0	-	-	
c	21.2	13.3	9.4	-	-	
4a	8.63	4.3	145.4	.200	117.8	4.8
b	1095.6	210.2	965.3	-	-	
c	940.5	120.3	516.7	-	-	
5a	6.0	3.6	80.6	.097	82.2	2.4
b	764.1	124.8	101.2	-	-	
c	9.5	0	0	-	-	
6a	2.4	.1	26.6	.013	9.4	3.6
b	780.2	258.9	341.8	-	-	
c	18.4	16.5	0	-	-	
8a	6.1	.8	35.4	.026	13.4	3.6
b	581.1	105.6	18.9	-	-	
c	3.4	0	0	-	-	
9a	1.5	.2	14.4	.017	10.6	3
b	198.2	47.7	127.3	-	-	
c	0	0	0	-	-	
10a	1.4	0	23.0	.029	15.8	3
b	215.0	108.2	59.0	-	-	
c	2.3	0	0	-	-	
11a	.9	0	13.3	.019	9.8	3.45
b	248.3	36.5	71.9	-	-	
c	5.9	84	0	-	-	
13a	2.8	1.35	16.6	.040	37.4	2.64
b	199.8	20.0	25.1	-	-	
c	0	22.4	0	-	-	
15a	1.2	0	71.4	.014	25.8	6.12
b	869.9	201.9	82.5	-	-	
c	265.7	34.4	129.5	-	-	
16a	4.1	1.4	53.0	.038	23.8	2.832
b	725.7	146.4	277.2	-	-	
c	16.5	0	0	-	-	
17a	.7	0	11.9	.020	12.6	2.457
b	134.1	37.3	86.2	-	-	
c	60.8	60.8	19.5	-	-	

Table C.2.b. Blank corrected data for 1993 - 47mm filters (ug/filter)

E93-	S	F	Cl	In	Na	vol.(m3)
52a	2.5	1.3	44.5	.058	30.8	1.584
b	711.0	316.0	783.9	-	-	
c	174.9	8.4	9.6	-	-	
54a	.9	1.1	23.1	.027	17.4	1.584
b	399.5	145.7	422.9	-	-	
c	254.3	60.0	148.9	-	-	
55a	.1	.9	10.6	.012	5.4	.63
b	69.5	72.0	103.7	-	-	
c	51.6	36.4	70.3	-	-	
56a	1.4	1.4	29.5	.027	12.8	1.8
b	635.2	238.3	236.5	-	-	
c	105.8	0	23.3	-	-	
58a	.1	1.0	10.6	.012	7.6	.6
b	145.1	62.0	73.5	-	-	
c	24.2	16.2	28.2	-	-	
59a	1.1	1.4	22.2	.024	11.4	1.2
b	1003.1	445.2	489.1	-	-	
c	21.1	0	8.7	-	-	
60a	1.4	1.6	7.5	.011	5.6	.69
b	180.5	62.2	108.4	-	-	
c	46.4	10.7	37.7	-	-	
61a	.6	.7	29.0	.037	16.6	2.156
b	406.9	298.7	463.0	-	-	
c	48.2	3.6	17.3	-	-	
62a	.2	1.1	5.7	.008	4.2	1.38
b	89.5	47.8	257.8	-	-	
c	1.7	0	25.8	-	-	
63a	1.3	1.6	11.8	.021	10.4	1.625
b	213.2	97.2	567.7	-	-	
c	23.6	0	4.4	-	-	

Table C.2.c. Blank corrected data for 1993 Staplex 100mm filters.

E93-	S	F	Cl	In	Na	vol.(m3)
101	2.9	0	28.1	n.a.	n.a.	148.6
102	6.5	0	0	n.a.	n.a.	182.8
103	7.5	319.7	3566.7	.356	190.2	6.4
104	50.9	279.8	3859.0	.272	207.0	8.5
105	12.0	206.7	1570.0	.127	116.2	4.3
107	15.0	570.7	1356.1	.093	87.8	1.1
108	478.3	551.4	1078.4	n.a.	n.a.	.9
109	0	70.2	1017.2	n.a.	n.a.	6.4
110	.5	21.9	459.3	n.a.	n.a.	6.4
111	0	15.8	488.6	n.a.	n.a.	5.1
112	4.4	43.0	1035.6	n.a.	n.a.	5.1
113	827.0	121.8	1502.0	n.a.	n.a.	3.4
114	145.7	107.5	279.4	n.a.	n.a.	1.0

* indicates treated, all others Whatman 41.

Table C.3.a. Blank corrected data for 1994 - 100mm filters (ug/filter).

E94-	S	F	Cl	In	Na	vol.(m3)
1a	0	0	40.2	.027	72.3	2.743
b	307.2	228.2	332.8	n.a.	n.a.	
c	4.4	6.0	25.4	n.a.	n.a.	
3a	0	0	176.6	.069	85.8	2.725
b	400.3	342.2	405.1	n.a.	n.a.	
c	76.6	14.9	51.7	n.a.	n.a.	
4a	.5	0	50.4	.042	88.8	3.625
b	258.3	177.72	208.9	n.a.	n.a.	
c	1.3	1.6	0	n.a.	n.a.	
6a	1.2	11.5	2.4	.014	38.4	5.04
b	138.7	74.6	255.1	n.a.	n.a.	
c	0	.4	0	n.a.	n.a.	
9a	0	0	.5	.002	19.3	2.34
b	2.4	1.3	47.9	n.a.	n.a.	
c	28.9	20.7	91.1	n.a.	n.a.	
11a	0	0	16.0	.012	1.9	3.25
b	308.8	44.4	100.2	n.a.	n.a.	
c	11.4	5.7	67.9	n.a.	n.a.	

Table C.3.b. Blank corrected data for 1994 size fraction (301) and hut aerosol samples (401)

E94-	S	F	Cl	In	Na	vol.(m3)
301 (8um)	1.8	0	.4	0	0	.495
(2um)	4.6	0	1.9	2.8	3.4	
(.2um)	4.8	0	0	0	0	
401a	0	0	0	0	0	11.463
b	6.3	7.4	27.6	n.a.	n.a.	
c	6.7	1.7	36.0	n.a.	n.a.	

Table C.3.c. Blank corrected data for 1994 - 47mm filters (ug/filter).

E94-	S	F	Cl	In	Na	vol.(m3)
51a	.8	0	13.0	.008	7.4	.57
b	76.3	35.5	43.7	n.a.	n.a.	
c	0	.1	0	n.a.	n.a.	
52a	.1	0	8.5	.005	.7	.465
b	35.6	15.9	13.5	n.a.	n.a.	
c	45.23	12.7	80.8	n.a.	n.a.	
53a	2.1	6.3	15.2	.006	10.5	.465
b	57.8	23.8	46.5	n.a.	n.a.	
c	23.7	10.5	23.6	n.a.	n.a.	
54a	.8	2.7	12.5	.007	2.6	.42
b	85.4	27.0	48.3	n.a.	n.a.	
c	12.1	0	0	n.a.	n.a.	
57a	1.6	5.2	1.2	.0003	.5	.396
b	3.2	1.1	2.5	n.a.	n.a.	
c	5.4	.9	0	n.a.	n.a.	
58a	0	0	6.3	.004	1.4	.396
b	27.1	7.1	11.6	n.a.	n.a.	
c	0	0	0	n.a.	n.a.	
59a	0	0	2.7	.002	2.8	.396
b	9.8	4.5	22.7	n.a.	n.a.	
c	0	.6	4.8	n.a.	n.a.	
60a	2.8	9.5	.8	.003	0	.462
b	17.9	8.9	34.7	n.a.	n.a.	
c	23.6	5.1	11.0	n.a.	n.a.	
61a	2.5	7.4	11.5	.010	6.9	.264
b	111.0	38.1	52.9	n.a.	n.a.	
c	3.3	1.3	17.0	n.a.	n.a.	
62a	0	0	5.8	.002	0	.81
b	2.5	2.3	9.6	n.a.	n.a.	
c	26.7	10.8	22.5	n.a.	n.a.	
63a	1.1	3.5	.7	.001	4.3	.573
b	17.2	4.5	14.2	n.a.	n.a.	
c	9.1	1.8	0	n.a.	n.a.	
65a	8.5	11.9	43.8	.038	26.3	3.64
b	451.8	168.6	360.9	n.a.	n.a.	
c	26.1	.5	0	n.a.	n.a.	
67a	5.1	8.1	26.1	.021	11.5	3.51
b	202.6	95.6	202.4	n.a.	n.a.	
c	10.5	1.4	8.4	n.a.	n.a.	
69a	9.3	11.5	33.4	.026	19.9	3.713
b	291.4	131.7	314.2	n.a.	n.a.	
c	32.7	0	16.6	n.a.	n.a.	
70a	4.0	6.0	54.8	.009	5.0	4.05
b	83.8	40.0	116.5	n.a.	n.a.	
c	10.7	.3	11.2	n.a.	n.a.	

Table C.4. Sample collection data for 1992.

Sample	Date	A filter	Start Time	Stop Time	Flow Rate (lpm) beginning	Flow Rate (lpm) end	Wind	Plume Conditions
92-1	12/7/92	S 1.2	12:51	13:41	40	45	S 10	poor
92-3	12/8/92	S 1.2	16:40	17:46	30	36	E 5	poor
92-4	Blank							
92-5	12/13/92	S 1.2	12:41	15:45	32	31	S 20	poor
92-6	12/12/92	S 1.2	17:27	20:06	25	31	S 10	poor
92-7	12/14/92	S 1.2	14:16	16:16	30	31	calm	int.
92-8	12/15/92	S 1.2	12:43	14:44	28	31		poor
92-9*	12/16/92	F 1	12:52	13:37	30	31		int.
92-10*	12/16/92	F 1	13:39	14:24	29	28		int.
92-11*	12/16/92	F 1	14:25	15:10	30	28		int.
92-12*	Blank							
92-13	12/18/92	S 1.2	14:16	15:16	31	31		poor
92-14	12/18/92	S 1.2	19:31	21:37	29	32		int.
92-15	12/19/92	S 1.2	13:48	14:33	30	32		
92-16	12/19/92	S 1.2	14:40	16:52	30	32		
92-19	12/25/92	S 1.2	09:53	11:27	28	34	S 2	poor
92-21	1/2/93	S 1.2	10:35	12:08	30	33	W 2	poor
92-22	1/2/93	S 1.2	12:12	15:51	30	30	W 2	poor

* indicates 47mm, all others 110mm. A filter types: S 1.2 = Sartorius 1.2um particulate filter, F 1 = Fluoropore 1um particulate filter. Flow rates (lpm) in liters per minute.

Table C.5.a. Sample collection data for 1993

Sample	Date	A filter	Start Time	Stop Time	Flow Rate (lpm) beginning	Flow Rate (lpm) end	Wind	Plume Conditions
110mm								
93-001	12/7	S 1.2	11:00	11:45	32	31	NW 5-10	Int.
93-002	12/7	S 1.2	11:50	?	32	0	N	Int.
93-003	12/8	Z 2	09:30	11:45	30	32	NW 5-10	Int.
93-004	12/8	Z 2	11:50	?	32	0	N 5-10	Poor
93-005	12/8	Z 2	17:15	18:30	32	32	N	Int.
93-006	12/9	Z 2	10:00	12:00	30	31	NE 5	Good
93-007	12/9	Z 2	Blank					
93-008	12/9	Z 2	12:00	14:00	20	30	N 5	Int.
93-009	12/9	Z 2	14:00	16:00	20	28		Int.
93-010	12/9	Z 2	16:00	18:00	20	28		Int.
93-011	12/10	Z 2	09:05	11:00	30	30		Good
93-012	12/10	Z 2	@					
93-013	12/10	Z 2	13:35	?	22	0		Int.
93-014	12/10	Z 2	Blank					
93-015	12/11	Z 2	09:45	14:00	24	24		Good
93-016	12/11	Z 2	14:00	17:00	24	26		Good
93-017	12/11	Z 2	17:03	19:00	21	22		Good
93-018	12/12	Z 2	12:00	14:05	24	30		Poor
93-019	12/12	Z 2	14:10	?	22	0		Poor
93-020	12/12	Z 2	Blank					
47mm								
93-051	12/9	Z 2	Blank					
93-052	12/10	Z 2	11:15	12:15	35	45	NW 10	Int.
93-053	12/10	Z 2	@					
93-054	12/10	Z 2	13:40	14:30	40	40		Int.
93-055	12/11	Z 2	09:50	10:20	32	32		Good
93-056	12/11	Z 2	10:22	?	30	0		Good
93-057	12/11	Z 2	Blank					
93-058	12/11	Z 2	14:00	14:30	30	30		Good
93-059	12/11	Z 2	14:30	?	30	0		Good
93-060	12/11	Z 2	17:10	17:40	35	35		Good
93-061	12/11	Z 2	17:43	19:00	42	40	NW 5-10	Good
93-062	12/12	Z 2	11:55	12:55	35	35		Poor
93-063	12/12	Z 2	13:00	14:05	38	39		Poor

@ samples were blown into crater. ? indicates unknown time (flow rate = 0 on collection). A filter types: S 1.2 = Sartorius 1.2um particulate filter, Z 2 = Zefluor 2um particulate filter.

Table C.5.b. Sample collection data for Staplex high volume sampler. All Staplex samples consist of a single filter.

Sample	Date	Filter Type	Start Time	Stop Time	Flow Rate (cfm) beginning	Flow Rate (cfm) end	Wind	Plume Conditions
93-101	12/8	Wh 41	18:00	23:50	15*	15*		Hut Aerosol
93-102	12/9	Wh 41	11:00	17:00	17*	17*		Hut Aerosol
93-103	12/11	Wh 41	14:05	14:20	15*	15*		Good
93-104	12/11	Wh 41	14:20	14:40	15*	15*		Good
93-105	12/11	Wh 41	14:40	14:50	15*	15*		Good
93-106	12/11	Wh 41	Blank					
93-107	12/11	Wh 41 LiOH	16:55	17:15	2*	2*		Good
93-108	12/12	Wh 41 LiOH	17:15	17:30	2*	2*		Good
93-109	12/12	Wh 41	12:07	12:22	14*	15*		Good
93-110	12/12	Wh 41	12:24	12:39	16*	15*		Good
93-111	12/12	Wh 41	12:41	12:56	12*	13*		Good
93-112	12/12	Wh 41	12:57	13:12	12*	12*		Poor
93-113	12/12	Wh 41 LiOH	18:07	18:22	0*	15*		Poor
93-114	12/12	Wh 41 LiOH	18:23	18:30	2*	2*		Poor
93-115	12/13	Wh 41 LiOH	Blank					
93-116	12/13	Wh 41 LiOH	Blank					
93-201	12/13	Wh 41 LiOH	15:20	18:20	%	%		Hut Aerosol
93-202	12/13	Wh 41 LiOH	18:25	21:25	%	%		Hut Aerosol
93-203	12/13	Wh 41 LiOH	21:30	23:50	%	%		Hut Aerosol

* Staplex sampler flow rates measured as cubic feet per minute (cfm). % unknown flow rate for this pump. Filter types: Wh41 = Whatman 41 cellulose filter, Wh41 LiOH = base-treated Whatman 41 cellulose filter.

Table C.6.a. Sample collection data for 1994.

Sample	Date	A filter	Start Time	Stop Time	Flow Rate (lpm) beginning	Flow Rate (lpm) end	Wind	Plume Conditions
100mm								
94-001	12/6	Z 2	15:45	17:55	30	34	N	Poor
94-003	12/7	Z 2	12:45	14:50	30	36		Poor
94-004	12/7	Z 2	12:45	14:50	28	30		Poor
94-006	12/7	Z 2	15:00	18:00	28	28		Poor
94-007	12/8	Z 2	Blank					
94-009	12/8	Z 2	10:30	11:15	20	20		Int.
94-011	12/8	Z 2	17:20	19:30	20	29		Good
94-015	12/9	Z 2	Blank					
47mm								
94-051	12/7	Z 2	11:45	12:00	26	30		Int.
94-052	12/7	Z 2	12:00	12:15	30	32		Int.
94-053	12/7	Z 2	12:15	12:30	30	32		Int.
94-054	12/7	Z 2	12:30	12:45	28	28		Int.
94-055	12/8	Z 2	Blank					
94-056	12/8	Z 2	13:45	14:15	20	20		Good
94-057	12/8	Z 2	14:15	14:45	20	20		Good
94-058	12/10	Z 2	12:15	12:45	20	20		Good
94-059	12/10	Z 2	12:45	13:15	20	20		Good
94-060	12/10	Z 2	13:15	13:50	20	20		Good
94-061	12/10	Z 2	13:50	?	20	0		Good
94-062	12/13	Z 2	12:40	13:10	26	29		Poor
94-063	12/13	Z 2	12:40	13:10	28	30		Poor
94-064	12/13	Z 2	Blank					
94-065	12/22	Z 2	14:30	16:40	20	35		Good
94-066	12/2	Z 2	16:40	18:45	22	27		Int.
94-067	12/23	Z 2	10:30	12:40	25	29		Poor
94-068	12/23	Z 2	12:45	?	22	0		Poor
94-069	12/25	Z 2	15:30	17:45	25	30		Int.
64-070	12/25	Z 2	17:45	20:00	30	30		Poor
94-071	12/25	Z 2	20:00	?	27	0		Poor

? indicates unknown time (flow rate = 0 on collection). A filter types: Z 2 = Zefluor 2um particulate filter.

Table C.6.b. Sample collection data for specialized samples

Sample	Date	A filter	B filter	C filter	Start Time	Stop Time	Flow Rate (lpm) beginning	Flow Rate (lpm) end	Sample Type
94-201*	12/12	Z 2	Nyl. 1.2	Nyl. 1.2	10:00	11:00	24	24	Sulfur Only
94-301*	12/12	Np 8	Z 2	Np .2	15:35	16:05	25	25	Size Fraction
94-401	12/13	Z 2	Wh41 LiOH	Wh41 LiOH	14:45	23:00	15	20	Hut Aerosol

* indicates 47mm, all others 100mm. Filter types: Z 2 = Zefluor 2um particulate filter, Nyl. 1.2 = Nylasorb 1.2um filter, Np 8 = Nucleopore 8um particulate filter, Np .2 = Nucleopore .2um particulate filter, Wh41 LiOH = base-treated Whatman 41 cellulose filters. Samples 201 and 301 were collected at the normal sampling location. Sample 401 was collected 20m west of the Lower Erebus Hut.

Appendix D.

Plume Model Results

Results for South Pole dispersion model (tables D.1, D.2) and ground level sector models for Mt. Erebus (tables D.3.a., D.3.b.).

Table D.1. Gaussian plume model results for South Pole using 1993 atmospheric data and Erebus emission rates. Units are as follows: Q (10^8 ug/sec), u (m/sec), x,y (10^3m), C (picograms/ m^3). C* represents a five hour average using a correction factor of $C^* = C \times (10/t)^{.5}$ where t=300 minutes. Values used for σy and σz were calculated using Briggs rural dispersion equations based on Pasquill stability class (Zanetti, 1990). Numbers in parentheses represent log (C).

Date	Time	Q (SO_2)	Q (Cl)	Q (F)	Wind Dir.	u (m/s)	St. Class	x	y	σ_y	σ_z	C* (SO_2)	C* (Cl)	C* (F)
10/3	12:00	4.86	1.8	.812	190	13.4	d	1363	240.3	9306	1808	(-141)	-	-
10/4	0:00	4.86	1.8	.812	176	13.8	e	1381	96.5	7025	99.8	(-35)	-	-
10/4	12:00	4.86	1.8	.812	189	27.3	e	1369	204.6	6994	99.8	(-180)	-	-
11/1	0:00	4.86	1.8	.812	183	10.0	e	1383	60.4	7030	99.8	(-10)	-	-
11/3	0:00	4.86	1.8	.812	170	16.7	e	1361	252.2	6974	99.8	(-278)	-	-
11/3	23:00	4.86	1.8	.812	182	15.1	d	1384	36.2	9376	1822	31	12	5.3
11/6	11:00	4.86	1.8	.812	186	5.1	d	1378	132.7	9356	1818	(-39)	-	-
11/7	23:00	4.86	1.8	.812	185	5.7	d	1380	108.6	9363	1819	(-26)	-	-
11/13	0:00	4.86	1.8	.812	190	3.7	d	1363	240.3	9306	1808	(-140)	-	-
11/27	0:00	4.86	1.8	.812	190	9.9	d	1363	240.3	9306	1808	(-140)	-	-
1/9	0:00	4.86	1.8	.812	180	14.7	d	1384	12.1	9378	1822	245E2	9080	4090
1/12	12:00	4.86	1.8	.812	174	10.3	e	1376	144.7	7014	99.8	(-87)	-	-
1/13	0:00	4.86	1.8	.812	171	11.2	e	1367	216.5	6990	99.8	(-203)	-	-
1/14	11:00	4.86	1.8	.812	174	17.0	d	1375	156.7	9347	1816	(-57)	-	-
1/15	10:00	4.86	1.8	.812	191	16.8	d	1359	264.1	9291	1805	(-171)	-	-
1/16	0:00	4.86	1.8	.812	168	171	d	1354	287.8	9274	1802	(-205)	-	-
1/16	10:00	4.86	1.8	.812	171	19.2	e	1365	228.4	6985	999.8	(-227)	-	-
1/17	0:00	4.86	1.8	.812	169	18.3	e	1356	275.9	6962	99.8	0	-	-
1/19	10:00	4.86	1.8	.812	180	6.3	d	1384	12.1	9378	1822	56870	21060	8500
1/21	12:00	4.86	1.8	.812	193	1.7	d	1349	311.3	9256	1799	(-240)	-	-
2/21	9:00	4.86	1.8	.812	170	2.7	d	1356	275.9	9282	1804	(-187)	-	-
Ave												**3880**	**1440**	**650**

- SO_2 values for this model were too low to be meaningfull; results for F and Cl were omitted accordingly.

Table D.2. Gaussian plume model results for South Pole using 1994 atmospheric data and Erebus emission rates. Units are as follows: Q (10^8 ug/sec), u (m/sec), x,y (10^3m), C (picograms/ m^3). C* represents a five hour average using a correction factor of $C^* = C \times (10/t)^{.5}$ where t=300 minutes. Values used for σy and σz were calculated using Briggs rural dispersion equations based on Pasquill stability class (Zanetti, 1990). Numbers in parentheses represent log (C).

Date	Time	Q (SO_2)	Q (Cl)	Q (F)	Wind Dir.	u (m/s)	St. Class	x	y	σ_y	σ_z	C* (SO_2)	C* (Cl)	C* (F)
11/8	12:00	8.33	4.95	1.8	179	5.3	d	1384	36.2	9376	1822	92	93	36
11/15	12:00	8.33	4.95	1.8	190	2.7	d	1365	228.4	9313	1810	(-132)	-	-
11/24	11:00	8.33	4.95	1.8	180	11.2	e	1384	0	7033	99.8	1.81E7	1.82E7	700190
11/29	0:00	8.33	4.95	1.8	181	2.0	d	1384	24.2	9377	1822	15020	15180	5820
12/12	0:00	8.33	4.95	1.8	173	5.0	e	1375	180.7	7003	99.8	(-144)	-	-
12/12	22:00	8.33	4.95	1.8	174	3.7	e	1376	144.7	7014	99.8	(-92)	-	-
12/15	23:00	8.33	4.95	1.8	173	5.3	e	1372	180.7	7003	99.8	(-144)		
12/22	0:00	8.33	4.95	1.8	182	4.5	e	1383	36.2	7032	99.8	7.8	7.9	3
12/22	12:00	8.33	4.95	1.8	189	5.1	e	1369	204.6	6994	99.8	(-186)	-	-
1/12	0:00	8.33	4.95	1.8	173	6.4	d	1372	180.7	9337	1814	(-83)	-	-
1/12	23:00	8.33	4.95	1.8	189	9.6	d	1369	204.6	9326	1812	(-106)	-	-
1/18	0:00	8.33	4.95	1.8	180	6.1	d	1384	12.1	9378	1822	59520	60130	23080
1/18	10:00	8.33	4.95	1.8	178	6.3	d	1383	60.4	9373	1821	.0001	.0001	.00005
1/21	12:00	8.33	4.95	1.8	179	3.6	d	1384	24.2	9377	1822	8430	8520	3270
1/23	12:00	8.33	4.95	1.8	171	10.6	d	1365	228.4	9313	1810	(-132)	-	-
1/24	0:00	8.33	4.95	1.8	170	9.2	d	1359	264.1	9291	1805	(-177)	-	-
1/24	9:00	8.33	4.95	1.8	173	3.0	e	1372	180.7	7003	99.8	(-144)	-	-
Ave												**111110**	**112240**	**43080**

- SO_2 values for this model were too low to be meaningfull; results for F and Cl were omitted accordingly.

Table D.3.a. 1993 ground level plume sector model results for SO_2 (ug/m^3). Units are as follows: Q (10^8 ug/s), u (m/s), h (meters), C (ug/m^3).

Sector	$Q(SO_2)$	f	n	u(m/s)	x(m)	σz	h	C
2000m CI								
0-30	4.86	.024	12	6.96	6250	153.9	1794	9.6 E -52
30-60	4.86	.016	12	3.15	6250	167.0	1794	1.4 E -51
60-90	4.86	.005	12	4.05	6000	193.6	1794	1.7 E -54
90-120	4.86	.043	12	6.53	5000	155.9	1794	9.4 E -66
120-150	4.86	.097	12	12.40	5500	154.9	1794	4.2 E -59
150-180	4.86	.0157	12	12.23	5000	150.0	1794	1.8 E -65
180-210	4.86	.135	12	9.85	4750	152.0	1794	2.6 E -69
210-240	4.86	.108	12	8.95	5250	159.7	1794	5.0 E -62
240-270	4.86	.092	12	7.69	5500	159.7	1794	6.4 E -59
270-300	4.86	.092	12	6.94	6250	167.0	1794	3.7 E -51
300-330	4.86	.119	12	6.81	7000	180.8	1794	4.1 E -45
330-360	4.86	.097	12	7.07	7250	188.9	1794	1.5 E -43
1000m CI								
0-30	4.86	.024	12	6.96	10500	153.9	2794	4.5 E -72
30-60	4.86	.016	12	3.15	12250	167.0	2794	2.99 E -61
60-90	4.86	.005	12	4.05	16250	193.6	2794	1.78 E -46
90-120	4.86	.043	12	6.53	10750	155.9	2794	4.88 E - 70
120-150	4.86	.097	12	12.40	10500	154.9	2794	1.04 E -70
150-180	4.86	.0157	12	12.23	10000	150.0	2794	2.89 E -75
180-210	4.86	.135	12	9.85	10250	152.0	2794	2.66 E -73
210-240	4.86	.108	12	8.95	11250	159.7	2794	1.56 E -66
240-270	4.86	.092	12	7.69	11250	159.7	2794	1.54 E -66
270-300	4.86	.092	12	6.94	12250	167.0	2794	7.67 E -61
300-330	4.86	.119	12	6.81	14250	180.8	2794	6.55 E -52
330-360	4.86	.097	12	7.07	15550	188.9	2794	1.03 E - 47

Table D.3.b. 1994 ground level plume sector model results for SO_2 (ug/m^3). Units are as follows: Q (10^8 ug/s), u (m/s), h (meters), C (ug/m^3).

Sector	Q(SO_2)	f	n	u(m/s)	x(m)	σz	h	C
2000m CI								
0-30	8.33	.0755	12	6.83	6250	150.0	1794	5.3 E -51
30-60	8.33	.0472	12	4.07	6250	167.0	1794	5.5 E -51
60-90	8.33	.066	12	4.39	6000	193.6	1794	3.3 E -53
90-120	8.33	.066	12	6.70	5000	155.9	1794	2.4 E -69
120-150	8.33	.1321	12	7.20	5500	153.9	1794	1.7 E -58
150-180	8.33	.1462	12	6.38	5000	150.0	1794	5.6 E -65
180-210	8.33	.066	12	7.36	4750	152.0	1794	2.9 E -69
210-240	8.33	.0708	12	6.15	5250	159.7	1794	8.1 E -62
240-270	8.33	.0613	12	7.65	5500	159.7	1794	7.4 E -59
270-300	8.33	.0613	12	5.46	6250	167.0	1794	5.9 E -51
300-330	8.33	.1274	12	7.06	7000	180.8	1794	7.2 E -45
330-360	8.33	.0802	12	5.22	7250	185.7	1794	2.9 E -43
1000m CI								
0-30	8.33	.0755	12	6.83	10500	150.0	2794	4.2 E -75
30-60	8.33	.0472	12	4.07	12250	167.0	2794	1.2 E -60
60-90	8.33	.066	12	4.39	16250	193.6	2794	3.4 E -45
90-120	8.33	.066	12	6.70	10750	155.9	2794	1.2 E -69
120-150	8.33	.1321	12	7.20	10500	153.9	2794	4.2 E -71
150-180	8.33	.1462	12	6.38	10000	150.0	2794	8.8 E -75
180-210	8.33	.066	12	7.36	10250	152.0	2794	3.0 E -73
210-240	8.33	.0708	12	6.15	11250	159.7	2794	2.5 E -66
240-270	8.33	.0613	12	7.65	11250	159.7	2794	1.8 E -66
270-300	8.33	.0613	12	5.46	12250	167.0	2794	1.1 E -60
300-330	8.33	.1274	12	7.06	14250	180.8	2794	1.2 E -51
330-360	8.33	.0802	12	5.22	15550	185.7	2794	4.6 E -49

References

ANDERSON A. T. (1974) Chlorine, sulfur, and water in magmas and oceans. *Geol. Soc. Amer. Bull.* **85**, 1485-1492.

ANDERSON A. T. (1975) Some basaltic and andesitic gases. *Rev. Geophys. Space Phys.* **13**, 37-55.

ARMSTRONG R. L. (1978) K-Ar dating: Late Cenozoic McMurdo Volcanic Group and dry valley glacial history, Victoria Land, Antarctica. *N.Z. Jour. Geol. Geophys.* **21**, 685-698.

BARNES S. J. (1993) Partitioning of the platinum group elements and gold between silicate and sulphide magmas in the Munni Munni Complex, Western Australia. *Geochim. Cosmochim. Acta* **57**, 1277-1290.

BLUTH G. J. S., DOIRON S. D., SCHNETZLER C. C., KRUEGER A. J. AND WALTER L. S. (1992) Global tracking of the SO2 clouds from the June, 1991 Mount Pinatubo eruptions. *Geophys. Res. Lett.* **19**, 151-154.

BOUTRON C. (1980) Respective influence of global pollution and volcanic eruptions on the past variations of the trace metals content of Antarctic snows since 1880's. *J. Geophys. Res.* **85**, 7426-7432.

BUAT-MENARD P. AND ARNOLD M. (1978) The heavy metal chemistry of atmospheric particulate matter emitted by Mount Etna volcano. *Geophys. Res. Lett.* **5**, 245-248.

CADLE R. D. (1975) Volcanic emissions of halides and sulfur compounds to troposphere and stratosphere. *J. Geophys. Res.* **80**, 1650-1652.

CALDWELL D. A. (1989) Physical and geochemical properties of summit flows and recent volcanic ejecta from Mount Erebus, Ross Island, Antarctica. M.S. Thesis, N.M. Institute of Mining and Technology.

CALDWELL D. A. AND KYLE P. R. (1994) Mineralogy and chemistry of ejecta erupted from Mount Erebus, Antarctica, between 1972 and 1986. In *Volcanological and Environmental Studies of Mount Erebus, Antarctica*, Antarctic Research Series ed. (ed. P. R. KYLE), Vol. 66, pp. 147-162. American Geophysical Union.

CAMPBELL I. H. AND BARNES S. J. (1984) A model for the geochemistry of the platinum-group elements in magmatic sulfide deposits. *Can. Min.* **22**, 151-160.

CARROLL M. R. AND WEBSTER J. D. (1994) Solubilities of Sulfur, Noble Gases, Nitrogen, Chlorine and Fluorine in Magmas. In *Volatiles in Magmas*, Reviews in Mineralogy ed. (eds. M. R. CARROLL and J. R. HOLLOWAY), Vol. 30, pp. 231-279. MIneralogical Society of America.

CASTLEMAN A. W., MUNKELWITZ H. R. AND MANOWITZ B. (1973) Contribution of volcanic sulfur compounds to the stratospheric aerosol layer. *Nature* **244**, 345-346.

CASTLEMAN A. W., MUNKELWITZ H. R. AND MANOWITZ B. (1974) Isotopic studies of the sulfur component of the stratospheric aerosol layer. *Tellus* **26**, 222-234.

CHUAN R. L. (1994) Dispersal of volcano-derived particles from Mount Erebus in the Antarctic atmosphere. In *Volcanological and Environmental Studies of Mount Erebus, Antarctica*, Antarctic Research Series ed. (ed. P. R. KYLE), Vol. 66, pp. 97-102. American Geophysical Union.

CLIFT R., GRACE J. R. AND WEBER M. E., eds. (1978) *Bubbles, Drops, and Particles*, 1st ed., Academic Press, 379p.

COLLINS R. L., BOWMAN K. P. AND GARDNER C. S. (1993) Polar stratospheric clouds at the South Pole in 1990: Lidar observations and analysis. *J. Geophys. Res.* **98**, 1001-1010.

DECKER R. W. AND DECKER B. B., eds. (1991) *Mountains of Fire: The Nature of Volcanoes*, Cambridge University Press, 221p.

DELMAS R. J. (1982) Antarctic sulphate budget. *Nature* **299**, 677-678.

DELMAS R., BRIAT M. AND LEGRAND M. (1982) Chemistry of south polar snow. *J. Geophys. Res.* **87**, 4314-4318.

DELMAS R. J., LEGRAND M., ARISTARAIN A. J. AND ZANOLINI F. (1985) Volcanic deposits in Antarctic snow and ice. *J. Geophys. Res.* **90**, 12901-12920.

DEVINE J. D., SIGURDSSON H. AND DAVIS A. N. (1984) Estimates of sulfur and chlorine yield to the atmosphere from volcanic eruptions and potential climatic effects. *J. Geophys. Res.* **89**, 6309-6325.

DIBBLE R. (1994) Velocity modeling in the erupting magma column of Mount Erebus, Antarctica. In *Volcanological and Environmental Studies of Mount Erebus, Antarctica*, Antarctic Research Series ed. (ed. P. R. KYLE), Vol. 66, pp. 17-33. American Geophysical Union.

DUNBAR N., CASHMAN K. V. AND DUPRE R. (1994) Crystallization processes of anorthoclase phenocrysts in the Mount Erebus magmatic system: evidence from crystal composition, crystal size distributions, and volatile content of melt inclusions. In *Volcanological and Environmental Studies of Mount Erebus, Antarctica*, Antarctic Research Series ed. (ed. P. R. KYLE), Vol. 66, pp. 129-146. American Geophysical Union.

FINNEGAN D. L. (1984) The chemistry of trace elements and acidic species in fumarolic emissions. Dept. of Geology Ph.D. dissertation, University of Maryland.

FISHER AND SCHMINKE (1984) *Pyroclastic Rocks*, Springer-Verlag, 472p.

FOLLOWS, M. J. (1992) On the cross-tropopause exchange of air. *J. Atmos. Sci.* **49**, 879-891.

GERLACH T. M. (1982) Interpretation of volcanic gas data from tholeiitic and alkaline mafic lavas. *Bull. Volcano.* **45**, 235-244.

GIGGENBACH W. F. (1980) Variations in the carbon, sulfur and chlorine contents of volcanic gas discharges from White Island, New Zealand. *J. Volcan. Geotherm. Res.* **27** , 1-13.

GIGGENBACH W. F., KYLE P. R. AND LYON G. (1973) Present volcanic activity on Mt. Erebus, Ross Island, Antarctica. *Geology* **1**, 135-136.

HANNA S. R., BRIGGS G. A. AND HOSKER R. P. (1982) *Handbook on Atmospheric Diffusion*, Technical Information Center, US Dept. of Energy, 102p.

HAUGHTON D. R., ROEDER P. L. AND SKINNER B. J. (1974) Solubility of sulfur in mafic magmas. *Economic Geology* **69**, 451-462.

HEDENQUIST J. W., SIMMONS S. F., GIGGENBACH W. F. AND ELDRIDGE C. S. (1993) White Island, New Zealand, volcanic-hydrothermal system represents the geochemical environment of high-sulfidation Cu and Au ore deposition. *Geology* **21**, 731-734.

HERRON M. M. (1982) Impurity sources of F^-, Cl^-, NO_3^-, and SO_4^{2-} in Greenland and Antarctic precipitation. *J. Geophys. Res.* **87**, 3052-3060.

HIRABAYASHI J., OSSAKA J. AND OZAWA T. (1982) Relationship between volcanic activity and chemical composition of volcanic gases- a case study on the Sakurajima Volcano. *Geoch. J.* **16**, 11-21.

HOFFMAN D. J. AND SOLOMON S. (1989) Ozone destruction through heterogeneous chemistry following the eruption of El Chichon. *J. Geophys. Res.* **94**, 5029-5041.

HOFMANN D. J., OLTMANS S. J., HARRIS J. M., SOLOMON S., DESHLER T. AND JOHNSON B. J. (1992) Observations and possible causes of new ozone depletion in Antarctica in 1991. *Nature* **359**, 283-287.

JACKSON M. L. (1994) Energy effects in bubble nucleation. *Ind. Eng. & Chem. Res.* **33**, 929-933.

JAUPART C. AND VERGNIOLLE S. (1988) Laboratory models of Hawaiian and Strombolian eruptions. *Nature* **331**, 58-60.

JAUPART C. AND VERGNIOLLE S. (1989) The generation and collapse of a foam layer at the roof of a basaltic magma chamber. *J. Fluid Mech.* **203**, 347-380.

KAWARATANI R. K. AND FUJITA S. (1990) Wet deposition of volcanic gases and ash in the vicinity of Mount Sakurajima. *Atm. Env.* **24a**, 1487-1492.

KILINC I. A. AND BURNHAM C. W. (1972) Partitioning of chloride between a silicate melt and coexisting aqueous phase from 2 to 8 kilobars. *Economic Geology* **67**, 231-235.

KRAUSKOPF K. B. (1957) The heavy metal content of magmatic vapor at 600 deg. C. *Economic Geology* **52**, 786-807.

KRAUSKOPF K. B. (1964) The possible role of volatile metal compounds in ore genesis. *Economic Geology* **59**, 22-45.

KRAUSKOPF K. B. (1979) *Introduction to Geochemistry*, Second ed., McGraw-Hill, 617p.

KYLE P. R. (1977) Mineralogy and glass chemistry of recent volcanic ejecta from Mt. Erebus, Ross Island, Antarctica. *N.Z. Jour. Geol. Geophys.* **20**, 1123-1146.

KYLE P. R. (1989) Antarctica. In *Global Volcanism 1975-1985* (eds. L. MCCLELLAND, T. SIMKIN, M. SUMMERS, E. NIELSON and T. C. STEIN), pp. 573-580. Prentice-Hall.

KYLE P. R. (1990) Erebus Volcanic Province, in *Volcanoes of the Antarctic Plate and Southern Oceans,* (ed.s W. E. LeMasurier and J. W. Thompson), pp 81-88. American Geophysical Union.

KYLE P. R. AND COLE J. W. (1974) Structural control of volcanism in the McMurdo Volcanic Group, Antarctica. *Bull. Volcanol.* **38**, 16-25.

KYLE P. R., DIBBLE R. R., GIGGENBACH W. F. AND KEYS J. (1982) Volcanic activity associated with the anorthoclase phonolite lava lake, Mt. Erebus, Antarctica. In *Antarctic Geosciences* (ed. C. CRADDOCK), pp. 735-745. University of Wisconsin Press.

KYLE P. R., MEEKER K. AND FINNEGAN D. (1990) Emission rates of sulfur dioxide, trace gases and metals from Mount Erebus, Antarctica. *Geophys. Res. Lett.* **17**, 2125-2128.

KYLE P. R., MOORE J. A. AND THIRLWALL F. (1992) Petrologic evolution of anorthoclase phonolite lavas at Mount Erebus, Ross Island, Antarctica. *J. Petrol.* **33**, 849-875.

KYLE P. R., SYBELDON L. M., MCINTOSH W. C., MEEKER K. AND SYMONDS R. (1994) Sulfur dioxide emission rates from Mount Erebus, Antarctica. In *Volcanological and Environmental Studies of Mount Erebus, Antarctica*, Antarctic Research Series ed. (ed. P. R. KYLE), Vol. 66, pp. 69-82. American Geophysical Union.

KYLE P. R., MCINTOSH W. C. AND ZREDA G. (1995) Automated correlation spectrometer (COSPEC) measurements of degassing of the anorthoclase phonolite magmatic system, Mount Erebus, Antarctica. *Bull. Volcano.* **in press**.

LAZRUS A. L., GANDRUD B. W., WOODARD R. N. AND SEDLACEK W. A. (1976) Direct measurements of stratospheric chlorine and bromine. *J. Geophys. Res.* **81**, 1067-1070.

LAZRUS A. L., CADLE R. D., GANDRUD B. W., GREENBURG J. P., HUEBERT B. J. AND ROSE W. I. (1979) Sulfur and halogen chemistry of the stratosphere and of volcanic eruption plumes. *J. Geophys. Res.* **84**, 7869-7875.

LEGRAND M. R. AND DELMAS R. J. (1988) Formation of HCl in the Antarctic atmosphere. *J. Geophys. Res.* **93**, 7153-7168.

LEPEL E. A., STEFANSSON K. M. AND ZOLLER W. H. (1978) The enrichment of volatile elements in the atmosphere by volcanic activity: Augustine Volcano 1976. *J. Geophys. Res.* **83**, 6213-6220.

MAENHAUT W., ZOLLER W. H., DUCE R. A. AND HOFFMAN G. L. (1979) Concentration and size distribution of particulate trace elements in the South Polar atmosphere. *J. Geophys. Res.* **84**, 2421-2431.

MALINCONICO L. L. (1979) Fluctuations in SO2 emission during recent eruptions of Etna. *Nature* **278**, 43-45.

MATHEZ E. A. (1976) Sulfur solubility and magmatic sulfides in submarine basalt glass. *J. Geophys. Res.* **81**, 4269-4276.

MATHEZ E. A. (1984) Influence of degassing on oxidation states of basaltic magmas. *Nature* **310**, 371-375.

MCCORMICK M. P. (1992) Initial assessment of the stratospheric and climatic impact of the 1991 Mount Pinatubo eruption: prologue. *Geophys. Res. Lett.* **19**, 149.

MCCORMICK M. P., THOMASON L. W. AND TREPTE R. (1995) Atmospheric effects of the Mt. Pinatubo eruption. *Nature* **373**, 399-404.

MEEKER K. (1988) The emission of gases and aerosols from Mount Erebus volcano, Antarctica. M.S. dissertation, N.M. Institute of Mining and Technology.

MEEKER K. A., CHUAN R. L., KYLE P. R. AND PALAIS J. M. (1991) Emission of elemental gold particles from Mount Erebus, Ross Island, Antarctica. *Geophys. Res. Lett.* **18**, 1405-1408.

METRICH N. (1990) Chlorine and fluorine in tholeiitic and alkaline lavas of Etna (Sicily). *J. Volcan. Geotherm. Res.* **40**, 133-148.

METRICH N. AND RUTHERFORD M. J. (1992) Experimental study of chlorine behavior in hydrous silicic melts. *Geochim. Cosmochim. Acta* **56**, 607-616.

METRICH N., CLOCHIATTI R., MOSBAH M. AND CHAUSSIDON M. (1993) The 1989-1990 activity of Etna magma mingling and ascent of H2O-Cl-S-rich basaltic magma. Evidence from melt inclusions. *J. Volcan. Geotherm. Res.* **59**, 131-144.

MILLER T. M., ZOLLER W. H., CROWE B. M. AND FINNEGAN D. L. (1990) Variations in trace metal and halogen ratios in magmatic gases through an eruptive cycle of the Pu'u O'o Vent, Kilauea, Hawaii: July-August 1985. *J. Geophys. Res.* **95**, 12607-12615.

NISBET E. G. (1986) RNA, hydrothermal systems, zeolites and the origin of life. *Episodes* **9**, 83-90.

OXTOBY D. W. AND EVANS R. (1988) Nonclassical nucleation theory for the gas-liquid transition. *J. Chem. Phys.* **89**, 7521-7530.

PALAIS J. M., SPENCER M. J. AND CHUAN R. L. (1994) Elemental tracers of volcanic emissions from Mount Erebus in Antarctic snow samples. In *Volcanological and Environmental Studies of Mount Erebus, Antarctica,* Antarctic Research Series ed. (ed. P. R. Kyle), Vol 66, pp. 103-113. American Geophysical Union.

POULSON S. R. AND OHMOTO H. (1990) An evaluation of the solubility of sulfide sulfur in silicate melts from experimental data and natural samples. *Chemical Geology* **85**, 57-75.

ROSE W. I., CHUAN R. L. AND KYLE P. R. (1985) Rate of sulphur dioxide emission from Erebus volcano, Antarctica, December 1983. *Nature* **316**, 710-712.

RUNCA E., MELLI P. AND ZANNETI P. (1976) Computation of long-term average SO2 concentration in the Venetian area. *Applied Mathematical Modeling* **1**, 9-15.

RYAN J. A. AND MUKHERJEE N. R. (1975) Sources of stratospheric gaseous chlorine. *Rev. Geophys. Space Phys.* **13**, 650-658.

SHAW G. E. (1983) X-ray spectrometry of polar aerosols. *Atm. Env.* **17**, 329-339.

SHINOHARA H., IIYAMA J. T. AND MATSUO S. (1989) Partition of chlorine compounds between silicate melt and hydrothermal solutions: I. Partition of NaCl-KCl. *Geochim. Cosmochim. Acta* **53**, 2617-2630.

SMIRNOV V. I. (1976) Ore-forming elements in juvenile gases of Tolbachik volcanoes. *Int. Geo. Rvws.* **20**, 286-288.

SOLOMON S., GARCIA R. R., ROWLAND F. S. AND WUEBBLES D. J. (1986) On the depletion of Antarctic ozone. *Nature* **321**, 755-758.

SOLOMON S., SANDERS R. W., GARCIA R. R. AND KEYS J. G. (1993) Increased chlorine dioxide over Antarctica caused by volcanic aerosols from Mount Pinatubo. *Nature* **363**, 245-248.

SPARKS R. S. J. (1978) The dynamics of bubble formation and growth in magmas: a review and analysis. *J. Volcan. Geotherm. Res.* **8**, 1-37.

SYBELDON L. (1991) Sulfur dioxide emissions from Pu'u O'o vent, Kilauea, Hawaii and Mount Erebus, Antarctica. M.S. thesis, N.M. Institute of Mining and Technology.

SYMONDS R. B. AND REED M. H. (1993) Calculation of multicomponent chemical equilibria in gas-solid-liquid systems: calculation methods, thermochemical data, and applications to studies of high temperature volcanic gases with examples from Mt. St. Helens. *Amer. J. Sci.* **293**, 758-864.

SYMONDS R. B., KYLE P. R. AND ROSE W. I. (1985) SO_2 emission rates and the 1984 activity at Mount Erebus Volcano, Antarctica. *EOS* **66**, 417.

SYMONDS R. B., ROSE W. I., GERLACH T. M., BRIGGS P. H. AND HARMON R. S. (1990) Evaluation of gases, condensate, and SO2 emissions from Augustine volcano, Alaska: the degassing of a Cl-rich volcanic system. *Bull. Volcano.* **52**, 355-374.

SYMONDS R. B., ROSE W. I., BLUTH G. J. S. AND GERLACH T. M. (1994) Volcanic gas studies: methods, results and applications. In *Volatiles in Magmas*, Reviews in Mineralogy ed. (eds. M. R. CARROLL and J. R. HOLLOWAY), Vol. 30, pp. 1-66. Mineralogical Society of America.

TABAZADEH A. AND TURCO R. P. (1993) Stratospheric chlorine injection by volcanic eruption: HCl scavenging and implications for ozone. *Science* **260**, 1082-1085.

TAIT S., JAUPART C. AND VERGNIOLLE S. (1989) Pressure, gas content and eruption periodicity of a shallow, crystallising magma chamber. *Earth. Planet. Sci. Lett.* **92**, 107-123.

TOUTAIN J. P., ALOUPOGIANNIS P., DELORME H., PERSON A., BLANC P. AND ROBAYE G. (1990) Vapor deposition of trace elements from degassed basaltic lava, Piton de la Fournaise volcano, Reunion Island. *J. Volcan. Geotherm. Res.* **40**, 257-268.

VOIGHT B. (1990) The Nevado del Ruiz catastrophe: anatomy and retrospection. *J. Volcan. Geotherm. Res.* **44**, 349-386.

WALLACE P. AND CARMICHAEL I. S. E. (1992) Sulfur in basaltic magmas. *Geochim. Cosmochim. Acta* **56**, 1863-1874.

WEBSTER J. D. (1990) Partitioning of F between H2O and CO2 fluids and topaz rhyolite melt. *Contrib. Mineral. Petrol.* **104**, 424-438.

WENDLANDT R. F. (1982) Sulfide saturation of basalt and andesite melts at high pressures and temperatures. *Am. Mineral.* **67**, 877-885.

WORNER G. AND SCHMINKE H. U. (1984) Mineralogical and Chemical Zonation of the Laacher See Tephra Sequence (East Eifel, W. Germany). *J. Petrol.* **25**, 805-835.

YOSHIDA M. (1990) Fractionation of Fluorine and Chlorine Through the Volcanic Process. In *Geochemistry of Gaseous Elements and Compounds* (eds. E. M. DURRANCE, E. M. GALIMOV, M. E. HINKLE, G. M. REINER, R. SUGISAKI and S. S. AUGUSTITHIS), pp. 163-183. Theophrastus Publications, S.A.

YOSHIDA M., UCHIKAWA K. AND HIRABAYASHI J. (1994) Fluorine and chlorine contents in the lavas and ejecta of the 1986 eruption of Izu-Oshima volcano. *J. Volcan. Geotherm. Res.* **63**, 231-241.

ZANETTI P. (1990) *Air Pollution Modeling: Theories, Computational Methods and Available Software*, Van Nostrand Reinhold, 443p.

ZREDA-GOSTYNSKA G. (1993) Chlorine, fluorine and sulfur emissions from Mt. Erebus Antarctic and estimated contributions to the Antarctic atmosphere. *Geophys. Res. Lett.* **20**, 1959-1962.

ZREDA-GOSTYNSKA G. (1995) Characterization of gas and aerosol emissions from Mt. Erebus Volcano, Antarctica. Ph.D. dissertation, New Mexico Tech, Socorro, NM.